

Stephen F. Austin State University

SFA ScholarWorks

Electronic Theses and Dissertations

Winter 12-15-2020

Species Distribution Modeling for Arid Adapted Habitat Specialists in Zion National Park

Sam Driver

Stephen F Austin State University, driversm@jacks.sfasu.edu

Chris M. Schalk

Stephen F Austin State University, schalkc@sfasu.edu

Daniel Unger

Stephen F Austin State University, unger@sfasu.edu

David Kulhavy

Stephen F Austin State University, dkulhavy@sfasu.edu

Follow this and additional works at: <https://scholarworks.sfasu.edu/etds>



Part of the [Desert Ecology Commons](#), [Environmental Studies Commons](#), [Geomorphology Commons](#), [Natural Resources and Conservation Commons](#), and the [Other Earth Sciences Commons](#)

Tell us how this article helped you.

Repository Citation

Driver, Sam; Schalk, Chris M.; Unger, Daniel; and Kulhavy, David, "Species Distribution Modeling for Arid Adapted Habitat Specialists in Zion National Park" (2020). *Electronic Theses and Dissertations*. 354. <https://scholarworks.sfasu.edu/etds/354>

This Thesis is brought to you for free and open access by SFA ScholarWorks. It has been accepted for inclusion in Electronic Theses and Dissertations by an authorized administrator of SFA ScholarWorks. For more information, please contact cdsscholarworks@sfasu.edu.

Species Distribution Modeling for Arid Adapted Habitat Specialists in Zion National Park

SPECIES DISTRIBUTION MODELING FOR ARID ADAPTED
HABITAT SPECIALISTS IN ZION NATIONAL PARK

by

Samuel Macon Driver, B.S.

Presented to the Faculty of the Graduate School of

Stephen F. Austin State University

In Partial Fulfillment

of the Requirements

For the Degree of

Master of Science

Stephen F. Austin State University

December 2020

SPECIES DISTRIBUTION MODELING FOR ARID ADAPTED
HABITAT SPECIALISTS IN ZION NATIONAL PARK

by

Samuel Macon Driver, B.S.

APPROVED:

Dr. Daniel R. Unger, Committee Chair

Dr. David L. Kulhavy, Committee Member

Dr. Christopher M. Schalk, Committee Member

Pauline M. Sampson, Ph.D.
Dean of Research and Graduate Studies

ABSTRACT

The Arizona toad (*Anaxyrus microscaphus*) and Jones' waxy dogbane (*Cycladenia humilis* var. *jonesii*) are habitat specialists with historical ranges in the desert southwest and specifically, Zion National Park (ZION). The machine learning method, MaxEnt, constructed species distribution models (SDMs) in ZION for the two study species at 30 m and 900 m spatial resolutions using climate, topographic, and remotely sensed data. Additionally, 900 m forecasting models were constructed to observe the shifts in suitable habitat for the years 2050 and 2070, based off two representative concentration pathway scenarios. Results indicate promising predictive power for both high resolution models (30m) for *C. humilis* var. *jonesii* and *A. microscaphus* with area under curve (AUC) test analysis of 0.715 and 0.810, respectively. Forecasting models displayed decreasing suitability for *A. microscaphus* with both climate scenarios applied to the model. However, *C. humilis* var. *jonesii* habitat increased with future scenarios applied to the MaxEnt models.

ACKNOWLEDGEMENTS

I'd first like to express my gratitude to Stephen F. Austin State University for allowing me to develop, pursue, and achieve my academic goals. To all my professors in the environmental and spatial science divisions at the SFA Forestry Department, I am beyond grateful for all that you've helped me accomplish. To my thesis advisor, Dr. Daniel Unger, thank you for equipping me with the tools to succeed in my future career field. Thank you to my thesis committee member, Dr. David Kulhavy, for your guidance and steadfast belief in me. To my graduate representative, Dr. Yanli Zhang, your intro GIS class was the first I attended at SFA and your advanced GIS class happened to be my last at SFA; thank you for keeping my intellectual curiosity up from beginning to end. And how could I forget my thesis committee member, Dr. Christopher Schalk, thank you for continuously checking in on my progress and staying on me to learn the ecology behind species modeling. "Bonesaw is ready!!!"

Special thank you to Dr. Kenneth Farrish and Mary Ramos. Thank you, Shauna, Adam, and Aven for taking me in for the summer in beautiful Zion National Park while also planting the seed for this research project. I'll cherish our adventures for a lifetime and can't wait to make more.

Above all, I will never be able to thank my family enough. You constantly believe in my dreams and have supported me through all my life endeavors. To my brother,

Daniel, thank you for cookin' up gumbos, smoking briskets, and playing that squeezebox till them roosters' crow, and above all, always providing the brightest of outlooks when the odds seemed stacked up against me. *Laissez les bons temps rouler!* To my mother and father, Margaret and Paul, thank you for allowing your adult son to park and live in an ugly RV for two years in your front yard. On a serious note, words don't do justice for how grateful I am to have two amazing role models to always look up to, thank you for everything.

*"The only way to get there son is one mile at a time. This road's crooked
steep and rocky as she winds."*

– Uncle Steve Hartz



TABLE OF CONTENTS

ABSTRACT.....	i
ACKNOWLEDGEMENTS.....	ii
TABLE OF CONTENTS.....	iv
LIST OF FIGURES	vii
LIST OF TABLES	xiii
INTRODUCTION	1
OBJECTIVES.....	7
LITERATURE REVIEW	8
<u>Zion National Park</u>	8
<u>Arizona Toad (<i>Anaxyrus microscaphus</i>)</u>	10
<u>Jones' waxy dogbane (<i>Cycladenia humilis</i> var. <i>jonesii</i>)</u>	12
<u>Species Distribution Models</u>	15
<u>Niche Concepts</u>	16
<u>Maximum Entropy (MaxEnt)</u>	17
<u>Sample Size</u>	19

<i>Variable Selection</i>	19
<i>Spatial Scale</i>	20
<i>Spatial Resolution</i>	21
<i>Thresholds</i>	23
<i>Sampling Bias</i>	26
<i>Forecasting</i>	27
METHODS	30
<u>Study Area</u>	30
<u>Occurrence Data</u>	32
<u>Data Acquisition</u>	32
<i>Digital Elevation Model Acquisition</i>	32
<i>Remote Sensing Acquisition</i>	33
<i>Climatic Data Acquisition</i>	33
<u>Environmental Variable Justification</u>	35
<u>Variable Selection</u>	45
<u>Model Parameters</u>	46
<i>Spatial Scale</i>	46

<i>Spatial Resolution</i>	49
<i>MaxEnt Calibration</i>	49
<u>Model Performance</u>	51
<i>30-m and 900-m Current Models</i>	51
<i>Model Forecasting</i>	51
RESULTS	53
<u>Model Performance</u>	53
<u>Resolution Comparison</u>	62
<u>Future Climate Trends</u>	68
DISCUSSION & CONCLUSIONS	77
LITERATURE CITED	86
VITA.....	104

LIST OF FIGURES

Figure 1. ZION is in southwestern Utah and includes habitat for many threatened and endangered species, including habitat for *C. humilis* var. *jonesii* and the *A. microscaphus*.9

Figure 2. Location of the habitat range generated by the USGS for the Arizona toad (*Anaxyrus microscaphus*) in the states of California, Nevada, Utah, New Mexico, and Arizona. A portion of the habitat range is located inside of ZION (orange). The top-right inset displays an adult Arizona toad.11

Figure 3. Location of the habitat range generated by the Fish and Wildlife Service for Jones’ cycladenia (*Cycladenia humilis* var. *jonesii*) scattered throughout southeastern Utah and northern Arizona. Habitat for *C. humilis* var. *jonesii* is fragmented and is known to occur in only southeast Utah and far northern Arizona. The top-left inset displays a flowering *C. humilis* var. *jonesii*.....13

Figure 4. A demonstration of a representative concentration pathway depicting the four climate scenarios of (2.6, 4.5, 6.0, and 8.5). RCPs begin to differ from 2025-2030 and are extrapolated to the year 2100. RCP 2.6 is considered the best-case scenario while RCP 8.5 is the worst-case climate scenario ().29

Figure 5. ZION is the study area for the SDMs created for <i>A. microscaphus</i> and <i>C. humilis</i> var. <i>jonesii</i> . The inset in the top right displays the five national parks found within Utah.....	30
Figure 6. Flow chart displaying the procedures in creating the proper parameters from start to finish for use within the MaxEnt model for both study species.	31
Figure 7. Digital elevation model for ZION at 30 m resolution.	36
Figure 8. Slope derived from the original DEM for ZION at 30 m resolution.....	37
Figure 9. Aspect derived from the original DEM for ZION at 30 m resolution.....	39
Figure 10. Terrain ruggedness index derived from the original DEM for ZION at 30 m resolution.....	40
Figure 11. Topographic position index derived from the original DEM for ZION at 30 m resolution. This variable describes the valley bottom flatness in green and higher elevation peaks in the red.....	42
Figure 12. Normalized difference vegetation index derived from Landsat 5 satellite imagery for ZION at 30 m resolution. Green represents vegetation in this map and red represents lack of vegetation.....	43
Figure 13. Bare soil index derived from Landsat 5 satellite imagery for ZION at 30 m resolution.....	44
Figure 14. The model training for <i>A. microscaphus</i> was determined by constructing a 50 km buffer around the occurrence points obtained from GBIF.org. Of the 327 occurrence points, 87 points remained after spatial rarefying which were used to train the MaxEnt	

model. Occurrence localities used inside and outside of ZION were used to train the SDMs.47

Figure 15. The model training extent was determined by constructing a 50 km buffer around the occurrence points obtained from GBIF.org. Spatial rarefying was not conducted on the occurrence points for *C. humilis* var. *jonesii* due to the low volume of occurrence localities.....48

Figure 16. **A.** The average receiver operating curve (AUC) for *A. microscaphus* with the five replicates run in MaxEnt. The red line representing the fit of the model to the training data. The blue line represents the fit of the model to the 25% testing data. AUC over 0.7 assumes positive predictive power for the model. **B.** Represents the test omission rate and predicted area as a function of the cumulative threshold.54

Figure 17. **A.** The average receiver operating curve (AUC) for *C. humilis* var. *jonesii* with the five replicates run in MaxEnt. The red line representing the fit of the model to the training data. The blue line represents the fit of the model to the 25% testing data. AUC over 0.7 assumes positive predictive power for the model. **B.** Represents the test omission rate and predicted area as a function of the cumulative threshold.55

Figure 18. Partial dependence plots displaying the marginal response of the 12 environmental variables selected for *A. microscaphus* in the MaxEnt model. Each response curve demonstrates the range of suitability for each environmental variable if each variable were used to create a MaxEnt model independent of other variables.57

Figure 19. Partial dependence plots displaying the marginal response of the 13 environmental variable selected for *Cycladenia humilis* var. *jonesii* in the MaxEnt model. Each response curve demonstrates the range of suitability for each environmental variable if each variable were used to create a MaxEnt model independent of other variables.59

Figure 20. MaxEnt model output for 30 m resolution habitat suitability maps for *A. microscaphus* in ZION. Suitability classes describe the ranking of habitat preference for the species being modeled. Models were created using MaxEnt.....60

Figure 21. MaxEnt model output for 30 m resolution habitat suitability maps for *C. humilis* var. *jonesii* in ZION. Suitability classes describe the ranking of habitat preference for the species being modeled. Models were created using ArcMap and MaxEnt.61

Figure 22. MaxEnt habitat suitability outputs for *A. microscaphus* with differing resolution sizes to compare low to high suitability habitat for ZION. Highest suitability habitat increased within the park with the higher resolution. All environmental variables (topographic, remotely-sensed, and climate) were applied to these two outputs.66

Figure 23. MaxEnt habitat suitability outputs for *C. humilis* var. *jonesii* with differing resolution sizes to compare low to high suitability habitat for ZION. Highest suitability habitat decreased within the park with the higher resolution. All environmental variables (topographic, remotely-sensed, and climate) were applied to these two maps.....67

Figure 24. Forecasting SDM of *A. microscaphus* contrasting the suitable habitat for future climate scenarios for representative concentration pathways that describe greenhouse gas

concentration of 2.6 W/m² and 8.5 W/m² for the year 2050. The SDM covers the complete training extent of the toad to better understand changes in suitable habitat (see Figure 14). The ‘10 percentile training presence’ threshold was used to delineate suitable habitat in this analysis.....69

Figure 25. Forecasting SDM of *A. microscaphus* contrasting the suitable habitat for climate scenarios for representative concentration pathways, which describe greenhouse gas concentration of 2.6 W/m² and 8.5 W/m² for the year 2070 (see Figure 14). The SDM covers the complete training extent of the toad to better understand changes in suitable future habitat. The ‘10 percentile training presence’ calculated by the MaxEnt output was used as the threshold to delineate suitable habitat.70

Figure 26. Forecasting SDM of *A. microscaphus* for the current year (2020) and 2050 using binary distribution of suitable versus not suitable habitat. The ‘10 percentile training presence’ threshold was calculated by MaxEnt to delineate suitable habitat in this analysis.....71

Figure 27. Forecasting SDM of *A. microscaphus* for the current year (2020) and 2070 using binary distribution of suitable versus not suitable habitat. The ‘10 percentile training presence’ threshold was calculated by MaxEnt to delineate suitable habitat in this analysis.....72

Figure 28. Forecasting SDM of *C. humilis* var. *jonesii* contrasting the suitable habitat for future climate scenarios for representative concentration pathways that describe greenhouse gas concentration of 2.6 W/m² and 8.5 W/m² for the year 2050. The SDM

covers the complete training extent of the plant to better understand changes in suitable future habitat (see Figure 15). The ‘10 percentile training presence’ calculated by the MaxEnt output was used to delineate suitable habitat in this analysis.73

Figure 29. Forecasting SDM of *C. humilis* var. *jonesii* contrasting the suitable habitat for future climate scenarios for with representative concentration pathways that describe greenhouse gas concentration of 2.6 W/m² and 8.5 W/m² for the year 2070. The SDM covers the complete training extent of the plant to better understand changes in suitable habitat (see Figure 15). The ‘10 percentile training presence’ calculated by the MaxEnt output was used to delineate suitable habitat in this analysis.74

Figure 30. Forecasting SDM of *C. humilis* var. *jonesii* in ZION for the current year (2020) and 2050 using binary distribution of suitable versus not suitable habitat. The ‘10 percentile training presence’ threshold was calculated by MaxEnt to delineate suitable habitat in this analysis.75

Figure 31. Forecasting SDM of *C. humilis* var. *jonesii* in ZION for the current year (2020) and 2070 using binary distribution of suitable versus not suitable habitat. The ‘10 percentile training presence’ threshold was calculated by MaxEnt to delineate suitable habitat in this analysis.76

LIST OF TABLES

Table 1. List of the 19 bioclimatic variables taken from the WorldClim database and used for analysis within the target species' SDMs. Pearson's correlation test was first used to eliminate highly correlated variables with topographic and remotely sensed variables....	34
Table 2. Results from Pearson's correlation coefficient used to quantify correlation among environmental variables. Resulting variables were used to train the model within MaxEnt.....	45
Table 3. The MACHISPLIN package results for the climate variables downscaled to 30 m resolution and the r^2 values associated with each layer. Results are based off an ensemble approach using six algorithms. Independent variables used in the approach include elevation, slope, aspect, and topographic wetness index.	50
Table 4. Permutation importance values for each bioclimatic variable within the MaxEnt model for the 30 m <i>A. microscaphus</i> SDM. The permutation value is determined by randomly permuting the values of each independent variables against the training points. Values are then normalized to provide percentages; higher values suggest greater influence on the model.....	56
Table 5. Permutation importance values for each WorldClim variable for the MaxEnt model for the 30 m <i>C. humilis</i> var. <i>jonesii</i> SDM. The permutation value is determined by	

randomly permuting the values of each independent variables against the training points. Values are then normalized to provide percentages; higher values suggest greater influence on the model.....58

Table 6. Differing MaxEnt outputs for both study species comparing the contrast63
between 30 m and 900 m resolution.63

Table 7. The percent change between 30 m and 900 m SDM outputs for the study species within five habitat suitability classes.64

Table 8. Permutation importance values for each bioclimatic variable within the MaxEnt model for the 900 m *A. microscaphus* and *C. humilis* var. *jonesii* SDMs. The permutation value is determined by randomly permuting the values of each independent variables against the training points. Values are then normalized to provide percentages; higher values suggest greater influence on the model.65

Table 9. Area of suitable habitat for *A. microscaphus* within the training extent for future climate scenarios for 2050 and 2070 with differing RCPs of 2.6 and 8.5 W/m².....70

Table 10. Area of suitable habitat for *A. microscaphus* within ZION for current and future climate scenarios of 2050 and 2070 with differing RCPs of 2.6 and 8.5 W/m².....72

Table 11. Area of suitable habitat for *C. humilis* var. *jonesii* within the training extent for future climate scenarios of 2050 and 2070 with differing RCPs of 2.6 and 8.5 W/m².....74

Table 12. Area of suitable habitat for *C. humilis* var. *jonesii* within ZION for future climate scenarios of 2050 and 2070 with differing RCPs of 2.6 and 8.5 W/m².....76

INTRODUCTION

Since the incorporation of new statistical methods and GIS tools, the development of predictive species distribution models (SDMs) has expanded in the field of ecology, biogeography, and conservation biology (Raes, 2012). SDMs describe how climatic and environmental factors relate to species occurrences in geographic space, in order to delineate suitable habitat over local, regional, and global scales. Common applications for SDMs include projecting species distribution for current, past, and future climates, studying relationships between environmental parameters and species richness, mapping invasive species habitat range, and conservation planning (Melo-Merino et al., 2020).

Of notable interest from a conservation and management standpoint, is the construction of SDMs to understand the current and future distribution of available habitat for species, particularly habitat specialist. Habitat specialists display a narrow range of environmental factors and have relatively limited geographic requirements, often constricting the species to a defined range of suitable habitats for which they are well-adapted (Hernandez et al., 2006; Büchi and Vuilleumier, 2014). In their optimal habitat, it is believed that specialists perform better than generalists, with a trade-off to generalists on performance and fitness in suboptimal habitats (Levins, 1968; Lawlor and Smith 1976; Marvier et al. 2004; Jasmin and Kassen 2007). However, alterations to resource

gradients can lead to unfavorable impacts on specialists. Specialist species are susceptible to anthropogenic factors, such as climate change and urbanization (McKinney and Lockwood, 1999). Interspecific competition also contributes to specialization within a species (Biedma et al. 2019). Generalists can alter ecosystems by outcompeting specialists, homogenizing ecosystems, and reducing biodiversity at the community level (Büchi and Vuilleumier, 2013). These reductions in availability and resources can fragment the available habitat, resulting in demographic isolation, population decline, species extirpation, and ultimately leading to biodiversity loss (Vrba, 1987; Ricketts, 2001; Büchi and Vuilleumier, 2013). Monitoring the loss of biodiversity, especially within specialist species is important to understand the identity, abundance, and shifts in their habitat range (Díaz et al., 2006).

Due to the effects of climate change and other factors on desert landscapes, understanding the available habitat to specialist species is of particular importance (IPCC, 2014). Globally, desert climates are changing faster than other non-polar terrestrial ecosystems due to climate change (IPCC, 2014). Increased effects of climate change are projected across the desert southwest in the 21st century with increases in aridity and temperatures, along with longer drought durations (Cayan et al., 2010; Dominguez et al., 2010; Seager and Vecchi, 2010). Arid environments, such as the desert southwest of the United States, provide an array of ecosystems and microclimates conducive to examine the current and projected availability of habitats for specialist species. Across regions of the southwest, seasonal precipitation is erratic and prolonged droughts are common,

leading to adverse effects on landscape and ecosystems (Notaro et al., 2011). These abiotic factors have shifted species to become better adapted to their xeric landscape. Plants have become drought tolerant by growing deeper tap roots, inducing seed dormancy, or utilizing paraheliotropism to minimize sun exposure (Canadell et al., 1996; Chávez et al., 2016). Desert anurans have adapted to diminishing water resources by becoming fossorial, utilizing explosive breeding behaviors, accelerating metamorphosis, and becoming restricted geographically to stable water sources (Kulkarni et al., 2011; Schalk et al., 2015).

To better understand species habitat requirements and the effects of future climate change scenarios on species, researchers use SDMs such as the maximum entropy modeling method (MaxEnt) to analyze these changes (Elith et al., 2010). MaxEnt is a machine-learning technique used in modeling the distribution of a species' habitat using presence-only occurrence records (Phillips et al., 2006). The maximum entropy algorithm attempts to estimate a probability distribution of species occurrence that is closest to uniform while maintaining its environmental constraints (Elith et al., 2010). MaxEnt has become a popular platform for species distribution modelling because of an ease of use interface, implementation of presence-only data, low occurrence data requirements, future forecasting ability, and its use of environmental data from across the study area rather than a discriminative approach (Phillips and Elith, 2013). MaxEnt is also capable of projecting one set of environmental layers to other locations using similarly formatted environmental layers. Projecting is often used to map species in areas of changing

climate, observing potential habitat for invasive species, or building models in unknown areas for target species evaluation (Phillips, 2017). MaxEnt is capable of handling both continuous and categorical (discrete) environmental variables within its algorithm (Phillips and Dudík, 2008). Using both continuous and categorical environmental data, occurrence locations of the target species are then included into the MaxEnt algorithm to build a model that projects a species habitat range across a geographic landscape to identify other potential locations of suitable habitat.

With changing climates and diminishing habitats for many species, forecasting SDMs has become a powerful tool for conservation practitioners and resource managers as changing climates impact ecological systems (Guisan et al. 2013). MaxEnt can construct SDMs to predict the changes in the geographic distribution of a species under different climate change scenarios. These climate change scenarios are represented by representative concentration pathways (RCPs), which are the developments of scenario sets containing emissions, concentrations, and land-use trajectories (Vuuren et al., 2011). RCPs project a potential future scenario and allow SDMs, such as MaxEnt, to capture the shifts in suitable habitat for a species. This provides an invaluable tool for proactively monitoring and planning conservation efforts for specialist species who are at risk of extirpation and declining habitat due to changing climates.

One of the most diverse protected landscapes in the desert southwest, Zion National Park (ZION) provides refuge to various protected species within its boundaries. ZION was chosen as the study area due to its diverse landscape characterized by high

plateaus and deep sandstone canyons carved out by the Virgin River and additional tributaries which support many microclimates. The southern section of the park is characterized by desert habitat while the norther portion of the park is covered with high plateau forests (US DOI, 2013a). An abundance of specialist species inhabit the park, including the Arizona toad (*Anaxyrus microscaphus*), desert tortoise (*Gopherus agassizii*), Gila monster (*Heloderma suspectum*), and Mexican spotted owl (*Strix occidentalis lucida*) (US DOI, 2009; US DOI, 2013a). These and many other species are sensitive to environmental alterations occurring such as habitat degradation, invasive species encroachment, changes in hydrologic regimes, and rising temperatures due to climate change (Ryan et al., 2014). To protect sensitive habitat within the park from the changes in habitat, ZION complies with the National Environmental Policy Act in addition to other environmental regulations, including the Endangered Species Act and the National Historic Preservation Act (US DOI, 2013a).

This study concentrates on the habitat range of two arid adapted habitat specialists within ZION, the Arizona toad (*Anaxyrus microscaphus*) and Jones' waxy dogbane (*Cycladenia humilis* var. *jonesii*) (Tilley et al., 2010; Ryan et al., 2015). Both species are endemic to the desert southwest and display morphological traits typically found in regions of prolonged drought and extreme temperatures. *Anaxyrus microscaphus* is a habitat specialist that requires slow moving streams, sandy floodplains for burrowing, and a narrow temperatures range for breeding (Sullivan, 1992; Ryan et al., 2017). Their habitat is currently threatened by changes in the hydrological cycle, habitat

modifications, forest fires, hybridization, and introduced pathogens (Sullivan and Lamb, 1988; Ryan et al., 2014). Reports have shown that on a regional scale, toads are declining, but locally have more stable populations based upon habitat conditions (Sullivan, 1993; Bradford et al., 2005; Ryan et al., 2017). The habitat for *C. humilis* var. *jonesii* is highly specialized, requiring gypsiferous and saline soils that are primarily fragmented rock surfaces with soils at least 50 cm in depth (Welsh et al., 1987; USFWS, 2008). Main threats to *C. humilis* var. *jonesii* habitat arise from shifts in climate and land use practice (Tilley et al., 2010). Populations for *C. humilis* var. *jonesii* are currently geographically disjunct across southeastern Utah, little is known about the taxon's historic range (Sipes et al., 1994; Sipes and Wolf, 1997). Suitable habitat currently remains for both study species inside of ZION, with common sightings of *A. microscaphus* along riparian zones and other ephemeral water sources (Dalh et al., 2000). Unfortunately, there have been no official sightings of *C. humilis* var. *jonesii* within the park. Nearest populations are to the east in Garfield County, Utah and Mohave County, Arizona (Welsh et al., 1987; Sipes et al. 1994).

Habitat specialists are known to have restricted spatial distribution patterns which typically leads to limited occurrences localities (Kattan, 1992; Segurado and Araújo, 2004; Elith et al., 2006). Furthermore, SDMs for habitat specialists are known to have narrow geographic ranges but have higher SDM accuracy than those of generalist species (Luoto et al., 2005; Elith et al., 2006). Within this study, MaxEnt is used to capture the distribution of *A. microscaphus* and *C. humilis* var. *jonesii*, with differing spatial

resolutions providing detail into the estimation of suitable habitat for higher resolution models. Forecasting models with MaxEnt also observed the long-term habitat shifts due to abiotic factors within the region and ZION.

OBJECTIVES

The goal of this study is to develop a SDM for arid adapted habitat specialist species within ZION using the maximum entropy modelling methods (MaxEnt).

Generating reliable SDMs will benefit environmental managers in mapping valuable species habitat to help establish a firm ecological background to assist in understanding complex management issues. Below are the following objectives for the study:

1. Create a species distribution model for both the Arizona toad (*Anaxyrus microscaphus*) and Jones' Waxy Dogbane (*Cycladenia humilis* var. *jonesii*) to delineate suitable habitat range within the ZION boundaries using the MaxEnt software to construct ecologically relevant climate, topographic, and remotely sensed variables to maximize effectiveness of model strength;
2. Construct SDMs for the target species at 30 m and 900 m spatial resolutions within ZION, for comparison of model strength between the two resolutions; and
3. Utilize forecasting techniques to project each species' distribution for the years 2050 and 2070 to understand the effect of climate change on habitat suitability for the target species based on 2.6 and 8.5 W/m² RCP scenarios. Future habitat scenarios will be estimated by representative concentration pathways that predict the measurement of greenhouse gas concentration for alternative future climates.

LITERATURE REVIEW

Zion National Park

ZION is in southwestern Utah (Figure 1) within Washington, Iron, and Kane counties. ZION entered the national park system in 1919 under the signing of President Woodrow Wilson. The park has an area of 601.9 km², with 84% designated as wilderness (US DOI, 2013a). The park is located at the juncture of the Colorado Plateau, Mojave Desert, and Great Basin ecoregions. The elevation ranges from 2,660 m at its highest point (Horse Ranch Mountain) to 1,117 meters (Coal Pits Wash) at its lowest point (US DOI, 2013a). More than 1,000 plant species inhabit ZION with approximately 78 species of mammals, 30 reptile species, 7 amphibians, 8 fish, and 291 species of birds (NPS, 2018). The last known stable population studied in ZION was located along the Virgin River and Oak Creek riparian zones from 1998-1999 (Dahl et al., 2000). They are believed to still inhabit the park, though no recent studies can support this claim. There is no known literature of *C. humilis* var. *jonesii* populations occurring inside of ZION, only potential suitable habitat remains within the park boundaries for the plant (US DOI, 2013b).

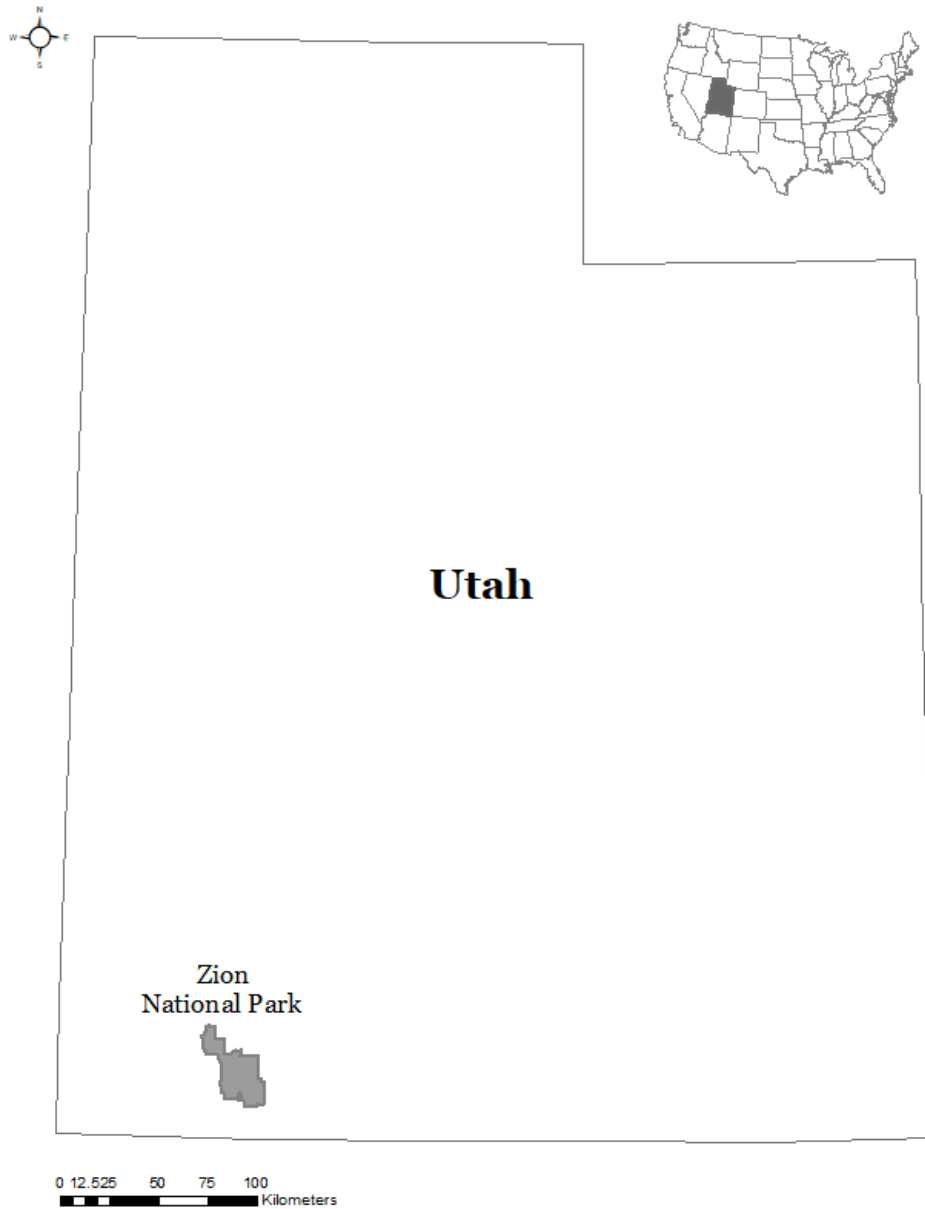


Figure 1. ZION is in southwestern Utah and includes habitat for many threatened and endangered species, including habitat for *C. humilis* var. *jonesii* and the *A. microscaphus*.

Arizona Toad (*Anaxyrus microscaphus*)

Anaxyrus microscaphus was originally described by Cope (1867) as *Bufo microscaphus*. The toads' habitat range expands primarily along the Mogollon Plateau in western New Mexico, expanding through Arizona into far southwestern Utah and eastern Nevada along the Virgin and Colorado River basins and its tributaries (Figure 2) (Dodd, 2013; Blais et al., 2016). Aside from the Virgin and Colorado River locations, historical occurrences for the toad have been found in the Agua Fria, Salt, Verde, Bill Williams, and Hassayampa Rivers in Arizona and the Gila, Mimbres, and San Francisco Rivers in New Mexico (Sullivan and Lamb, 1988; Ryan et al., 2015). In New Mexico, roughly 70% of historical sites monitored for *A. microscaphus* recorded no observations in past decades, implying a decline in New Mexico populations over that time span (Ryan et al., 2017). Monitoring of *A. microscaphus* populations by Ryan et al. (2017) between 2013 and 2016 along the Gila and San Francisco River showed that toad populations were stable within those years, although local populations were vulnerable to local extirpation, mainly due to random weather events. Currently, *A. microscaphus* is considered a Species of Greatest Conservation Need in New Mexico and a state 'sensitive' species in Arizona, Nevada, and Utah (New Mexico DGF, 2006; Dodd, 2013).

The toad is found at elevations of 365-2700 m and typically occupies marginal zones or terraces, preferring mixtures of dense willow clumps and open flats or flood channels (Sweet, 1992). Toads are typically observed from February to September where they enter torpor for winter months (Schwaner and Sullivan, 2009). During the breeding

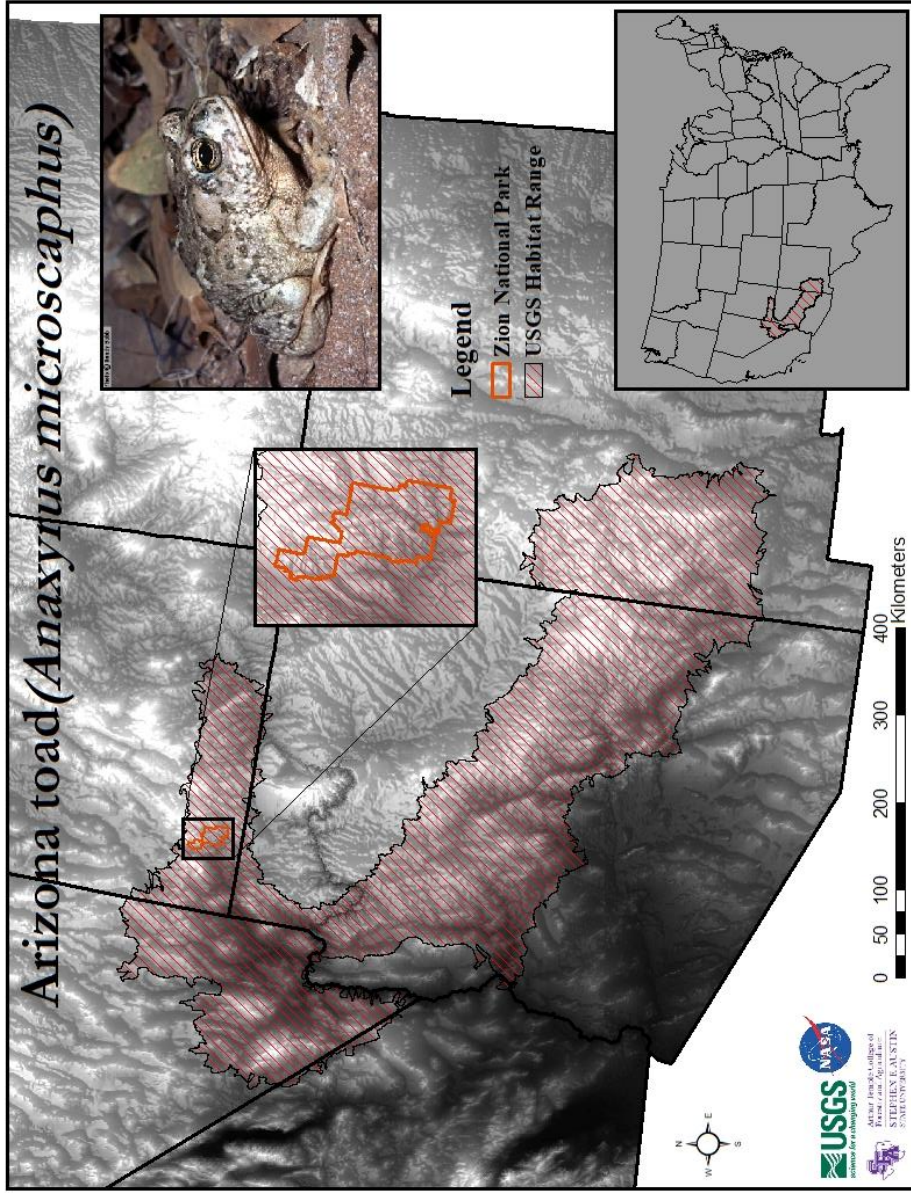


Figure 2. Location of the habitat range generated by the USGS for the Arizona toad (*Anaxyrus microscaphus*) in the states of California, Nevada, Utah, New Mexico, and Arizona. A portion of the habitat range is located inside of ZION (orange). The top-right inset displays an adult Arizona toad.

season, males begin their calling when air temperatures range anywhere from 8 to 18°C (Sullivan, 1992). Arizona toads remain close to flowing water sources during warmer months and seldom migrate further than 200 m, typically remaining within floodplain habitat (Schwaner and Sullivan, 2005). Clutch size average is around 4,500 eggs per clutch and eggs are deposited in riparian areas of streams, shallows, backwashes, and side-pools, where they hatch anywhere from 3-6 days (Blair, 1955; Schwaner and Sullivan, 2005). Under normal conditions, tadpoles require relatively shallow, slow flowing streams, and avoid faster moving water (Ryan et al, 2017).

Jones' waxy dogbane (*Cycladenia humilis* var. *jonesii*)

Jones' waxy dogbane is found in southern Utah counties (Emery, Grand, Garfield, and Kane Counties) and Northern Arizona (Figure 3), occurring at a narrow range of latitudes between 36° and 39° north (USFWS, 2008). *Cycladenia humilis* var. *jonesii* can be found at elevations ranging from 1,300-1,800 meters on side slopes or at the base of mesas, and typically within plant communities of mixed desert scrub, juniper, or wild buckwheat-Mormon tea receiving 6 to 9 inches of mean annual precipitation (Tilley et al., 2010). *Cycladenia humilis* var. *jonesii* is a long-lived herbaceous perennial in the Dogbane family and grows 10-15 cm in height (USFWS, 2008). Flowering of the plant takes place typically in April through June and produces a pink or rose-colored, trumpet shaped flower. Soil requirements are edaphic and most if not all plants are found in gypsiferous and saline soils of the Cutler, Summerville, and Chinle formations (USFWS, 2008). Often, habitat has been found on (80 to 100%) rock fragments, with shallow soils

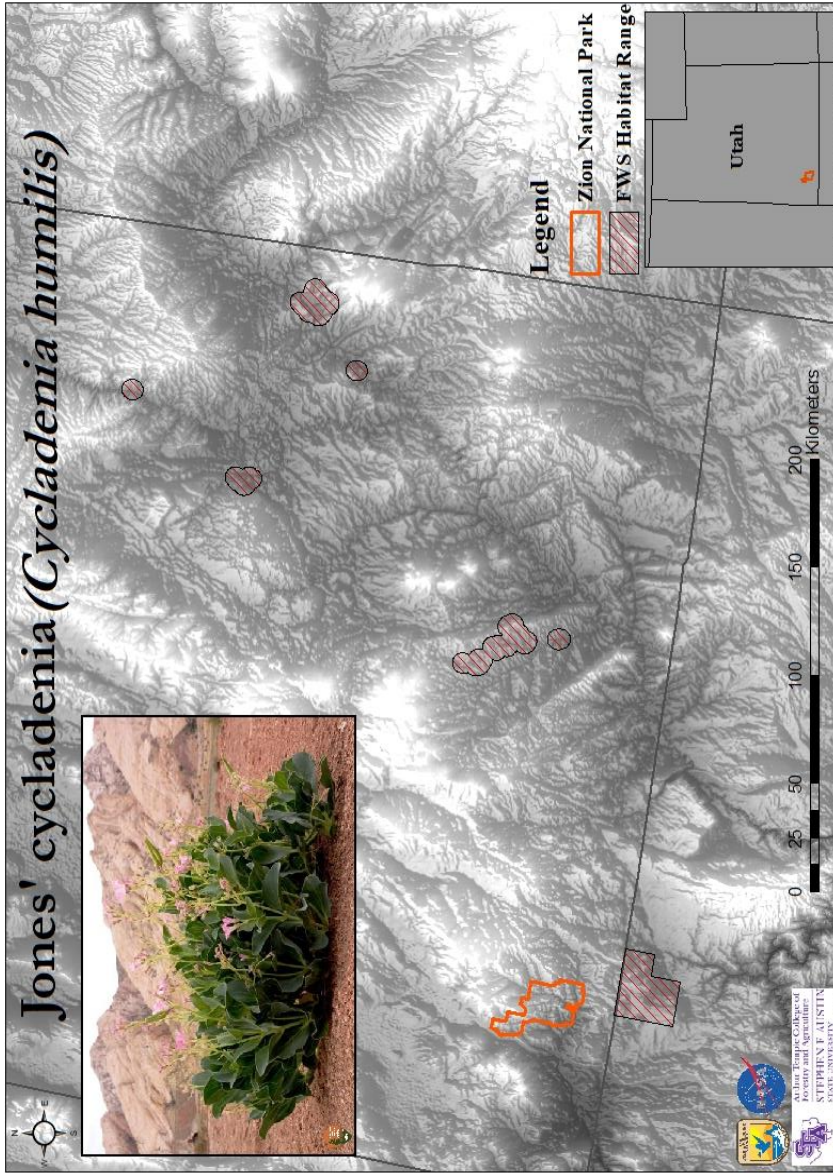


Figure 3. Location of the habitat range generated by the Fish and Wildlife Service for Jones' cycladenia (*Cycladenia humilis* var. *jonesii*) scattered throughout southeastern Utah and northern Arizona. Habitat for *C. humilis* var. *jonesii* is fragmented and is known to occur in only southeast Utah and far northern Arizona. The top-left inset displays a flowering *C. humilis* var. *jonesii*.

less than 50 cm deep (Welsh et al., 1987). *Cycladenia humilis* replicates mainly by the spreading of its rhizomes rather than by sexual reproduction, according to a study by Sipes et al. (1994), supporting the theory of a lack of active primary pollinators to the flower. It overwinters as a subterranean rhizome and is considered rhizomatous, meaning it contains a long underground stem system not viewable from the ground surface. Because *C. humilis* var. *jonesii* is a rhizomatous plant species it is made up of ramets, which is an underground system of genetically identical individuals, the colony of ramets makes up a genet (Sipes and Tepedino, 1996; USFWS, 2008).

Cycladenia humilis is a genus with three varieties currently recognized within the species: *C. humilis* var. *humilis*, *C. humilis* var. *venusta*, and *C. humilis* var. *jonesii*. *Cycladenia humilis* var. *humilis* is endemic to northern California while *C. humilis* var. *venusta* is endemic to southern California (Hickman, 1993). Results from a study by Brabazon (2015) supports the variation of *jonesii* indicates significant genetic structure, supporting a possible delineation of *jonesii* as its own distinct species apart from the two California variations. *Cycladenia humilis* var. *jonesii* was listed as a threatened species in June of 1986 with an estimated total of 7,500 known individuals in the habitat range during that time. As of 2008, there is believed to only be 1,100 individuals (Sipes and Tepedino, 1996). Threats to *C. humilis* var. *jonesii* habitat are anthropogenic in nature with disturbances including off-highway vehicle (OHV), oil and gas exploration, livestock grazing, and the threat of rising temperatures due to climate change (Welsh et al., 1987; Sipes et al., 1994). According to the recovery plan documented by FWS,

further monitoring and implementing of management plans for conservation of habitat is currently being conducted (USFWS, 2008).

Species Distribution Models

SDM or environmental niche model (ENM) is an algorithmic method for the modeling of a species habitat range based on the correlation between known occurrences and the environmental conditions of occurrence localities (Elith and Leathwick, 2009). In a Grinnellian sense, habitat modelling of an organism is adapted to tolerance zones or niches, which are considered abiotic requirements in which a species is capable of surviving within (Lorini and Vail, 2015). The utilization of species modelling has become ubiquitous in many fields, especially those of analytical biology and can be used extensively in conservation, natural resource management, ecology, evolution, and invasive-species management (McShea, 2014; Pollock et al., 2014).

Among many types of models used in mapping species range habitat, some of the more prevalently known statistical models fall under regression-based techniques, such as: generalized linear model (GLM), generalized additive models (GAM), and multivariate adaptive regression splines (Guisan et al., 2002; Elith and Leathwick, 2007). The advancement of these particular analyses pioneered the development and growth of innovative statistical methods and led to a renaissance of mechanistic models and machine learning approaches. Between the years of 1992 and 2010 the increase in published SDM related articles in ecological literature has increased from ten articles in 1992 up to 350 articles per year in 2010 (Brotons, 2014). As of 2019, the increase on

mendely.com has risen to 2,769 published articles on species distribution modelling. Increasing in popularity, with the aid of highly effective computer system machine learning techniques like those of MaxEnt, artificial neural networks (ANN), Genetic algorithm for rule set production (GARP), boosted regression trees (BRT), random forest (RF), support vector machines (SVM), and also ensemble models (Pearson et al., 2002; Phillips et al., 2006; Elith et al., 2008; Evans et al., 2011; Grenouillet et al., 2011). Many factors have contributed to the quick growth in the usage of species distribution modelling such as the expanding accessibility in occurrence databases like that of websites like International Union for Conservation of Nature (IUCN), iNaturalist, Global Biodiversity Information Facility (GBIF), Biodiversity Heritage Library, Birdlife International, or FishBase. These species occurrence databases are typically open source websites that accumulate data by use of citizen scientists, uploading species sightings to the website with exact coordinate location and additional detailed locality data. Digitization of historical museum specimens has also contributed to the expanding database collection for species occurrences.

Niche Concepts

Araujo and Guisan (2006) proposed that one of the biggest challenges and most overlooked elements of modelling species distribution is understanding and clarifying the niche concept. Recognizing the differences between a fundamental niche and realized niche is vital in comprehending the fluidity of the ever-shifting interactions with interspecific interactions (i.e. predation, competition, mutualism). A Hutchinsonian

definition of a fundamental niche is the set of all conditions that allow for a species long-term survival in the absence of competition, whereas a realized niche is a subset of the fundamental niche that the species currently occupies with the presence of competition. Chase and Leibold (2003) proposed a contrarian approach to defining a niche by excluding the idea of a fundamental niche and realized niche altogether, they stated a niche is limited by environmental factors that allows a population to reproduce at a rate that is higher than the rate of mortality. Ambiguity on what a model represents often results in misleading or inaccurate models. Soberón and Peterson (2005) supported the idea that niche models provide an approximation of the species' fundamental niche. Conversely, other researchers have supported that models are spatial representations of the realized niche (Guisan and Zimmerman, 2000; Pearson et al., 2002). Whether or not a model represents a fundamental niche or a realized niche, the condition is dependent on the parameters, variables, and algorithm representing the range in which a species occupies.

Maximum Entropy (MaxEnt)

The principle of maximum entropy was presented by Edwin Thompson Jaynes in 1957, and since has helped expand disciplines such as thermodynamics, economics, forensics, and ecology. MaxEnt software became available in 2004 and is a general-purpose statistical machine-learning algorithm for making predictions from incomplete datasets using presence-only data. MaxEnt contrasts presence data against background samples, which are often called pseudo-absences (Phillips et al., 2009). Entropy is a

concept in information theory that measures the amount of information lost when the value of a random variable is not known (Shannon, 1948). Lowering this amount of entropy is key in developing a strong model. The more background information that we have available the more entropy is lowered and the more uncertainty is reduced. Increasing the data that indicates a species is present within an environment of ecological conditions is information that will theoretically reduce the entropy within the model. Within the MaxEnt model, entropy is measured on a grid cell (raster), the grid cell is made up of pixels and within each pixel an occurrence point is either present or absent. Any pixel that contains an occurrence point would be expected to demonstrate a relatively low amount of entropy, while a pixel absent of an occurrence point would be expected to have a high level of entropy (Phillips and Dudík, 2008). Occurrence points are any coordinates denoting localities of where a particular species has been previously recorded, typically using latitude and longitude. Many of these occurrence points are derived from historical museum records or citizen science websites.

After each completion of a model, MaxEnt computes the area under the receiver operating characteristic curve (AUC) as a tool for evaluating the predicted distribution of species in a model. AUC was first developed for radar signal detection before being used in medical research field and later accepted as the standard for assessing accuracy of SDMs (Pepe, 2000; Jiménez-Valverde, 2012). Li and He (2018) proposed an approximate guide for classifying the accuracy of AUC on scale ranging from 0-1: 0.90–1.00 = excellent, 0.80–0.90 = good, 0.70–0.80 = fair, 0.60–0.70 = poor, and 0.50–0.60 = fail.

AUC values characterize the model's ability to distinguish presence records from background data.

Sample Size

Sample size in a species distribution model refers to the quantity of occurrence point data collected for a species. The effects of sample size on a model are often weakly considered in SDMs but can greatly influence the success rate of predicting suitable species habitat (Stockwell and Peterson, 2002). Depending on the rarity of the species, there is often a limit on occurrence data and exceptions must be implemented in situations dealing with low occurrence records. Model performance is known to decrease with samples sizes smaller than 15 and decrease dramatically for sample sizes smaller than five (Pearson et al., 2006; Papeş and Gaubert, 2007). With small sample sizes, outliers carry more weight in analyses, whereas more occurrence points help balance outlier effects (Wisiz et al., 2008). Also, uncertainty related to parameter estimates (e.g. means, modes, medians) decrease with an increase in sample size (Crawley, 2002). Though many model techniques are available, Hernandez et al. (2006) concluded in a study that MaxEnt is the most capable in producing useful model results with smaller sample sizes.

Variable Selection

Selection of environmental variables for SDMs should correspond with a deep ideology and understanding of the species biogeography, ecology, population dynamics and human disturbance. Careful selection of environmental variables is important in

producing a high quality, low bias model (Araújo and Guisan, 2006). MaxEnt, along with many other machine learning models can use topographic, climatic, soil, and remotely sensed variables. Yiwen et al. (2016) presents two methods for selecting environmental variables in MaxEnt. The first method consists of selecting environmental variables based from *a priori* or pre-selected ecological and biological knowledge. The second approach utilizes a reiterative process of a stepwise removal of least contributing variables, both approaches reduce overfitting and increase model accuracy.

In an article produced by Brown (2014) he outlines the use of a computer program called “SDM Toolbox”, intended to work as a platform connecting both Python and ArcGIS 10.1 (or higher). The toolbox consists of 59 scripts for use in macroecology, landscape genetics, landscape ecology, and evolutionary studies. Among the many scripts in the toolbox is the jackknifing tool, which measures variable importance and systematically excludes one environmental variable at a time when running the model. This process informs the user of variable contribution within the model while also identifying highly correlated variables.

Spatial Scale

Spatial scale, commonly referred to as spatial extent or training range, is simply the overall size of the study area in an SDM (Turner et. al, 1989). A common challenge when constructing a species model is determining the appropriate extent of the study area. Many study areas are determined by geographical or political borders, resulting in poor model calibration leading to an incomplete range of environmental conditions. This

issue can lead to errors when extrapolating beyond the training range or when using forecasting techniques for future modelling (El-Gabbas and Dormann, 2018).

A study by Williams et al. (2009) implemented a spatial scale design by producing a 50-km buffer around occurrence points using a convex hull. Likewise, Brown (2014) implements a convex hull buffer solution by buffering a set distance around the occurrence points, in most cases 50-km. This helps eliminate overfitting by reducing the spatial extent range and allows the model to select background points at only feasible areas of dispersion (Brown, 2014).

Spatial Resolution

Spatial resolution, or grain size, is the minimum unit of a pixel or cell size within a spatial grid. Studies suggest that consideration of pixel size and study extent can greatly influence SDM performance (Martes and Jetz, 2018; Morgan and Guénard, 2019). Natural environments are made up of geologic, climatic, topographic, and biological processes with varying characteristics and spatial scales. Within each of these environmental factors, species respond differently as spatial scales range from small (local) to large (global) (Morgan and Guénard, 2019).

As computing power and high spatial resolution imagery become more powerful, model performance and increasing model accuracy has proceeded. As is common with SDMs, higher computational power for finer grain size resolution is often unnecessary when modeling at larger extents. Coarser scaled models require less computational power but can pose issues with overestimation of species models when mapping out species

distribution for local scaled habitats. Understanding and considering overestimation of SDMs is important because a species' actual distribution and geographic range may be distorted at coarser scales (Jetz et al., 2007).

Advantages arise when modelling for local scale with higher grain resolution rather than coarse-resolution models. Finer grain size enhances the details of the landscape by sharpening the features and making the landscape more prominent and distinguishable (Gottschalk et al., 2011). Spatial resolutions ranging from 10-100 m can capture species distributions of features not visible at lower resolutions (1,000-10,000 m) (Morgan and Guénard, 2019). In a study conducted by Nezer et al. (2017) on the grain size effects of species distribution models of the Asiatic wild ass (*Equus hemionus*), high resolution mapping allowed for detection of four habitat components essential to the wild ass: potential movement corridors, isolated habitat patches, important topographic features, and anthropogenic effect on distribution. The study demonstrated that environmental variables such as slope and vegetation were nearly meaningless when approaching 1 km resolution and that consideration must be considered for environmental variables selection with respect to study extent (Nezer et al., 2017). In summary, fine-scale distribution models are preferred for management and conservation planning when modeling species at local scales (Hess et al., 2006).

Downscaling approaches for climate grids have only recently been introduced and accepted in climate grid construction (Wang et al., 2011; Meineri and Hylander, 2017; Morgan and Guénard, 2019). There are two known forms of downscaling: statistical and

dynamical. Dynamical downscaling utilizes regional climate models to extrapolate global climate models to a regional or local resolution (Tang et al., 2016). Statistical downscaling uses statistical relationships to predict regional or local climate grids from low resolution variables (Benestad, 2004). The Worldclim climate grids, for example, is a very well-known statistically downscaled database for climate surfaces that implements thin-plate splines with covariates that include elevation, distance to the coast, minimum and maximum land surface temperature, and cloud cover (Fick and Hijmans, 2017).

A study by Meineri and Hylander (2017) challenged the viewpoint that climate station data are inadequate for producing downscaled climate data with justifiable results. The study used data from climate stations, rather than weather data loggers, to build high resolution climate grids over a large extent. Linear models regressing the temperature against topographic variables were constructed, with thin-plate spline interpolation on the regression residuals. Topographic variables of 30 m resolution were used which included latitude, altitude, solar radiation, aspect, relative elevation, distance to sea and water body, and topographic wetness index.

Thresholds

Primarily, the output for a typical SDM is a raster that displays the probability of a species occurring in an area based on an algorithm with input data including both environmental variables and species location datasets. This representation transforms continuous results into a binary format and displays classes such as suitable, unsuitable, or marginally suitable. Binary model results are often required when assessing ecological

issues such as climate change impacts, invasive species impacts, reintroduction sites identification, and conservation planning. Selection of the threshold parameters greatly influence model outcome and thoughtful consideration should be given in determining the preferred requirements. Mismanagement of threshold selection can lead to overfitting or underfitting of a model. Overfitting occurs when a model fits the calibration data too closely in environmental or geographic space, whereas an underfit model fails to provide adequate discrimination. Both overfitting and underfitting models lead to complications when transferring the model to another region due to a lack of generality, this is known as transferability (Radosavljevic and Anderson, 2014).

The simplest technique for displaying habitat suitability was presented by Phillips and Dudík (2008); in order for an area to be considered suitable, the pixel value encompassing areas of suitability must contain a probability greater than 0.5 as 'present' and all areas below 0.5 as 'absent'. This leads to a clear distinction in determining the rate of sensitivity and specificity, where sensitivity is the percent of 'true' presences correctly classified as present in the model and specificity is the percent of 'true' absences labeled absent. Although this approach seems straight forward, it has been drawn into question based on the ratio of presences to absences in that models are seldom equal, providing bias when selecting arbitrary values such as 0.5 (Liu et al., 2005)

The lowest presence threshold was used by Philips et al. (2006), which implements the minimum predicted value for the training sites as the threshold. This technique of threshold selection is extremely sensitive to low sample sizes and should

only be used when using presence-only data. Once the threshold has been applied, model performance can be evaluated using the extrinsic omission rate, which is a percentage of test localities that fall into a pixel not predicted as suitable, and the proportional predicted area, which is a percentage of the pixels that are predicted as suitable for the species (Phillips et al., 2006) . Low omission rates are typically preferred for an above average model (Anderson et al., 2003)

Liu et al. (2005) produced one of the most well-known threshold selection methods for presence/absence data, referred to as maximizing the sum of sensitivity and specificity (maxSSS). This method is supported as valid in use with presence-only data when pseudo-absences are used instead of true absence data. This form of threshold selection considers three criteria (objectivity, equality, and discriminability). Liu et al. (2005) mathematically determined that maxSSS produced higher sensitivity, higher true skill statistic, and higher *kappa* while also supporting that maxSSS produces the same threshold using either presence/absence or presence-only data. Among other threshold selection methods tested against maxSSS include: 1) training data prevalence (trainPrev), 2) mean predicted value (meanPred), 3) mid-point between the average predicted values (midpoint), 4) maximizing *kappa* (max *kappa*), 5) maximizing overall accuracy (max OA), 6) maximizing the F measure (max F), 7) minimizing the difference between sensitivity and specificity (min DSS), 8) receiver operating characteristics (ROC), 9) minimizing the distance between the precision-recall curve and the point (min D_{11}) and 12) the predicted and observed prevalence equalization (equalPrev) (Liu et al., 2013). As

is the case with calculating sensitivity and specificity in a four-cell confusion matrix, the same technique is used when applying to SDMs. Presence-only data uses computer generated random points (pseudo-absences) rather than surveyed absence data. True presences and false absences are calculated the same as with presence/absences data, and the ‘true absences’ and ‘false absences’ are calculated using pseudo-absences (Liu et al., 2015). MaxSSS is capable of being produced in both MaxEnt and open-source R software.

Sampling Bias

Accuracy and validity of any species model is dependent upon the quality of the input data. Sampling bias artificially increases spatial autocorrelation of the localities and can lead to a model overfitting locality data in geographic space. Yackulic et al. (2013) found that 87% of MaxEnt models used occurrence data likely influenced by sample selection bias. MaxEnt models are commonly constructed on occurrence data that are spatially biased towards easily accessed or better-surveyed areas, such as roads, populated areas, or common water features (Reddy and Dávalos, 2003; Phillips et al., 2009; Ruiz-Gutierrez and Zipkin, 2011). Consequently, it is of utmost importance to be aware of inaccurate data due to the ramifications of incorrect models that in turn lead to inappropriate management decisions (Phillips et al., 2009). Beck et al. (2014) detailed that reducing spatial bias, at the loss of reduced input data, increases the predictive species models to a degree. Fortunately, sampling bias can be reduced by spatially filtering the occurrence dataset to reduce the degree of overfitting in a model. This

process considers the clustering of occurrence points within a particular radius and randomly removes the localities, reducing the overall occurrences but in return, improving model accuracy (Boria et al., 2014).

Forecasting

Forecasting has become a powerful tool for conservation practitioners and resource managers as climate change impacts ecological systems. Resource managers must constantly adapt to species shifting their distribution ranges in response to changing temperature and precipitation. Deciphering how a species will respond to patterns of land-use change allows land managers to design landscapes to better accommodate both human and non-human resource needs. Many species respond to rising temperatures by moving upward in elevation or poleward in latitude (Parmesan et al., 1999; Lenoir et al., 2008). Over the past century, global average temperatures have risen 0.6 °C with projections to rise between 1.1 and 6.4 °C in the next 100 years (IPCC 2014). Climate change has become an extremely impactful ecological manipulator as it drives alterations in hydrology, fire regimes, pathogen distribution, and distribution and cultures of human populations (Lawler et al., 2011).

Often referred to as climate-envelope models, these forecasting models can provide insight into future climate scenarios by projecting habitat suitability based on potential changes in environmental conditions. These environmental conditions are commonly composed of measured habitat attributes such as the structure of vegetation, landscape patterns, soil type, and topography (Lawler et al., 2011). A study developed by

Hijmans et al. (2005) produced 1 km² spatially interpolated climate data using thin-plate smoothing spline algorithm to compile monthly averages using weather data from the years (1950-2000). The data included in the forecast models include latitude, longitude, and elevation variables to construct climate surfaces for monthly minimum, maximum, and average temperature and precipitation. These climate surfaces are regularly used in forecasting for species distribution and are available for download at <http://www.worldclim.org>.

Future climate models are based on global climate model (GCMs), which use representative concentration pathways (RCPs), an RCP is a call to the scientific community to the request by the Intergovernmental Panel on Climate Change (IPCC) to develop a set of scenarios to facilitate the future of climate change (IPCC, 2007). An RCP is based on simulations from a set of integrated assessment models that provide scenarios on concentrations and emissions of greenhouse gases, emissions of aerosols, and associated land cover change scenarios (Arora et al., 2011). Based on Moss et al. (2008) process on RCP design criteria, the following must be contained in the design: 1) the RCP should be based on literature and contain an internally consistent description of the future; 2) the RCP should provide information on all components of radiative forcing in a geographically explicit way; 3) the RCP should have smooth transition between analyses of historical and future periods; and 4) the RCPs should cover the time period up to 2100. RCPs are based off four emission scenarios (Figure 4), a very low forcing level (RCP 2.6), two medium stabilization scenarios (RCP 4.5 and 6), and (RCP 8.5). RCP

measures of units are based on watts per square meter (W/m^2), that is, the sum of all contributing emission sources (Vuuren et al., 2011).

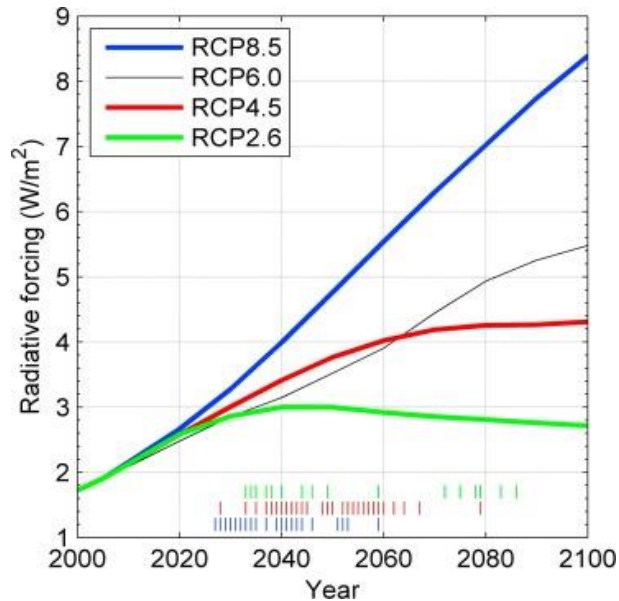


Figure 4. A demonstration of a representative concentration pathway depicting the four climate scenarios of (2.6, 4.5, 6.0, and 8.5). RCPs begin to differ from 2025-2030 and are extrapolated to the year 2100. RCP 2.6 is considered the best-case scenario while RCP 8.5 is the worst-case climate scenario.

A common RCP chosen for forecasting models is the Community Climate System Model (CCSM4). This RCP was made available to public use in April 2010 and is used by a community of scientists, national laboratories, universities, and other institutions. CCSM4 is a general circulation model consisting of atmosphere, land, ocean, and sea components that are linked by state information and fluxes between components (Gent et al., 2011). CCSM4 bioclimatic layers can be retrieved from the WorldClim website for the years 2050 and 2070 with the RCPs of (2.6, 4.5, 6.0, and 8.5).

METHODS

Study Area

The primary study area was focused in Zion National Park, located in southwestern Utah. ZION has an area of 601.81 km² within the boundaries of the park (Figure 5). All proceeding MaxEnt models, excluding the forecasting models, were used to project SDMs into the ZION boundary. A workflow for data collection was constructed to display the steps taken before model execution and analysis (Figure 6).

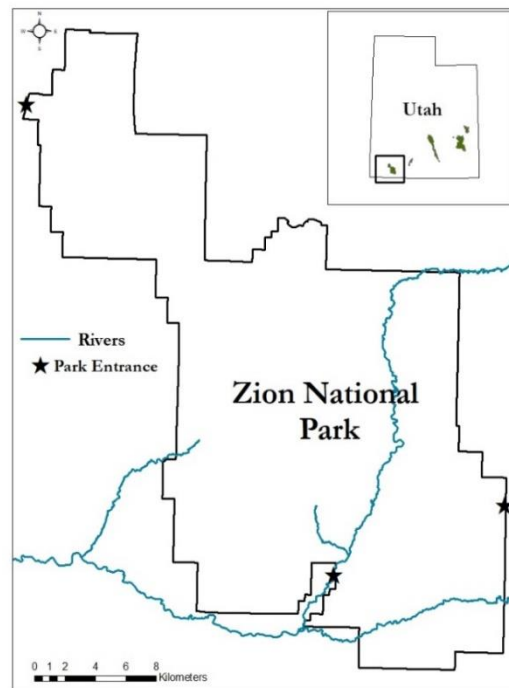


Figure 5. ZION is the study area for the SDMs created for *A. microscaphus* and *C. humilis* var. *jonesii*. The inset in the top right displays the five national parks found within

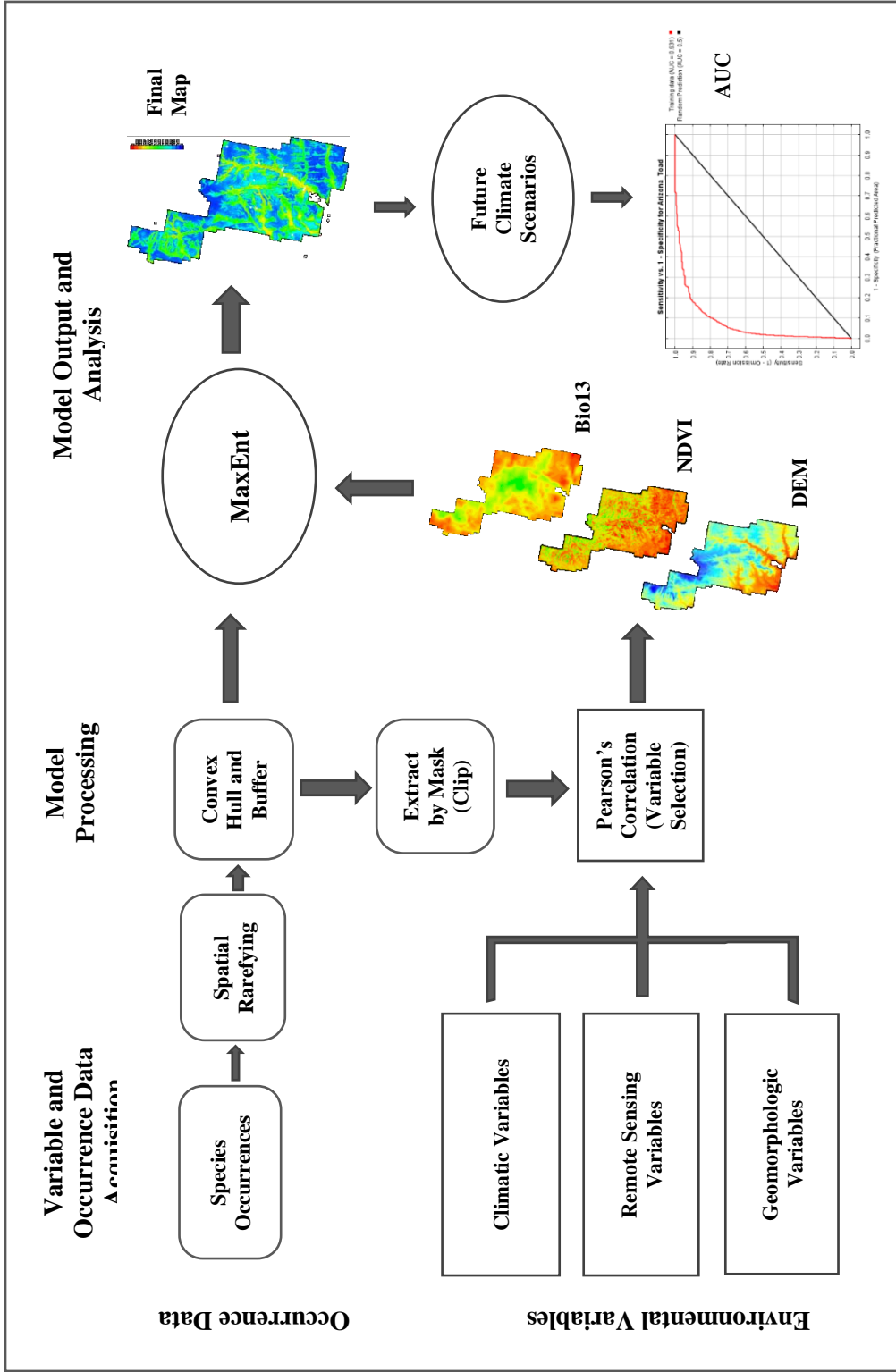


Figure 6. Flow chart displaying the procedures in creating the proper parameters from start to finish for use within the MaxEnt model for both study species.

Occurrence Data

Occurrence data were obtained using the Global Biodiversity Information Facility (GBIF) (<https://www.gbif.org/>), the largest online open source provider of distribution records. To prepare the coordinate data for the model, the occurrence points were downloaded to an Excel sheet and were subjected to data cleaning (i.e. duplicate removal and extreme outlier removal). After acquiring occurrence data for *A. microscaphus*, a spatial filtering process was executed to reduce spatial autocorrelation. Filtering was not done for *A. humilis* due to the limited amount of occurrence points available for modeling, a total of 16 localities (Pearson et al., 2006; Papeş and Gaubert, 2007). Spatial filter was completed by removing localities within a 30 km radius of one another. The spatial filtering step was performed using the SDMtoolbox with the tool ‘Spatially Rarefy Occurrence Data’ (Brown, 2014). Of the 327 occurrence points for *A. microscaphus*, 87 rarified occurrence localities were used in analyses.

Data Acquisition

Digital Elevation Model Acquisition

Digital elevation model (DEM) rasters were obtained from the NASA Earthdata website (<https://earthdata.nasa.gov/>) and mosaiced together using ESRI ArcMap 10.6.1 to form a master DEM. The master DEM was responsible for creating topographic environmental variables for the model. North America Albers Equal Area Conic was chosen as the projected coordinate system for creating environmental variables for both study species, due to the regional scale of the model training area extent.

Remote Sensing Acquisition

Data acquisition for the remote sensing aspect of the environmental variables were acquired using the USGS website (<https://earthexplorer.usgs.gov/>). The scenes collected were atmospherically corrected by ordering the level two Landsat satellite imagery. Landsat scenes were chosen and date back to a time frame that correlates with average temperature, which coincides positively during breeding seasons for *A. microscaphus* and flowering months for *C. humilis* var. *jonesii*. Imagery for *A. microscaphus* used Landsat 7 imagery with <5% cloud cover with dates ranging in May 2002. Remote sensing covariates for both target species used normalized difference vegetation index (NDVI), for characterizing various aspects of vegetation growth, and bare soil index (BSI), to characterize areas of bare soil. *C. humilis* var. *jonesii* used Landsat 5 imagery with <5% cloud cover and included scenes taken from May of 2009.

Climatic Data Acquisition

Climate data rasters were downloaded from the WorldClim website <https://www.worldclim.org/data/index.html> at a 30 second resolution, roughly 1 km² at the equator, but varying resolution in the desert southwest at ~ 800 km². WorldClim climate data were extracted from global weather stations ranging from (1970-2000). The 19 variables (Table 1) represent annual trends and included the following: annual mean temperature (BIO1), mean diurnal range (BIO2), isothermality (BIO3), temperature seasonality (BIO4), max temperature of warmest month (BIO5), min temperature of coldest month (BIO6), temperature annual range (BIO7), mean temperature of wettest

quarter (BIO8), mean temperature of driest quarter (BIO9), mean temperature of warmest quarter (BIO10), mean temperature of coldest quarter (BIO11), annual precipitation (BIO12), precipitation of wettest month (BIO13), precipitation of driest month (BIO14), precipitation seasonality (BIO15), precipitation of wettest quarter (BIO16), precipitation of driest quarter (BIO18), and precipitation of coldest quarter (BIO19).

Table 1. List of the 19 bioclimatic variables taken from the WorldClim database and used for analysis within the target species' SDMs. Pearson's correlation test was first used to eliminate highly correlated variables with topographic and remotely sensed variables.

BIO1	Annual Mean Temperature
BIO2	Mean Diurnal Range
BIO3	Isothermality
BIO4	Temperature Seasonality
BIO5	Max Temperature of Warmest Month
BIO6	Min Temperature of Coldest Month
BIO7	Temperature Annual Range
BIO8	Mean Temperature of Wettest Quarter
BIO9	Mean Temperature of Driest Quarter
BIO10	Mean Temperature of Warmest Quarter
BIO11	Mean Temperature of Coldest Quarter
BIO12	Annual Precipitation
BIO13	Precipitation of Wettest Month
BIO14	Precipitation of Driest Month
BIO15	Precipitation Seasonality
BIO16	Precipitation of Wettest Quarter
BIO17	Precipitation of Driest Quarter
BIO18	Precipitation of Warmest Quarter
BIO19	Precipitation of Coldest Quarter

Environmental Variable Justification

Digital Elevation Model

The digital elevation model was chosen to represent the elevation for each species preferred habitat (Figure 7). All proceeding variables were created using ArcMap 10.6.1.

Slope

The slope and steepness of a region significantly influences runoff, especially in mountainous areas like ZION. *Cycaldenia humilis* var. *jonesii* is known to reside on barren gypsiferous clay hills that form sides and lower slopes (USFWS, 1986).

Alternatively, *A. microscaphus* is commonly found in areas with little to no slope, although the toad prefers breeding and egg deposition in lightly flowing water (Ryan et al., 2017). Slope (Figure 8) was constructed using the master DEM by calculating the maximum rate of change from the target cell and the eight surrounding neighbors in the raster.

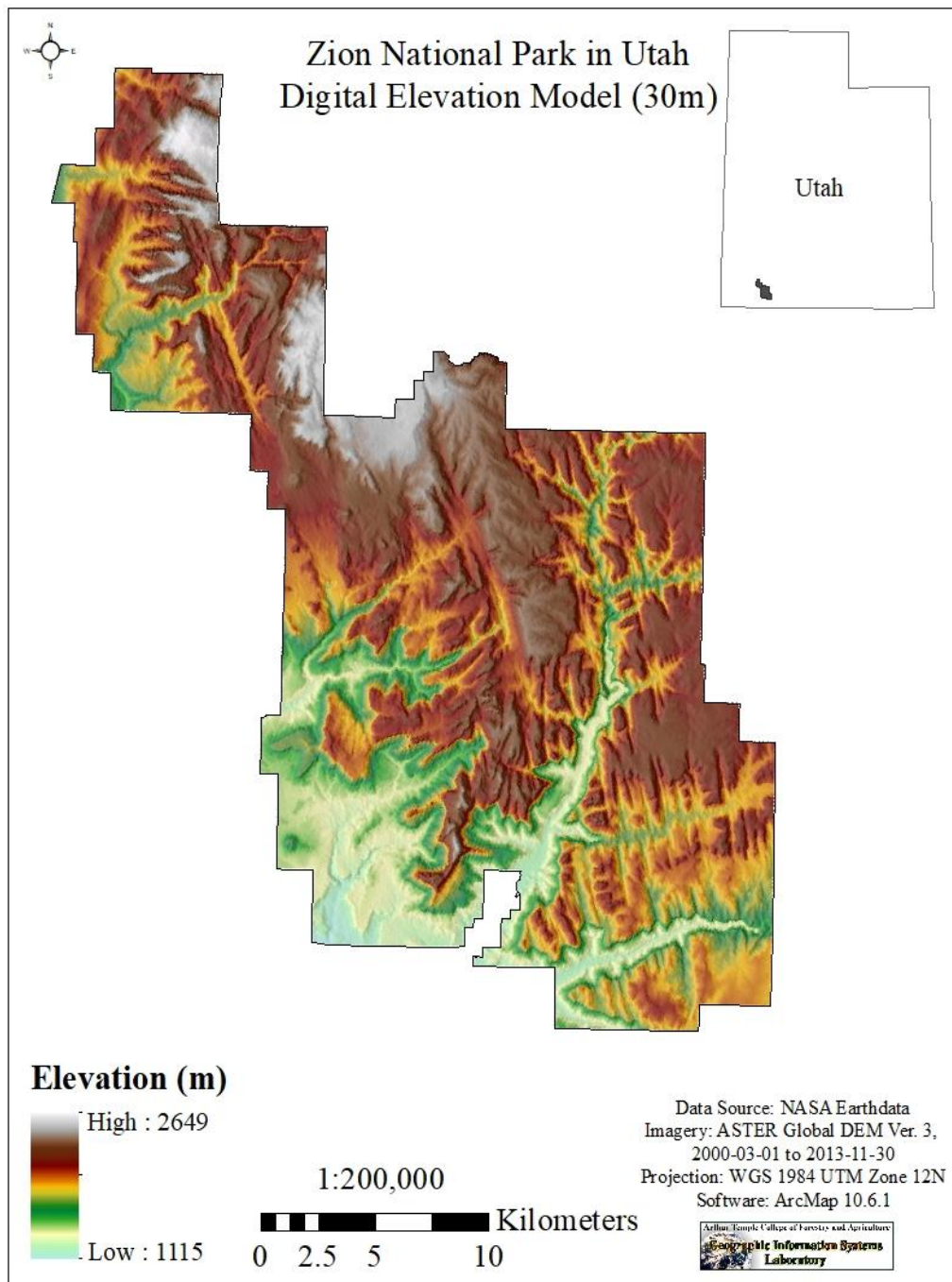


Figure 7. Digital elevation model for ZION at 30 m resolution.

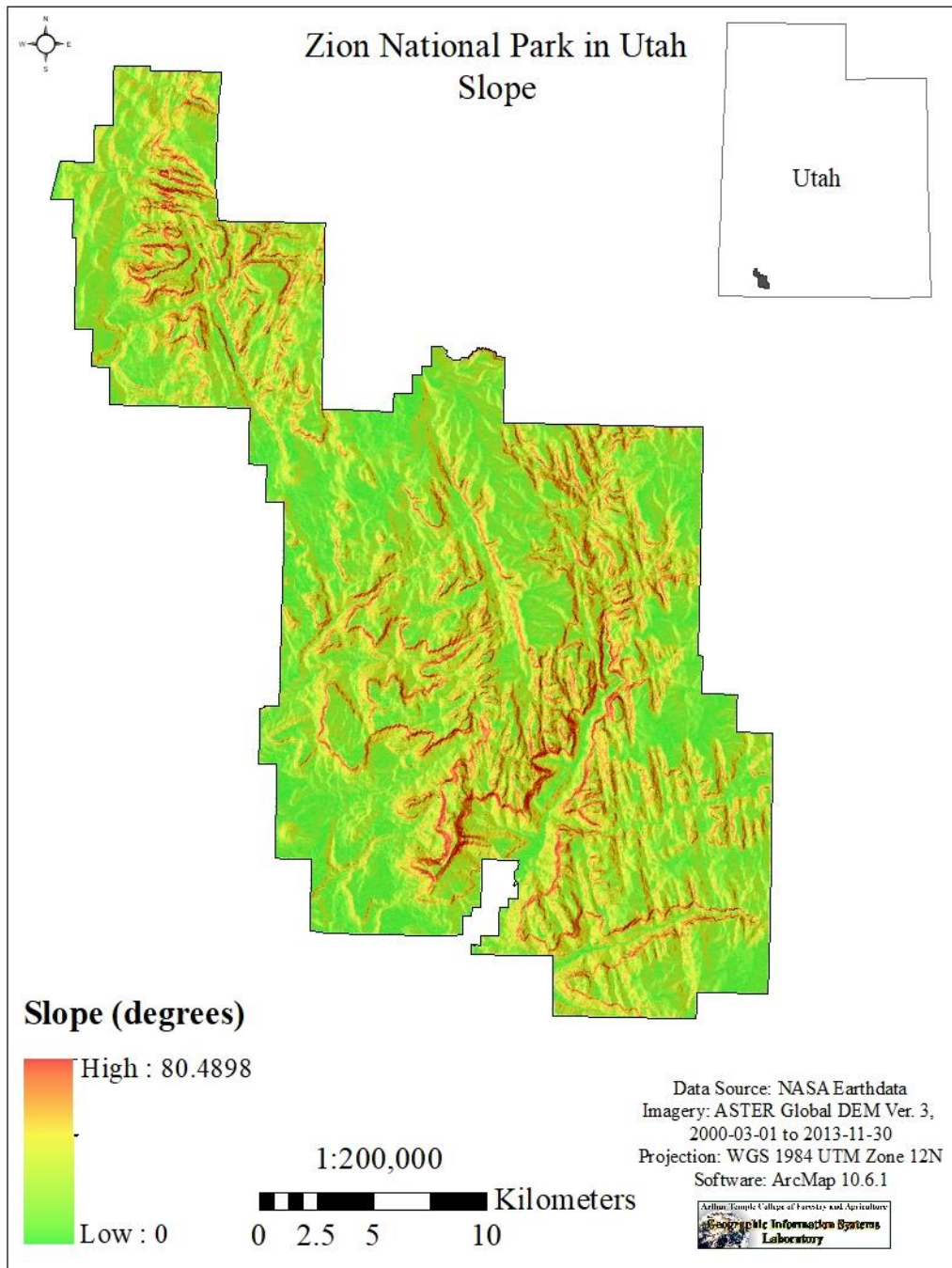


Figure 8. Slope derived from the original DEM for ZION at 30 m resolution.

Aspect

Anaxyrus microscaphus prefers habitat in valley bottom or areas with high canyon walls surrounding streams and rivers. This habitat could be influenced by solar exposure and a more southern facing valley could present preferred habitat for the toad. *C. humilis* var. *jonesii* prefers areas with moderate slopes, although there is no literature on preferred directional facing slopes. Surface temperatures between north- and south-facing slopes can vary by 20°C, which is equivalent to 2000 km change in latitude (Scherrer and Körner, 2010). Aspect (Figure 9) measures the direction the downhill slope faces and was constructed using the master DEM as the input data.

Terrain Ruggedness Index

Terrain Ruggedness Index (TRI) expresses the difference in elevation from the center cell and the eight cells directly surrounding it. The differences are then squared and averaged, the square root of this average results in the TRI for that cell (Riley et al., 1999). TRI was calculated and built (Figure 10) using the Vector Ruggedness Measure tool developed by Sappington et al. (2007).

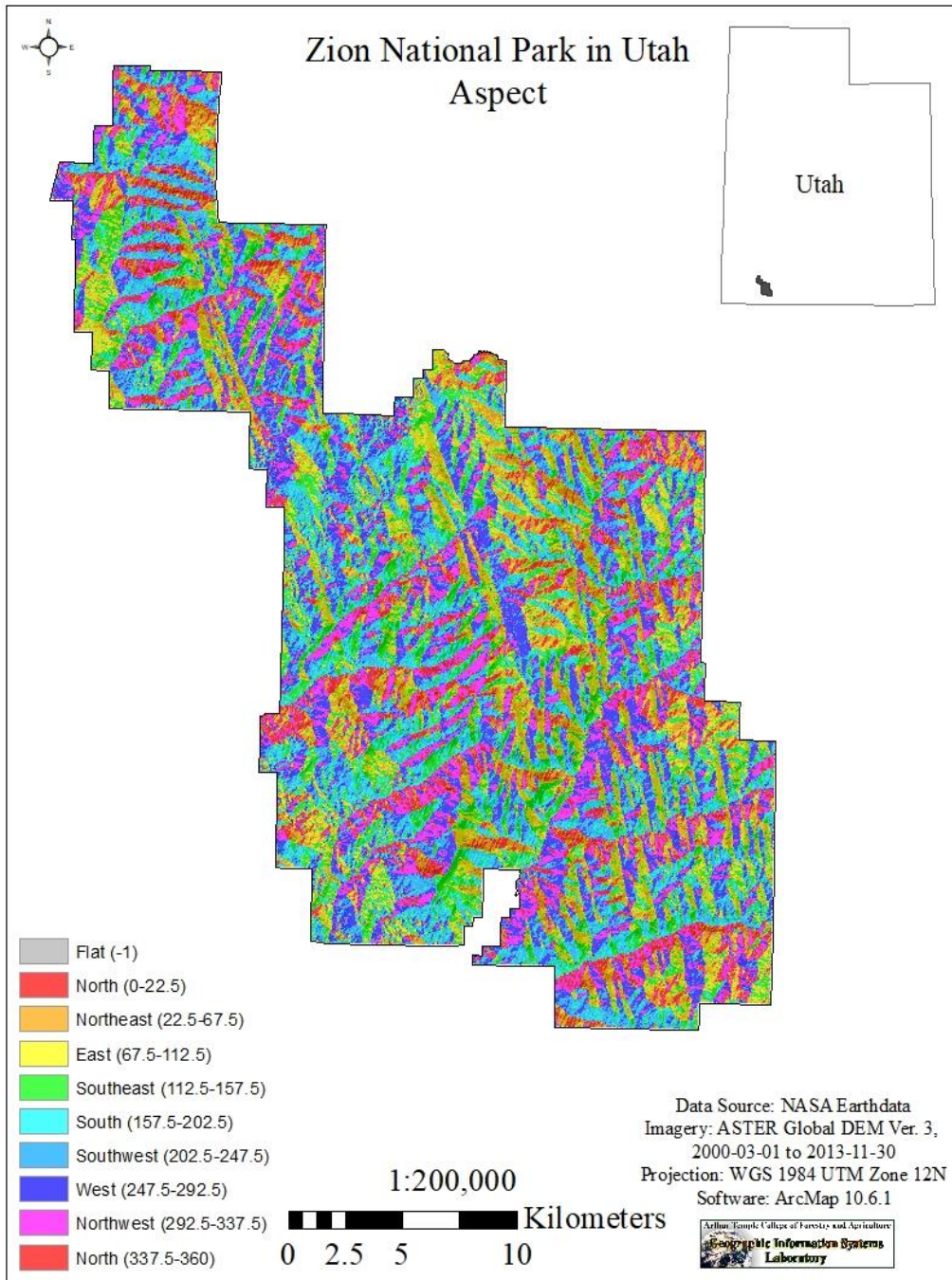


Figure 9. Aspect derived from the original DEM for ZION at 30 m resolution.

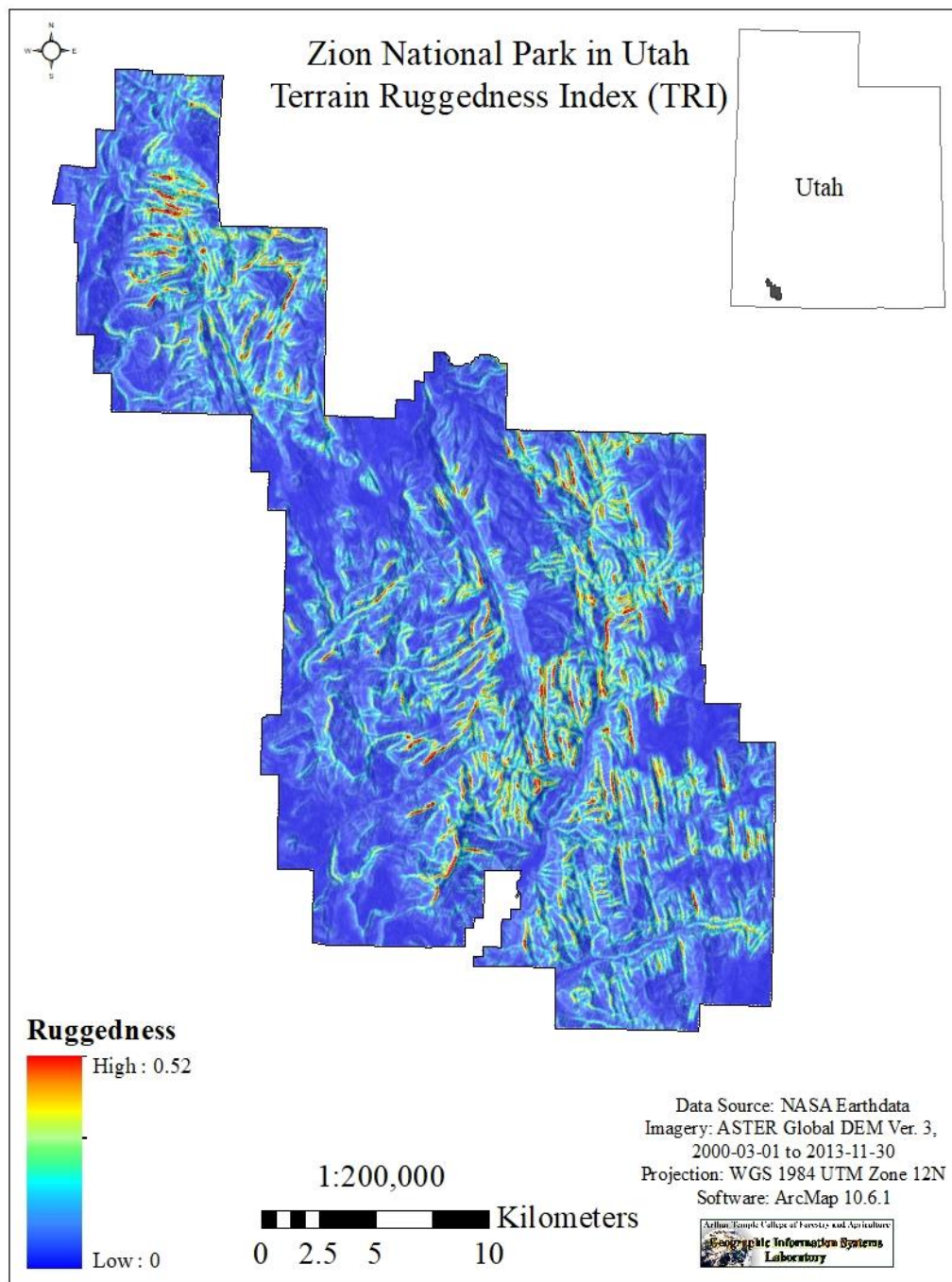


Figure 10. Terrain ruggedness index derived from the original DEM for ZION at 30 m resolution.

Topographic Position Index

Topographic position index was chosen for *A. microscaphus* to represent valley bottoms which typically display a high probability of habitat suitability due to the likelihood of alluvial accumulation and stream presence. TPI was calculated by the using difference between a cell elevation value and the average elevation of the surrounding neighborhood of the cell. TPI variables were created (Figure 11) using the Land Facet Corridor Analysis version 1.2.605 toolbox (Jenness, 2006).

Normalized Difference Vegetation Index

NDVI was chosen because it quantifies vegetation along riparian areas where *A. microscaphus* spends the majority of their life cycle near (Sweet, 1992). Additionally, *C. humilis* var. *jonesii* has been observed in various plant communities (Tilley et al., 2010).). NDVI (Figure 12) was calculated by obtaining temporally relevant Landsat imagery and using the near-infrared and red color bands to generate an image displaying vegetation abundance.

Bare Soil Index

Bare soil index (BSI) was selected to quantify the localities inhabiting terrain displaying a lack of vegetation. BSI relies on the short-wave infrared and red spectral bands to quantify soil mineral composition while the blue and near infrared bands display vegetative density. BSI environmental variables (Figure 13) were created using the 'Raster Calculator'.

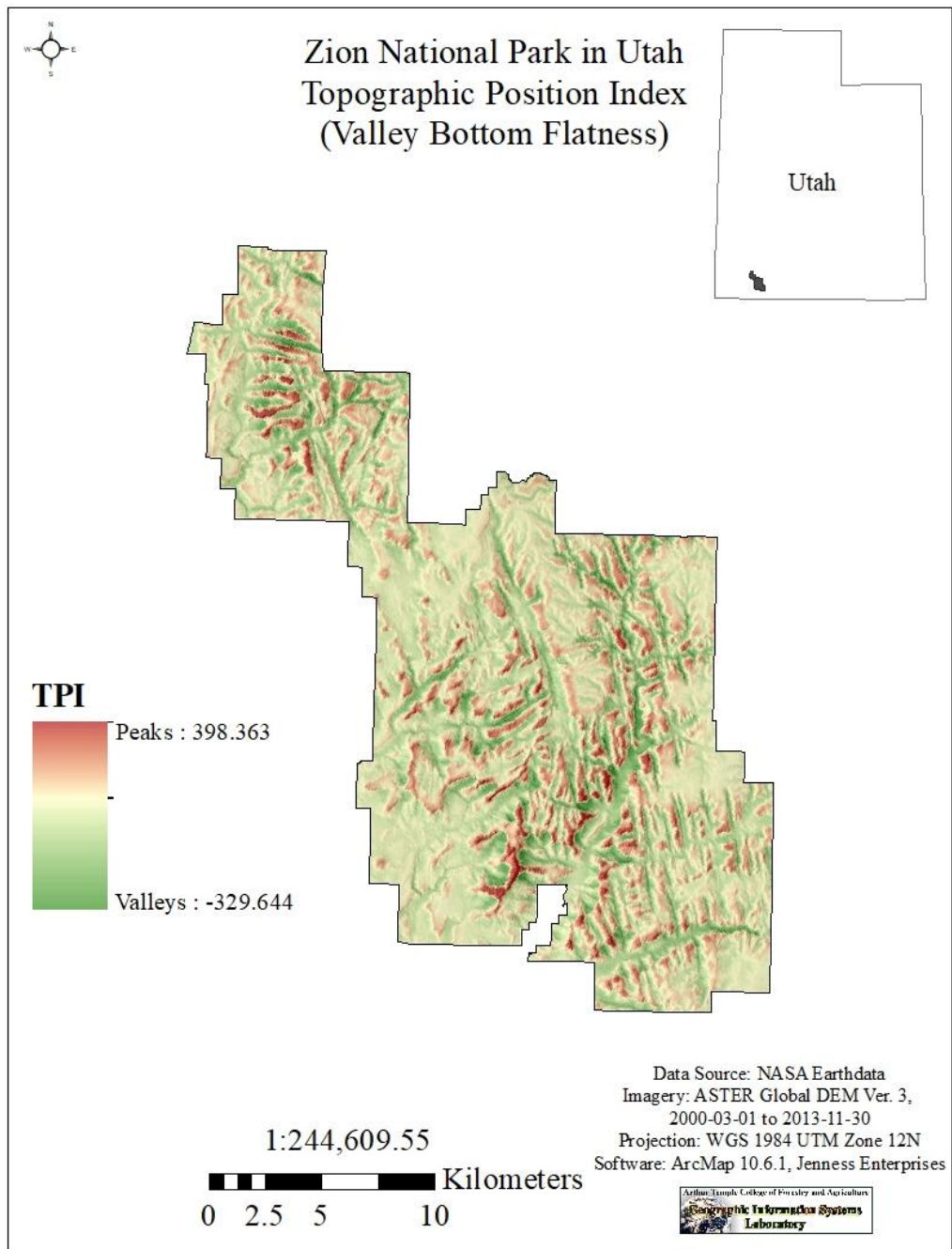


Figure 11. Topographic position index derived from the original DEM for ZION at 30 m resolution. This variable describes the valley bottom flatness in green and higher elevation peaks in the red.

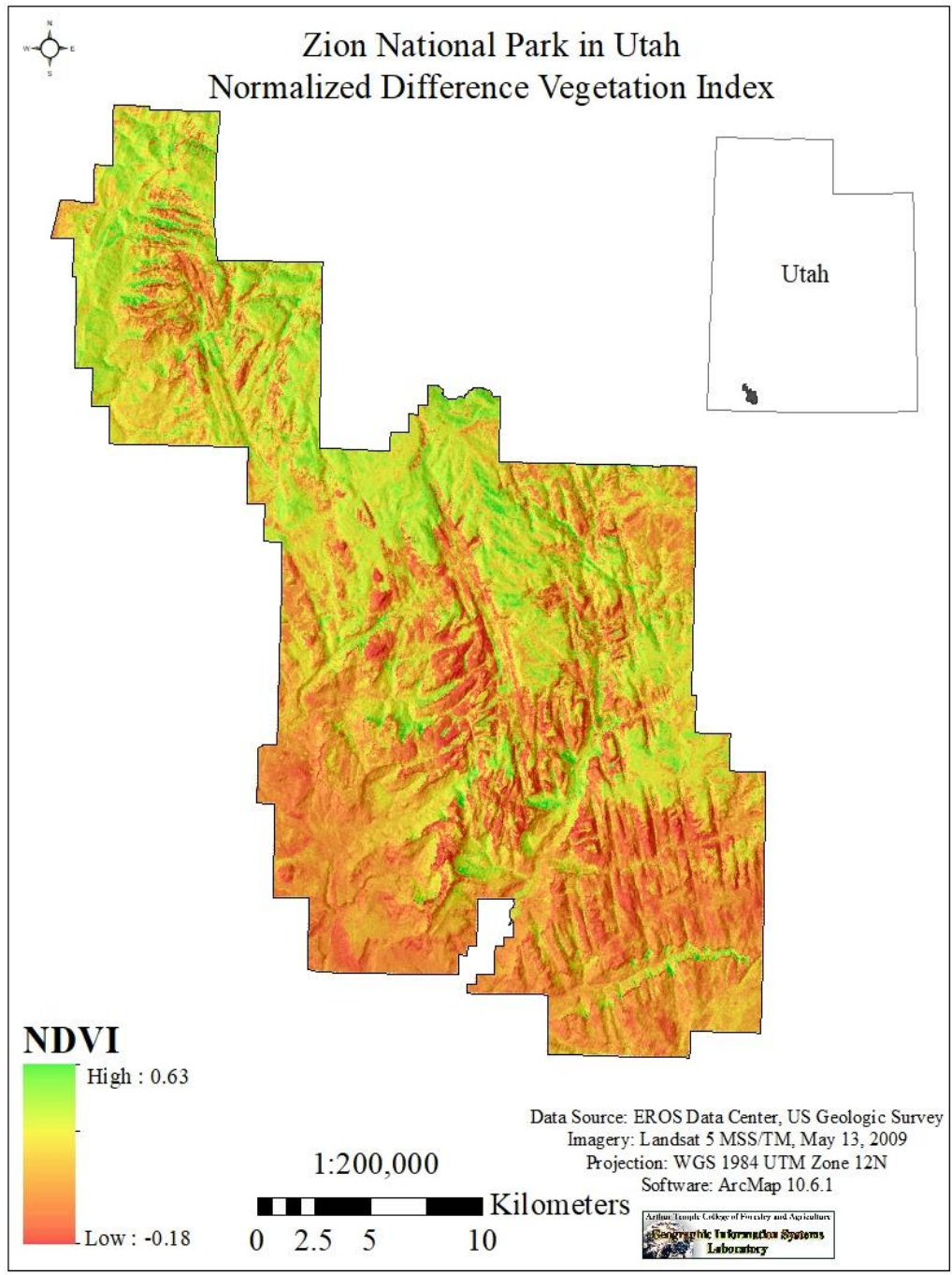


Figure 12. Normalized difference vegetation index derived from Landsat 5 satellite imagery for ZION at 30 m resolution. Green represents vegetation in this map and red represents lack of vegetation.

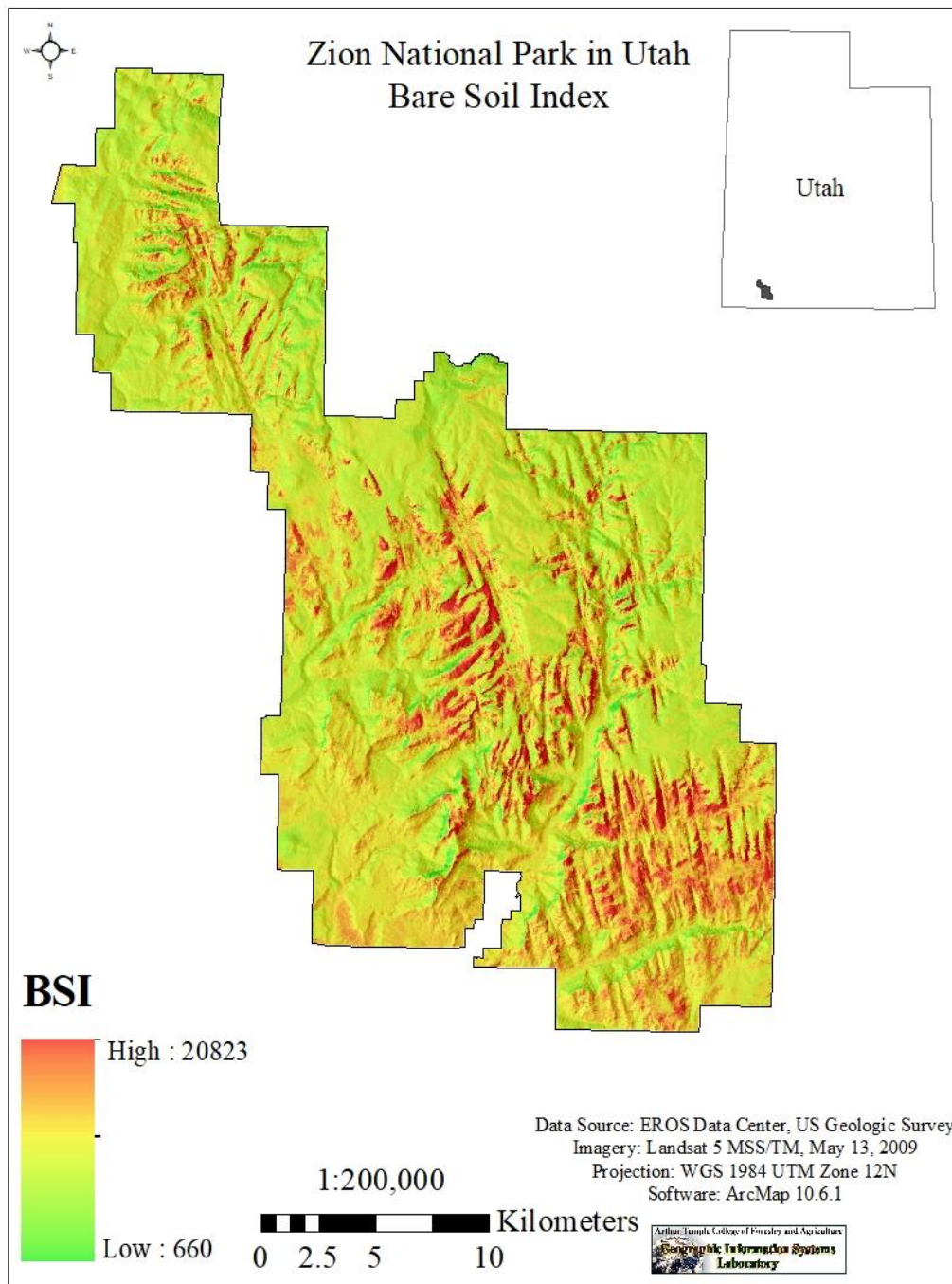


Figure 13. Bare soil index derived from Landsat 5 satellite imagery for ZION at 30 m resolution.

Variable Selection

Environmental variables for both *A. microscaphus* and *C. humilis* var. *jonesii* were constructed using the *a priori* process followed by removal of highly correlated variables using Pearson’s correlation coefficient. To adjust for multicollinearity, covariates displaying a high correlation above 0.9 were excluded from the model (Table 2). Within SDM Toolbox v2.4 in ArcMap, all the topographic, remotely sensed, and climate layers were inserted into the ‘Remove Highly Correlated Variables’ in ASCII file format. To reduce computational issues, the rasters were first resampled to a coarser scale.

Table 2. Results from Pearson’s correlation coefficient used to quantify correlation among environmental variables. Resulting variables were used to train the model within MaxEnt.

<i>Anaxyrus microscaphus</i>	<i>Cycladenia humilis</i> var. <i>jonesii</i>
BIO1 Annual Mean Temperature	BIO1 Annual Mean Temperature
BIO2 Mean Diurnal Range	BIO4 Temperature Seasonality
BIO3 Isothermality	BIO6 Min Temperature of Coldest Month
BIO15 Precipitation Seasonality	BIO9 Mean Temperature of Driest Quarter
BIO19 Precipitation of Coldest Quarter	BIO13 Precipitation of Wettest Month
Digital Elevation Model	BIO15 Precipitation Seasonality
Slope	BIO17 Precipitation of Driest Quarter
Aspect	Digital Elevation Model
Topographic Position Index	Slope
Normalized Difference Vegetation Index	Aspect
Bare Soil Index	Normalized Difference Vegetation Index
	Bare Soil Index

Model Parameters

Spatial Scale

The training extent for both species was determined by constructing a convex hull fitted to the spatially filtered occurrence points followed by a 50 km buffer around the hull. The hull is a perimeter that is fitted around the most outside group of points. The convex hull was generated in ArcMap 10.6.1 using the 'convex hull' tool followed by a buffer around the hull. The 50 km buffer allowed adequate background data to be sampled outside the known habitat of each species (Figures 14 & 15). The hull was then used to clip proceeding environmental variable rasters using the same extent, coordinate system, pixel count, and resolution. Although the training extent is outside of ZION, it was still used to train the model, in which case MaxEnt then projected the species distribution for both species into ZION using the training extent.

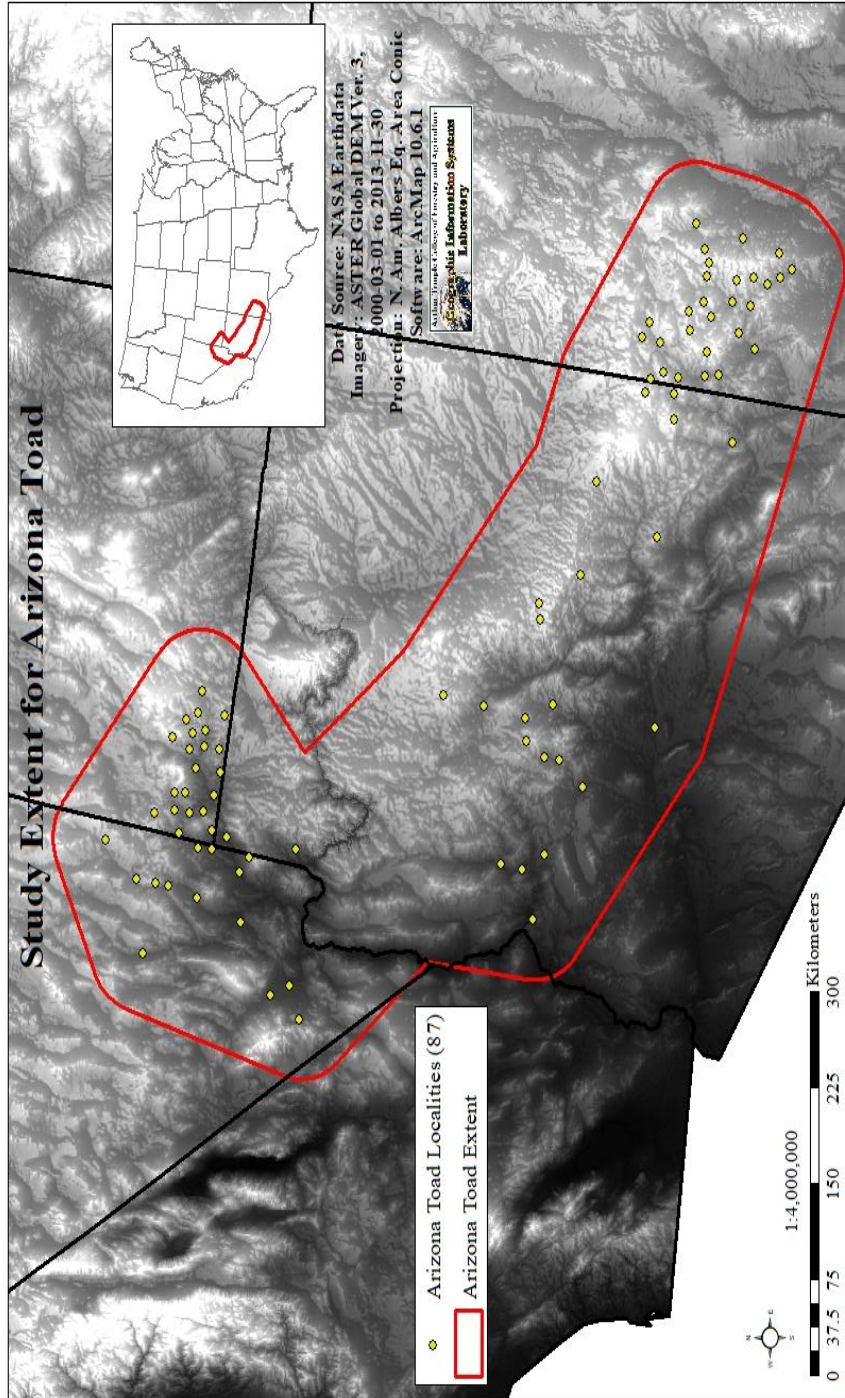


Figure 14. The model training for *A. microscaphus* was determined by constructing a 50 km buffer around the occurrence points obtained from GBIF.org. Of the 327 occurrence points, 87 points remained after spatial rarefying which were used to train the MaxEnt model. Occurrence localities used inside and outside of ZION were used to train the SDMs.

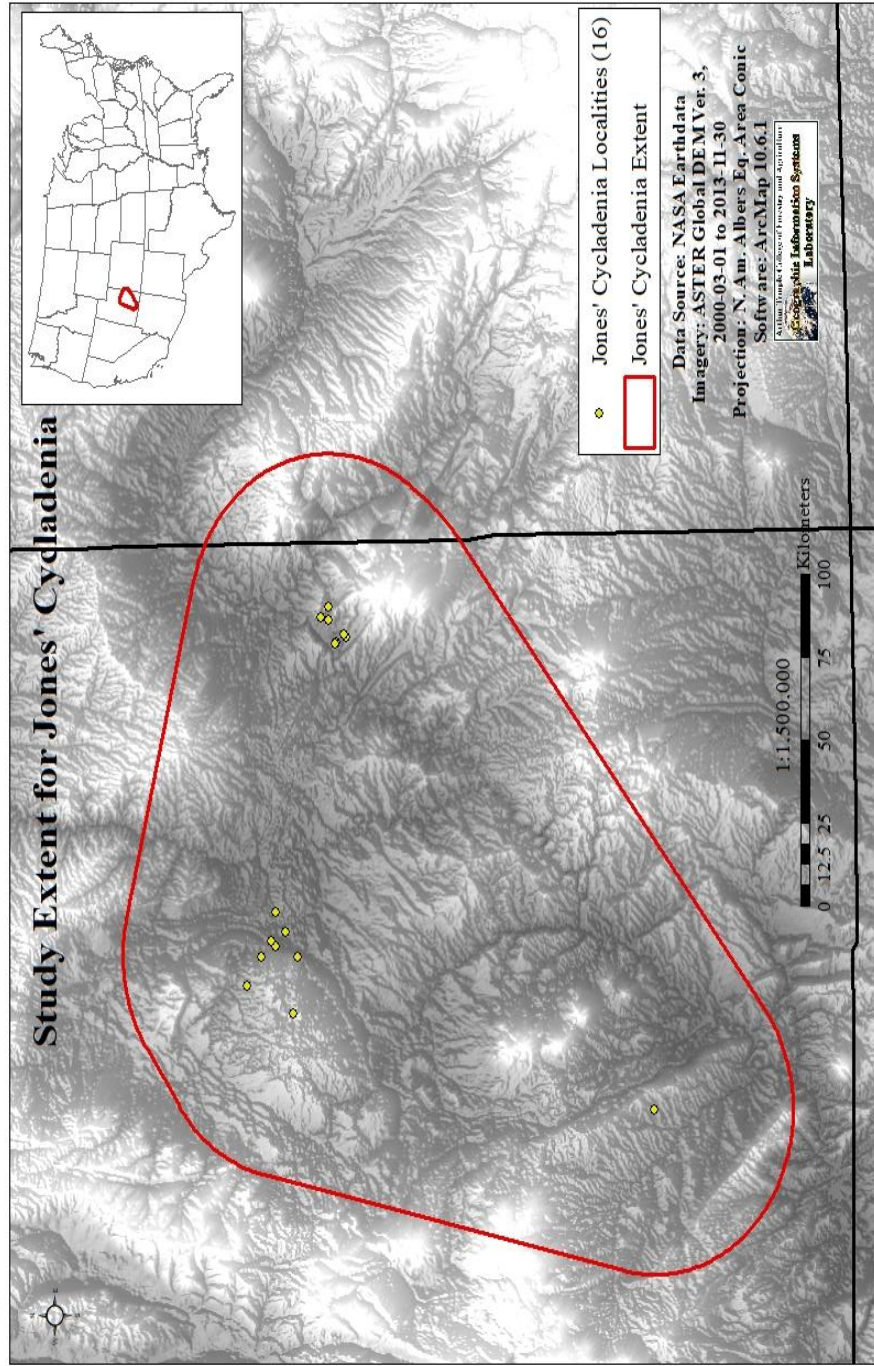


Figure 15. The model training extent was determined by constructing a 50 km buffer around the occurrence points obtained from GBIF.org. Spatial rarefying was not conducted on the occurrence points for *C. humilis* var. *jonesii* due to the low volume of occurrence localities.

Spatial Resolution

The resolution for the environmental variable rasters were constructed using both 30 m and 900- m spatial resolutions. Topographic and remotely sensed covariates had a predetermined spatial resolution of 30 m grain size and do not need further modifications to meet grain size requirements. To create the 900 m topographic and remotely sensed environmental variables, the 30 m resolution environmental variables were upscaled in ArcMap to 900 m using cubic convolution.

In order to downscale climate data, the ‘R’ package MACHISPLIN was used to interpolate Worldclim climate grids to 30 m spatial resolution through a machine learning ensemble approach that used six algorithms: boosted regression trees, neural networks, generalized additive model, multivariate adaptive regression splines, support vector machines, and random forests (Hutchinson and Xu, 2013). The ensemble model approach applied climate-forcing covariates of DEM, slope, aspect, and topographic wetness index. Thin plate spline geographic interpolation was then used with the residuals for smoothing of the climate rasters. Final r^2 values and weighted model algorithms used in the ensemble model were then displayed as an output from the MACHISPLIN package (Table 3).

MaxEnt Calibration

Preconditioned settings were applied to MaxEnt to ‘cross-validate’ all replicates for *C. humilis* var. *jonesii*, meaning the 16 occurrence points were divided into subsections and each iteration used different occurrence points per iteration to avoid

duplicates (Phillips, 2017). The ‘bootstrap’ method was chosen for *A. microscaphus* to account for larger sample size. MaxEnt used 25% of localities for testing (Phillips, 2017). MaxEnt used cloglog to provide output species maps that ranged from zero to one, with zero being least suitable and one being most suitable. A total of five iterations were used to build each model, with the average of the five iterations being the final output.

Table 3. The MACHISPLIN package results for the climate variables downscaled to 30 m resolution and the r^2 values associated with each layer. Results are based off an ensemble approach using six algorithms. Independent variables used in the approach include elevation, slope, aspect, and topographic wetness index.

Variable	01	02	03	04	05
Best Model	br	b	b	mr	b
Weight	76.3:23.7	100	100	25.3:60.2:14.5	100
R²	0.996	0.888	0.870	0.986	0.992
Variable	06	07	08	09	10
Best Model	b	b	br	bmr	br
Weight	100	100	69.4:30.6	52.4:17.8:168.8:13.1	80:20
R²	0.966	0.920	0.926	0.996	0.888
Variable	11	12	13	14	15
Best Model	br	mr	b	bmr	b
Weight	80.5:19.5	33.5:42.9:23.6	100	61.3:21.5:17.2	100
R²	0.870	0.986	0.992	0.966	0.920
Variable	16	17	18	19	
Best Model	b	bv	bm	b	
Weight	100	88.4:11.6	79.4:20.6	100	
R²	0.926	0.996	0.888	0.870	

*Letters depict the model algorithms: b = boosted regression trees, g = generalized additive model, m = multivariate adaptive regression splines, v = support vector machines, r = random forests, n = neural networks

Model Performance

30-m and 900-m Current Models

Habitat suitability rasters were divided into 5 classes by reclassifying the pixel values in ArcMap and then assigning each pixel group to its suitability class. Suitability classes ranged from 0-100%, with 0-20% being the least likely habitat suitability and 80-100% being the most likely suitable habitat. Output rasters for the 30 m suitability maps calculated the area of ZION at 601.81 km² while 900 m maps calculated at 604.26 km². The shapefile used to extract the boundaries of ZION had an area of 601.81 km² so no discrepancies should have resulted due to inadequacies in measurement tools. Differing cell resolution in rasters will result in both outputs being slightly dissimilar due to the clip of the raster not having similar spatial extent and cell size. Many of the occurrence points occur outside of ZION, therefore, the projection feature in MaxEnt interface was used to map the habitat distribution for the target species within the park boundaries. Response curves and percent permutation for each variable were also chosen as an output in the MaxEnt settings to display model analyses. MaxEnt outputs for both *A. microscaphus* and *C. humilis* var. *jonesii* were calculated statistically by using the area under the receiver operating characteristic curve (AUC) to quantify strength of model.

Model Forecasting

Future climate scenario SDMs were based on representative concentration pathways (RPCs) involving two emission scenarios, 2.6 W/m² and 8.5 W/m², for the years 2050 and 2070. The Community Climate System Model version 4 (CCSM4) is the

climate model used for forecasting, it is composed of four models simultaneously simulating the earth's atmosphere, ocean, land surface, and sea-ice. The forecasting models used the same environmental variables as previously mentioned (See Table 2) but removed remotely sensed variables (NDVI and BSI). Remotely sensed variables were excluded from both models due to uncertainty in vegetation and bare soil abundance for future climates. Spatial resolution for the future climate data will be 30 second (900 m²) spatial resolution, the finest resolution available within the WorldClim database. ZION and the MaxEnt training extent (see Figures 14 & 15) were modeled for both species to observe larger shifts in habitat suitability. The extent for *A. microscaphus* has a training extent of 233,078 km². *Cycladenia humilis* var. *jonesii* has a training extent area of 35,923 km². In addition, ZION boundary forecasting models were also created for future SDMs. To keep analysis consistent, the '10 percentile training presence' was used as the threshold to delimit suitable habitat against unsuitable habitat for each model (Escalante et al., 2013). This threshold excludes all regions with habitat suitability lower than the suitability values for the lowest 10% or occurrence records MaxEnt was used to compare the differences between current day suitable habitat and the 2.6 and 8.5 W/m² scenarios.

RESULTS

Model Performance

Anaxyrus microscaphus was recorded at 0.853 for training data AUC and 0.810 for test data AUC (Figure 16). *Cycladenia humilis* var. *jonesii* returned an AUC value of 0.796 for training data and 0.715 for testing data (Figure 17). Both models displayed good predictive power with AUC for test data ranging above the 0.7 threshold and much higher than 0.5, which represents a model that is no better than random. Percent contribution to the model, based on permutation importance, showed that annual mean temperature, elevation, and isothermality were the most contributing environmental variables for *A. microscaphus* (Table 4 & Figure 18). Precipitation seasonality, NDVI, and isothermality were the leading contributing environmental variables for *C. humilis* var. *jonesii* (Table 5 & Figure 19). Maps displaying low against high habitat suitability were created for both target species within ZION (Figures 20 & 21).

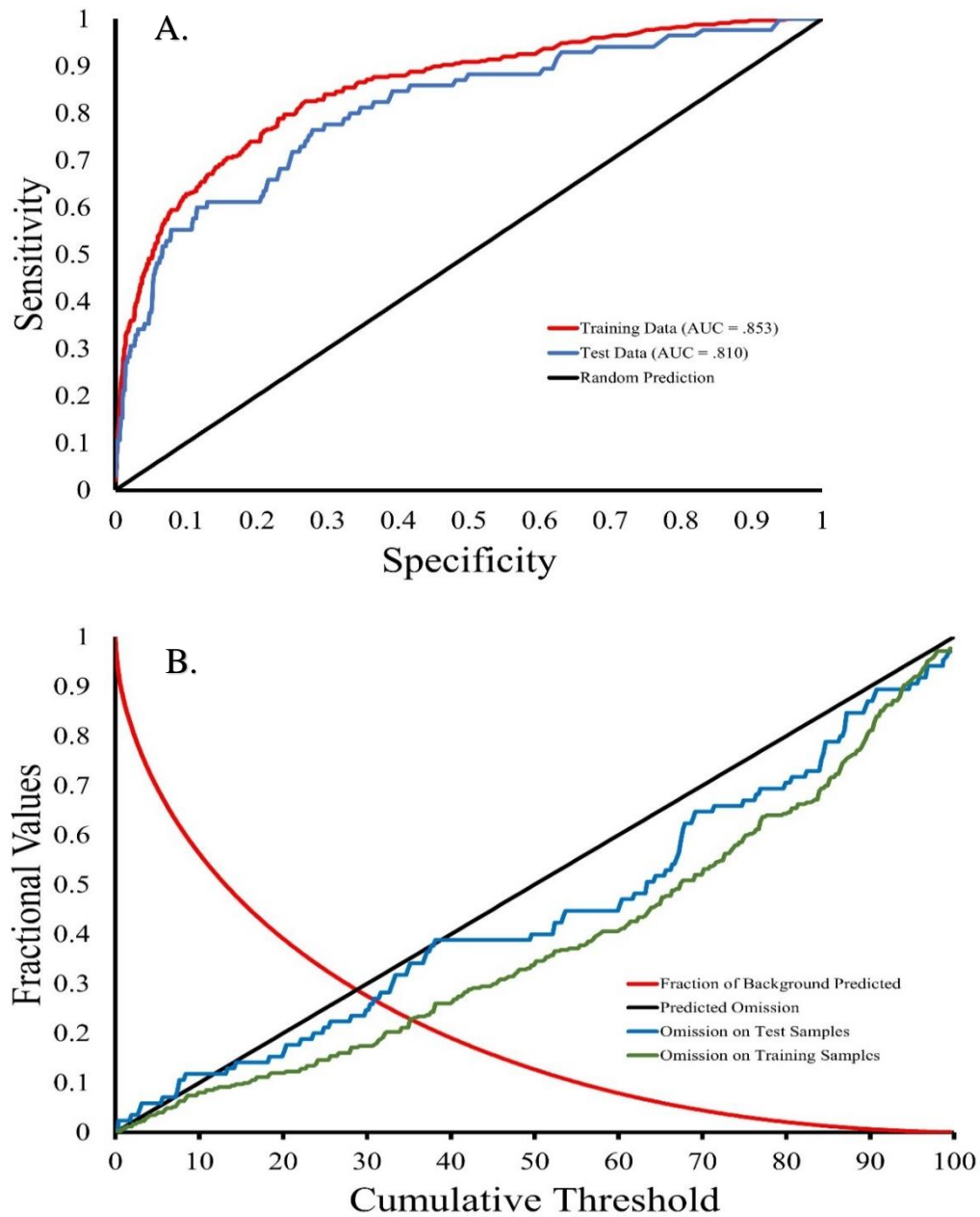


Figure 16. **A.** The average receiver operating curve (AUC) for *A. microscaphus* with the five replicates run in MaxEnt. The red line representing the fit of the model to the training data. The blue line represents the fit of the model to the 25% testing data. AUC over 0.7 assumes positive predictive power for the model. **B.** Represents the test omission rate and predicted area as a function of the cumulative threshold.

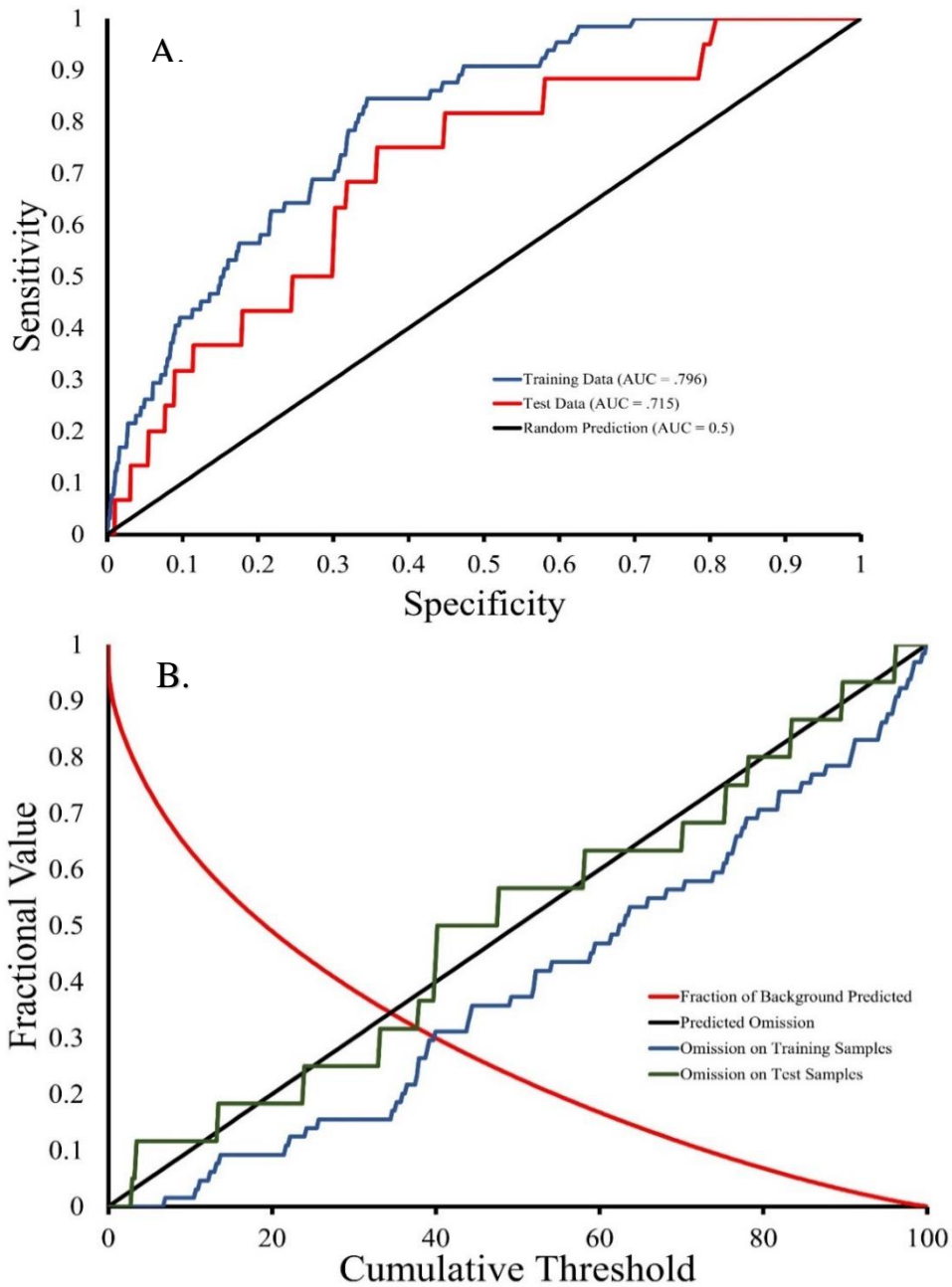


Figure 17. **A.** The average receiver operating curve (AUC) for *C. humilis* var. *jonesii* with the five replicates run in MaxEnt. The red line representing the fit of the model to the training data. The blue line represents the fit of the model to the 25% testing data. AUC over 0.7 assumes positive predictive power for the model. **B.** Represents the test omission rate and predicted area as a function of the cumulative threshold.

Table 4. Permutation importance values for each bioclimatic variable within the MaxEnt model for the 30 m *A. microscaphus* SDM. The permutation value is determined by randomly permuting the values of each independent variables against the training points. Values are then normalized to provide percentages; higher values suggest greater influence on the model.

Variable	Permutation Importance (%)
Annual Mean Temperature	22.9
Elevation	22.7
Isothermality	11.5
Normalized Difference Vegetation Index	11.1
Mean Diurnal Range	11
Precipitation Seasonality	5.7
Topographic Position Index	3.5
Slope	3.2
Precipitation of Coldest Quarter	2.7
Ruggedness	2.4
Aspect	2.1
Bare Soil Index	1.2

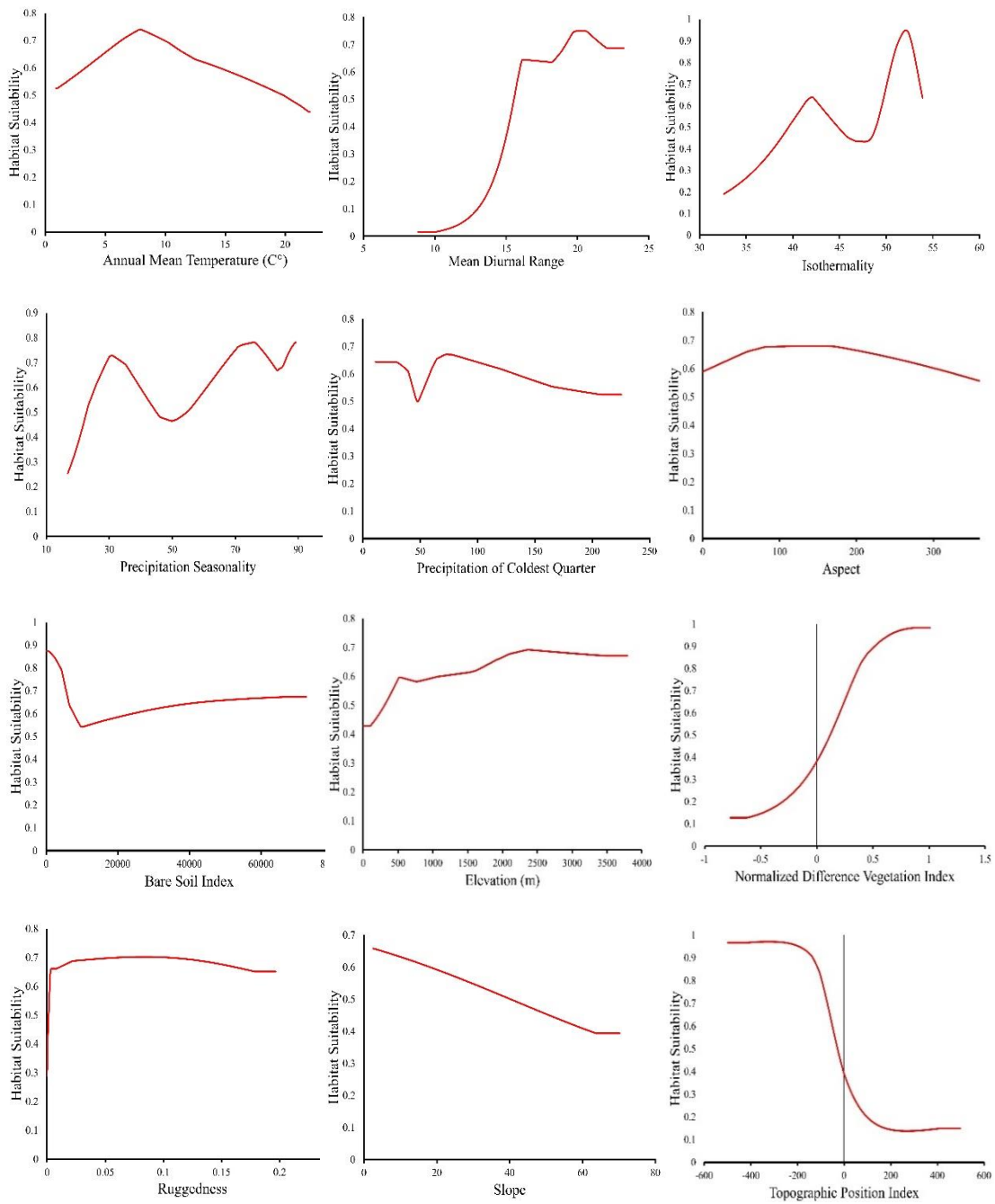


Figure 18. Partial dependence plots displaying the marginal response of the 12 environmental variables selected for *A. microscaphus* in the MaxEnt model. Each response curve demonstrates the range of suitability for each environmental variable if each variable were used to create a MaxEnt model independent of other variables.

Table 5. Permutation importance values for each WorldClim variable for the MaxEnt model for the 30 m *C. humilis* var. *jonesii* SDM. The permutation value is determined by randomly permuting the values of each independent variables against the training points. Values are then normalized to provide percentages; higher values suggest greater influence on the model.

Variable	Permutation Importance (%)
Precipitation Seasonality	47.2
Normalized Difference Vegetation Index	34.2
Minimum Temp of Coldest Quarter	8.9
Elevation	8.5
Slope	.4
Ruggedness	.3
Temperature Seasonality	0
Mean Temperature of Driest Quarter	0
Precipitation of Wettest Month	0
Aspect	0
Bare Soil Index	0
Precipitation of Driest Quarter	0
Annual Mean Temperature	0

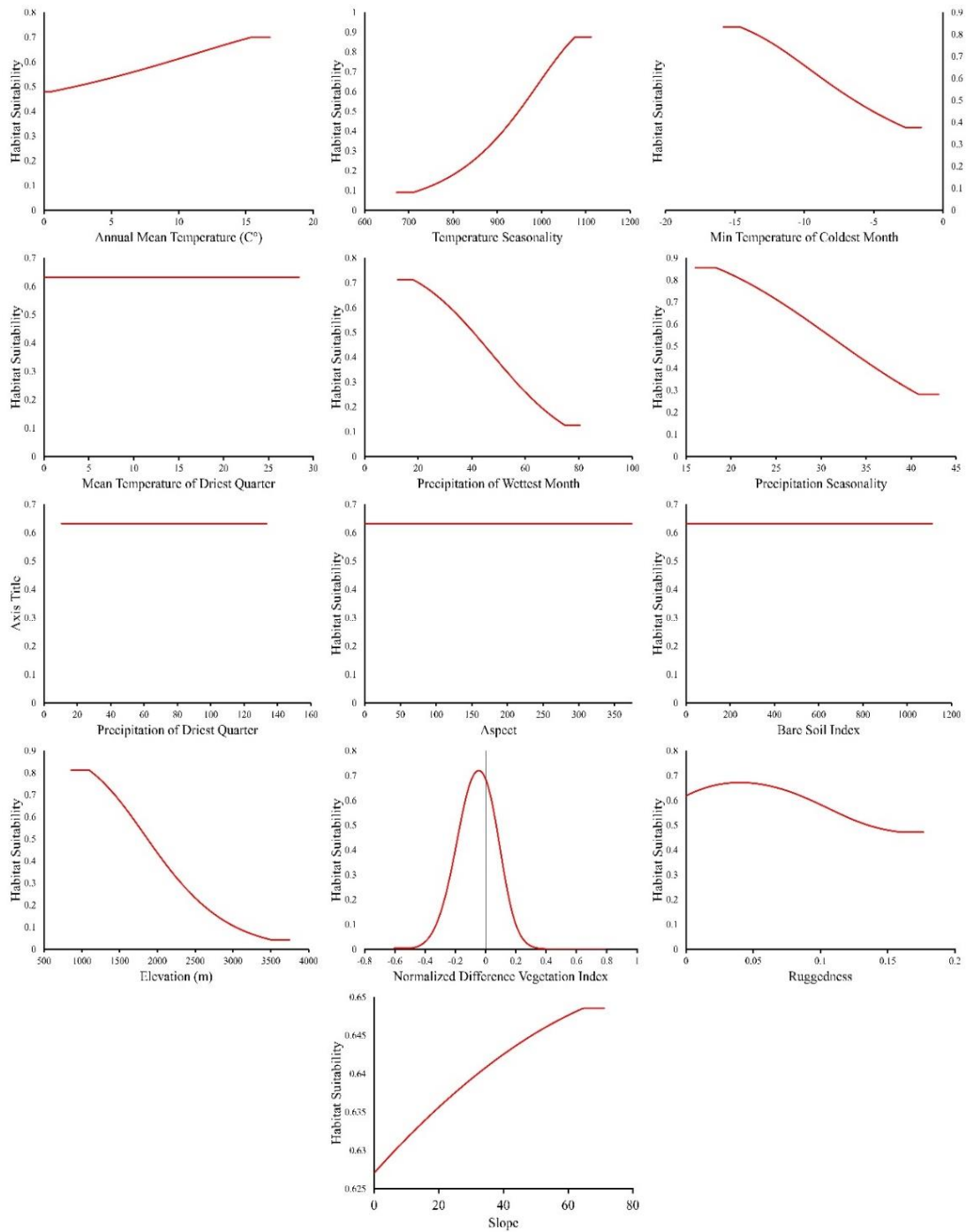


Figure 19. Partial dependence plots displaying the marginal response of the 13 environmental variable selected for *Cycladenia humilis* var. *jonesii* in the MaxEnt model. Each response curve demonstrates the range of suitability for each environmental variable if each variable were used to create a MaxEnt model independent of other variables.

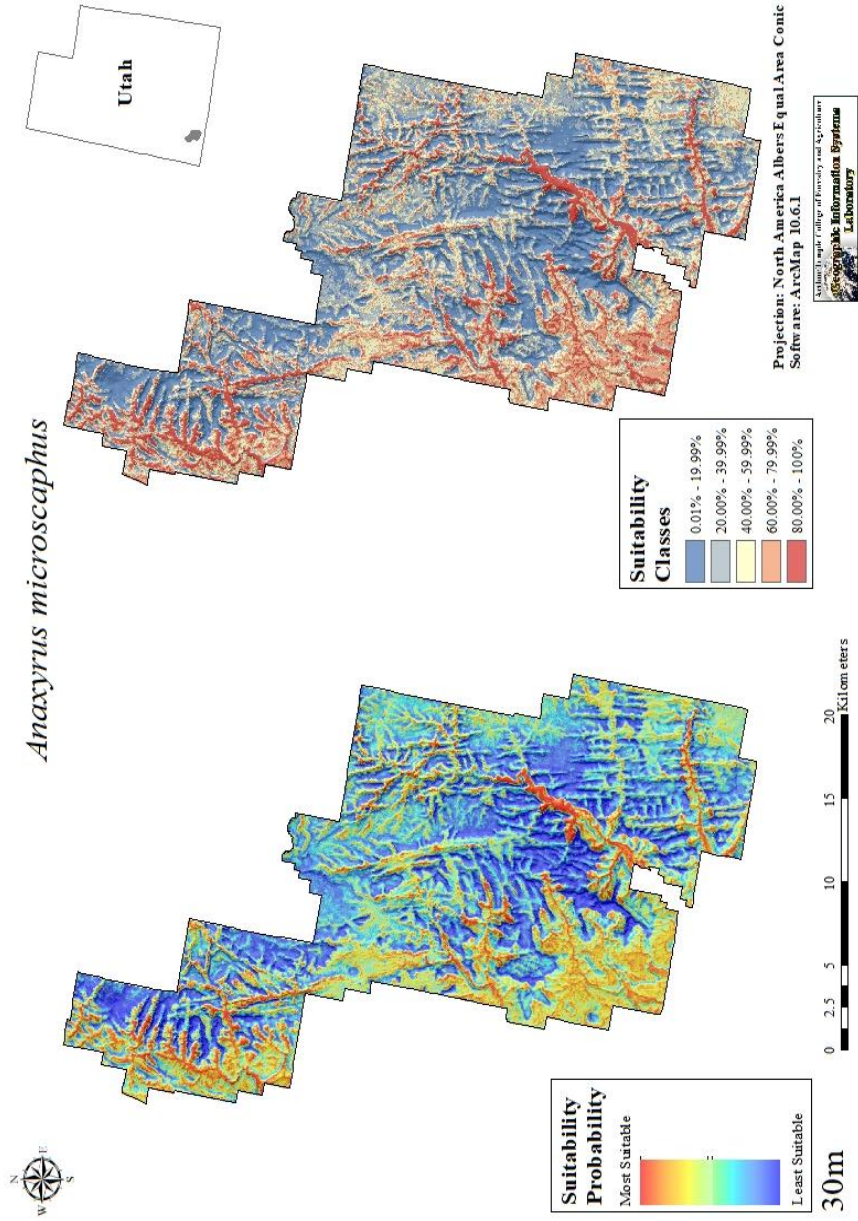


Figure 20. MaxEnt model output for 30 m resolution habitat suitability maps for *Anaxyrius microscaphus* in ZION. Suitability classes describe the ranking of habitat preference for the species being modeled. Models were created using MaxEnt.

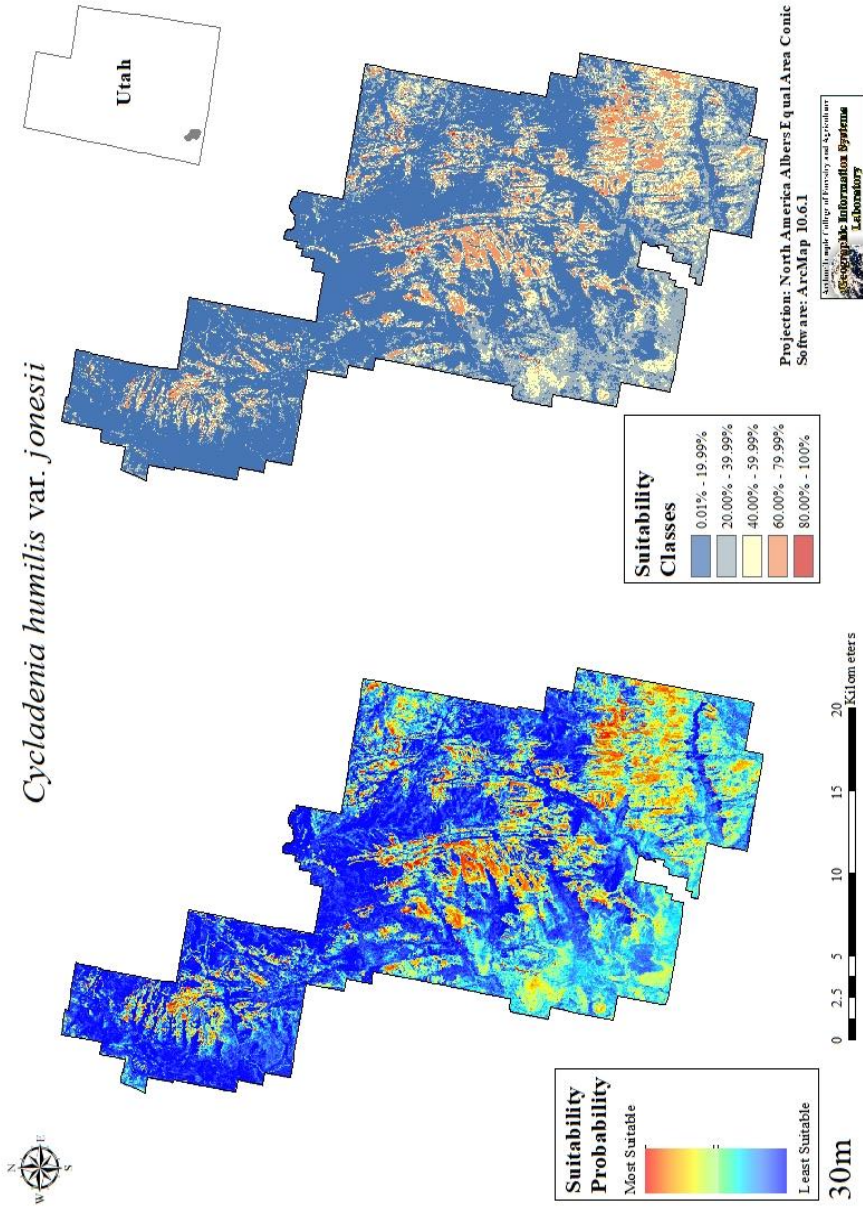


Figure 21. MaxEnt model output for 30 m resolution habitat suitability maps for *Cycladenia humilis* var. *jonesii* in ZION. Suitability classes describe the ranking of habitat preference for the species being modeled. Models were created using ArcMap and MaxEnt.

Resolution Comparison

The test AUC for *A. microscaphus* recorded an output of 0.815, while *C. humilis* var. *jonesii* recorded an output of 0.760. Both AUC outputs for the 900 m SDMs provided higher model prediction power than the 30 m SDMs (Table 6). Most suitable habitat increased from 900 m to 30 m for *A. microscaphus*, while the habitat decreased from 900 m to 30 m spatial resolution for *C. humilis* var. *jonesii*. The percent change for *A. microscaphus* was a 102% increase in the most suitable habitat range from 900 m to 30 m resolution. Percent change for *C. humilis* var. *jonesii* decreased by 68.7% for the most suitable habitat range (Table 7). Leading variable contribution for the 900 m *A. microscaphus* SDM was mean diurnal range, isothermality, and topographic position index. The most contributing variables for *C. humilis* var. *jonesii* were NDVI, precipitation seasonality, and aspect (Table 8). Maps displaying varying resolution sizes for both target species were created within ZION (Figures 22 & 23).

Table 6. Differing MaxEnt outputs for both study species comparing the contrast between 30 m and 900 m resolution.

Species	Resolution	Test AUC	Suitability Class	(km ²)	Hectare	Percent
<i>Anaxyrus microscaphus</i>	30m	.810	1-20%	174.28	17,428	28.96
			20.1-40%	144.90	14,489	24.08
			40.1-60%	123.21	12,321	20.47
			60.1-80%	98.88	9,888	16.43
			80.1-100%	60.54	6,054	10.06
	900m	.815	1-20%	283.5	28,350	46.92
			20.1-40%	127.17	12,717	21.05
			40.1-60%	97.2	9,720	16.09
			60.1-80%	66.42	6,642	10.99
			80.1-100%	29.97	2,997	4.96
<i>Cycladenia humilis</i> var. <i>jonesii</i>	30m	.715	1-20%	343.62	34,362	57.10
			20.1-40%	137.15	13,715	22.79
			40.1-60%	76.88	7,688	12.77
			60.1-80%	42.13	4,213	7.00
			80.1-100%	2.03	203	.33
	900m	.760	1-20%	469	46,899	77.61
			20.1-40%	65.61	6,561	10.86
			40.1-60%	36.45	3,645	6.03
			60.1-80%	26.73	2,673	4.42
			80.1-100%	6.48	648	1.07

Table 7. The percent change between 30 m and 900 m SDM outputs for the study species within five habitat suitability classes.

Species	Resolution	Suitability Class				
		1-20%	20.1-40%	40.1-60%	60.1-80%	80.1-100%
<i>Anaxyrus microscaphus</i>	900m	283.5	127.17	97.2	66.42	29.97
	30m	174.28	144.90	123.21	98.88	60.54
	% Change	-38.8	+13.9	+26.8	+48.9	+102.0
<i>Cycladenia humilis</i> var. <i>jonesii</i>	900m	469	65.61	36.45	26.73	6.48
	30m	343.62	137.15	76.88	42.13	2.03
	% Change	-26.7	+109.03	+110.92	+57.6	-68.7

Table 8. Permutation importance values for each bioclimatic variable within the MaxEnt model for the 900 m *A. microscaphus* and *C. humilis* var. *jonesii* SDMs. The permutation value is determined by randomly permuting the values of each independent variables against the training points. Values are then normalized to provide percentages; higher values suggest greater influence on the model.

<i>Anaxyrus microscaphus</i> Variables	Permutation Importance (%)
Mean Diurnal Range	22.1
Isothermality	17.2
Topographic Position Index	15.9
Normalized Difference Vegetation Index	10.6
Elevation	10.5
Annual Mean Temperature	6.6
Ruggedness	4.8
Aspect	3.6
Precipitation Seasonality	2.8
Bare Soil Index	2.4
Precipitation of Coldest Quarter	2.4
Slope	1.1
<i>Cycladenia humilis</i> var. <i>jonesii</i> Variables	Permutation Importance (%)
Normalized Difference Vegetation Index	35.7
Precipitation Seasonality	25.1
Aspect	15.5
Slope	10.3
Minimum Temp of Coldest Month	7.7
Elevation	2.7
Ruggedness	1.9
Annual Mean Temperature	0.6
Precipitation of Wettest Month	0.3
Bare Soil Index	0.1
Temperature Seasonality	0.0
Mean Temperature of Driest Quarter	0.0
Precipitation of Driest Quarter	0.0



Figure 22. MaxEnt habitat suitability outputs for *A. microscaphus* with differing resolution sizes to compare low to high suitability habitat for ZION. Highest suitability habitat increased within the park with the higher resolution. All environmental variables (topographic, remotely-sensed, and climate) were applied to these two outputs.

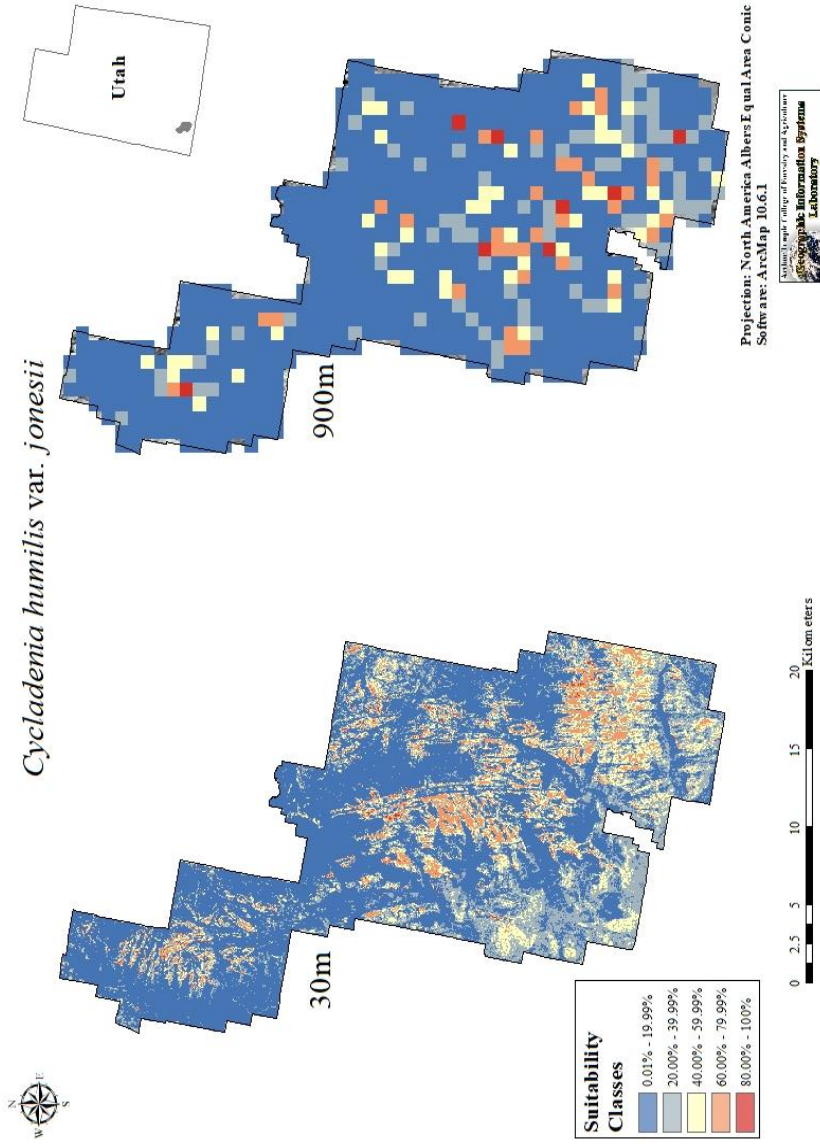


Figure 23. MaxEnt habitat suitability outputs for *C. humilis* var. *jonesii* with differing resolution sizes to compare low to high suitability habitat for ZION. Highest suitability habitat decreased within the park with the higher resolution. All environmental variables (topographic, remotely-sensed, and climate) were applied to these two maps.

Future Climate Trends

Based on the forecasting models for *A. microscaphus*, habitat suitability for the training extent maps diminish as projections into the future for both 2.6 and 8.5 W/m² scenarios. The 2070 8.5 W/m² scenario projects a 5.14% suitable habitat compared to the current day projection of 42.63% (Figures 24 & 25) (Table 9). Additionally, the forecasting maps for ZION also display a reduction of suitable habitat within the park for future climate scenarios (Figures 26 & 27) (Table 10). Conversely, the training extent forecasting models for *C. humilis* var. *jonesii* projects minimal shifts in suitability for both RCPs in the years 2050 and 2070 compared to the 2020 SDMs (Figures 28 & 29) (Table 11). The *C. humilis* var. *jonesii* forecasting maps for ZION produced suitability maps that showed an increase in potential habitat for the 2050 2.6 W/m² RCP but a decrease for the 2050 8.5 W/m² RCP (Figure 30). Both 2070 RCPs displayed an increase in similar suitable habitat for 2.6 and 8.5 W/m² scenarios (Figures 31) (Table 12).



Anaxyrus microscaphus

900m

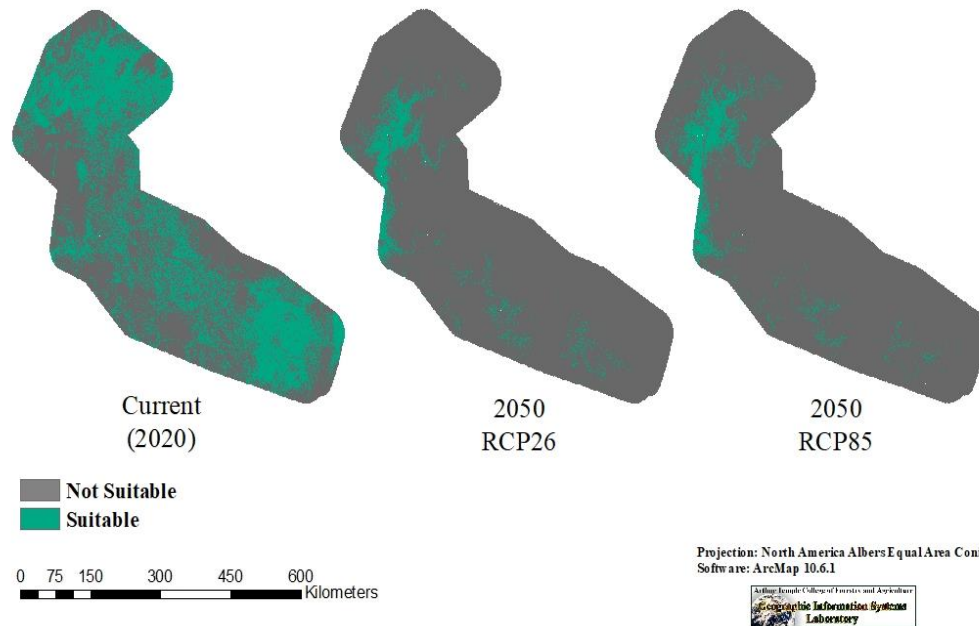


Figure 24. Forecasting SDM of *A. microscaphus* contrasting the suitable habitat for future climate scenarios for representative concentration pathways that describe greenhouse gas concentration of 2.6 W/m^2 and 8.5 W/m^2 for the year 2050. The SDM covers the complete training extent of the toad to better understand changes in suitable habitat (see Figure 14). The '10 percentile training presence' threshold was used to delineate suitable habitat in this analysis.

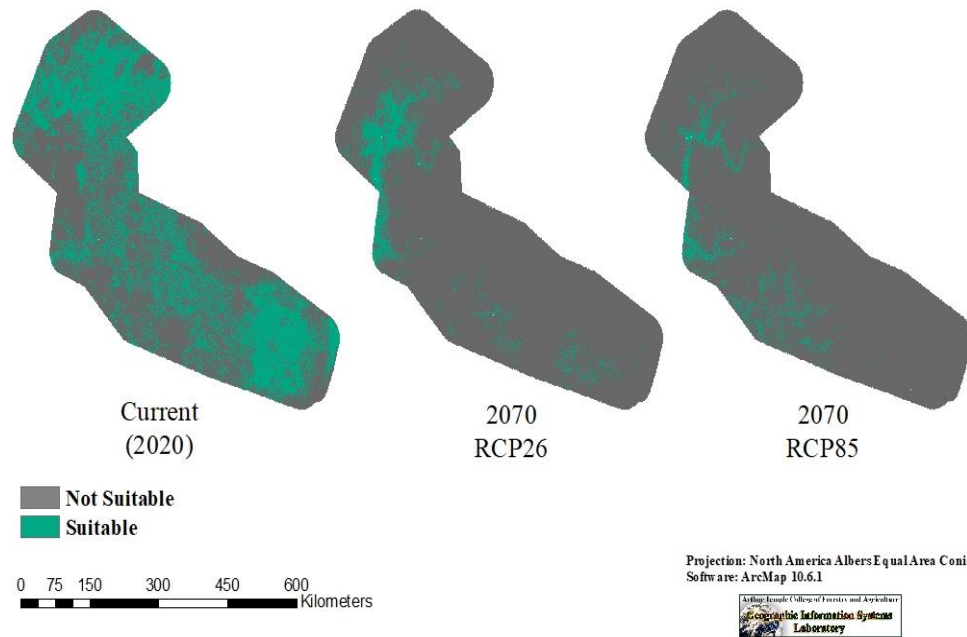


Figure 25. Forecasting SDM of *A. microscaphus* contrasting the suitable habitat for climate scenarios for representative concentration pathways, which describe greenhouse gas concentration of 2.6 W/m² and 8.5 W/m² for the year 2070 (see Figure 14). The SDM covers the complete training extent of the toad to better understand changes in suitable future habitat. The ‘10 percentile training presence’ calculated by the MaxEnt output was used as the threshold to delineate suitable habitat.

Table 9. Area of suitable habitat for *A. microscaphus* within the training extent for future climate scenarios for 2050 and 2070 with differing RCPs of 2.6 and 8.5 W/m².

Species	Year	RCP	(km ²) suitability	% suitability
<i>Anaxyrus microscaphus</i>	Current (2020)	Current	99,370	42.63%
	2050	2.6 W/m ²	15,125	6.48%
		8.5 W/m ²	17,702	7.59%
	2070	2.6 W/m ²	17,942	7.70%
		8.5 W/m ²	11,976	5.14%



Anaxyrus microscephus
in ZION

900m

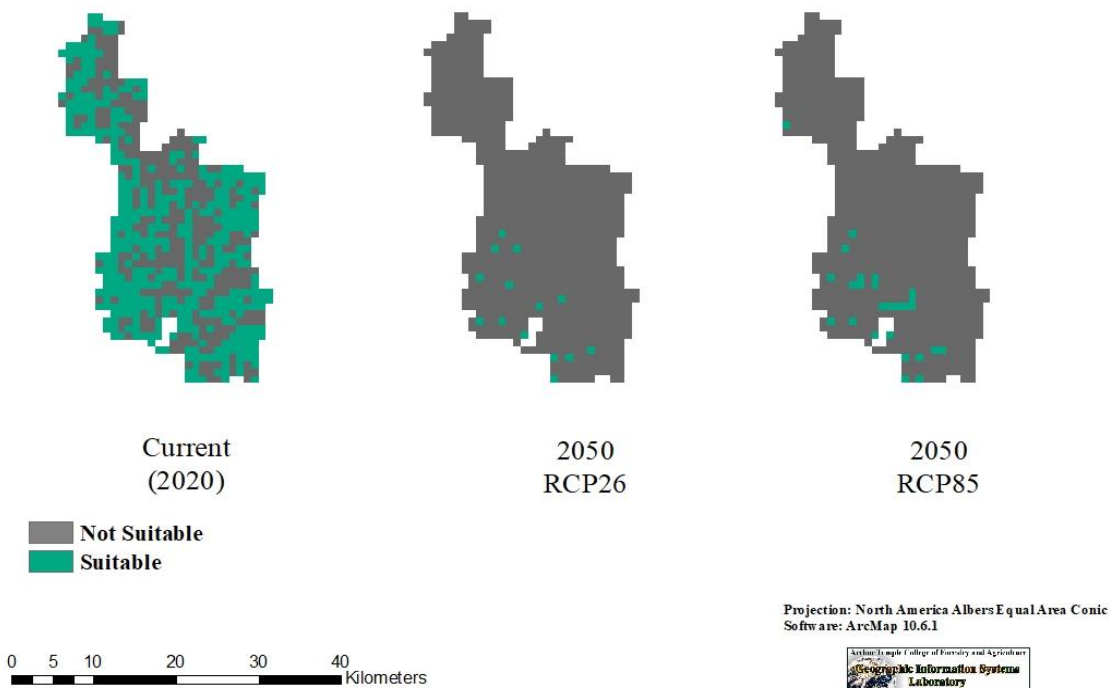


Figure 26. Forecasting SDM of *A. microscephus* for the current year (2020) and 2050 using binary distribution of suitable versus not suitable habitat. The ‘10 percentile training presence’ threshold was calculated by MaxEnt to delineate suitable habitat in this analysis.

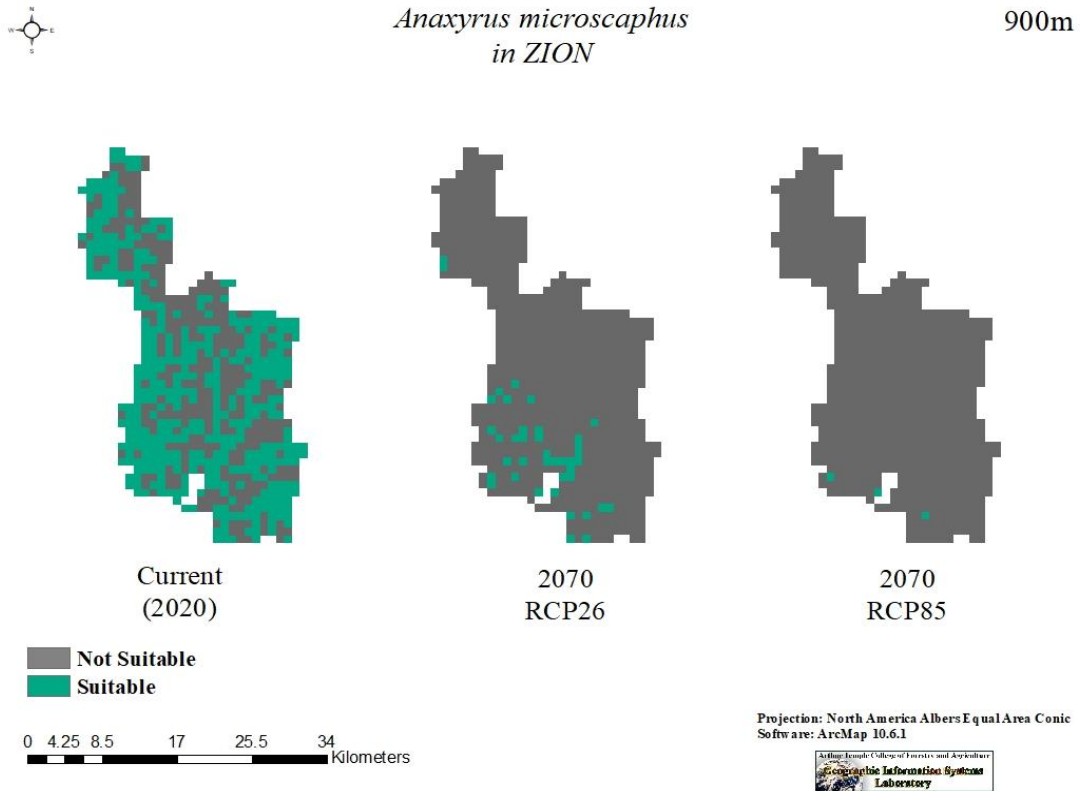


Figure 27. Forecasting SDM of *A. microscaphus* for the current year (2020) and 2070 using binary distribution of suitable versus not suitable habitat. The ‘10 percentile training presence’ threshold was calculated by MaxEnt to delineate suitable habitat in this analysis.

Table 10. Area of suitable habitat for *A. microscaphus* within ZION for current and future climate scenarios of 2050 and 2070 with differing RCPs of 2.6 and 8.5 W/m².

Species	Year	RCP	(km ²) suitability	% suitability
<i>Anaxyrus microscaphus</i>	Current (2020)	Current	343.4	57.22
	2050	2.6 W/m ²	11.34	1.8
		8.5 W/m ²	21.06	3.50
	2070	2.6 W/m ²	32.4	5.4
		8.5 W/m ²	2.43	0.4



Cycladenia humilis var. *jonesii*

900m

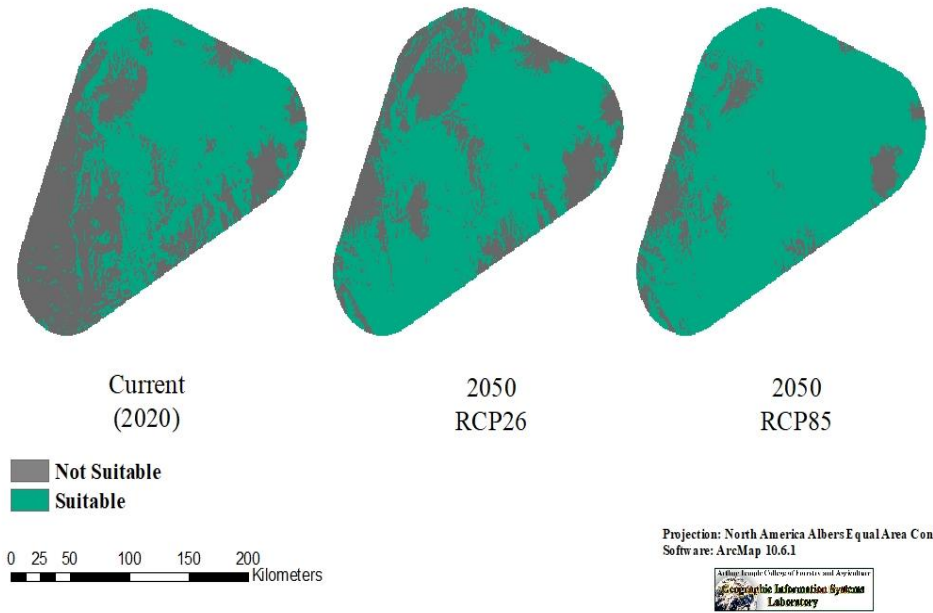


Figure 28. Forecasting SDM of *C. humilis* var. *jonesii* contrasting the suitable habitat for future climate scenarios for representative concentration pathways that describe greenhouse gas concentration of 2.6 W/m² and 8.5 W/m² for the year 2050. The SDM covers the complete training extent of the plant to better understand changes in suitable future habitat (see Figure 15). The ‘10 percentile training presence’ calculated by the MaxEnt output was used to delineate suitable habitat in this analysis.

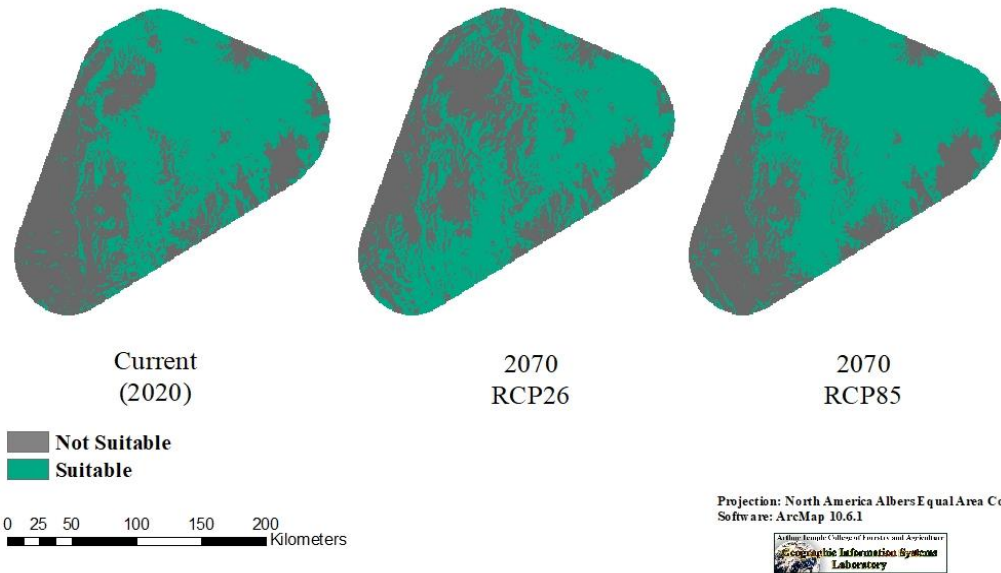


Figure 29. Forecasting SDM of *C. humilis* var. *jonesii* contrasting the suitable habitat for future climate scenarios for with representative concentration pathways that describe greenhouse gas concentration of 2.6 W/m² and 8.5 W/m² for the year 2070. The SDM covers the complete training extent of the plant to better understand changes in suitable habitat (see Figure 15). The ‘10 percentile training presence’ calculated by the MaxEnt output was used to delineate suitable habitat in this analysis.

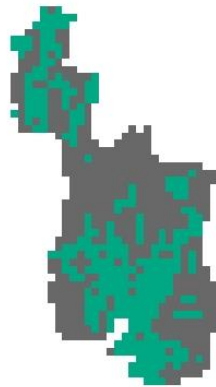
Table 11. Area of suitable habitat for *C. humilis* var. *jonesii* within the training extent for future climate scenarios of 2050 and 2070 with differing RCPs of 2.6 and 8.5 W/m².

Species	Year	RCP	(km²) suitability	% suitability
<i>Cycladenia humilis</i> var. <i>jonesii</i>	Current (2020)	Current	20,516	57.10%
	2050	2.6 W/m ²	25,347	70.55%
		8.5 W/m ²	31,371	87.32%
	2070	2.6 W/m ²	19,947	55.52%
		8.5 W/m ²	21,565	60.02%



Cycladenia humilis
in ZION

900m



Current
(2020)



2050
RCP26



2050
RCP85

Not Suitable
Suitable

Projection: North America Albers Equal Area Conic
Software: ArcMap 10.6.1

0 5 10 20 30 40
Kilometers



Figure 30. Forecasting SDM of *C. humilis* var. *jonesii* in ZION for the current year (2020) and 2050 using binary distribution of suitable versus not suitable habitat. The '10 percentile training presence' threshold was calculated by MaxEnt to delineate suitable habitat in this analysis.

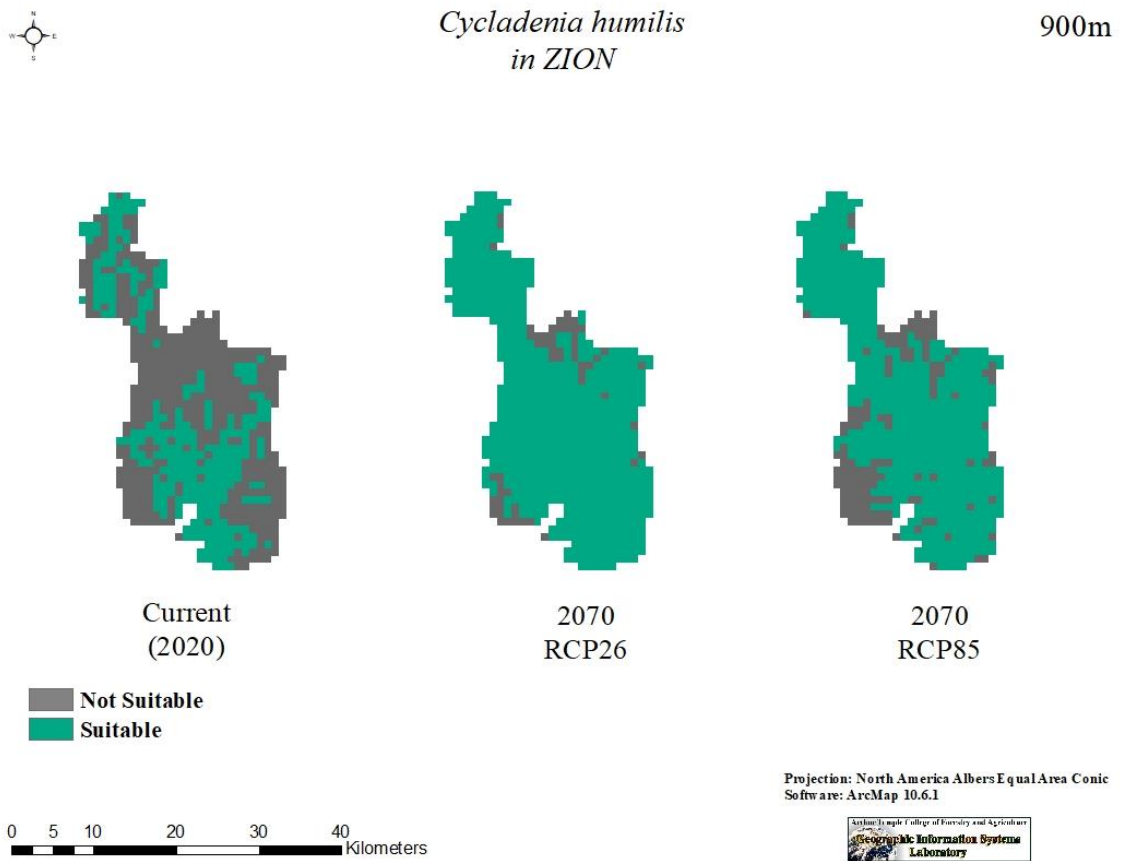


Figure 31. Forecasting SDM of *C. humilis* var. *jonesii* in ZION for the current year (2020) and 2070 using binary distribution of suitable versus not suitable habitat. The ‘10 percentile training presence’ threshold was calculated by MaxEnt to delineate suitable habitat in this analysis.

Table 12. Area of suitable habitat for *C. humilis* var. *jonesii* within ZION for future climate scenarios of 2050 and 2070 with differing RCPs of 2.6 and 8.5 W/m².

Species	Year	RCP	(km ²) suitability	% suitability
<i>Cycladenia humilis</i> var. <i>jonesii</i>	Current (2020)	Current	220.32	36.46
	2050	2.6 W/m ²	546.75	90.48
		8.5 W/m ²	42.12	6.97
	2070	2.6 W/m ²	557.28	92.22
		8.5 W/m ²	490.86	81.23

DISCUSSION & CONCLUSIONS

Results from this study displayed promising predictive power for the 30 m SDMs for *A. microscaphus* and *C. humilis* var. *jonesii*. The most contributing variables for both models varied across all three classes (topographic, remotely sensed, and climatic) and displayed little preference to one variable class type over the other. For the second objective, I observed comparable results for model performance based on AUC and contrasting results with respect to habitat suitability within ZION for the high versus low spatial resolutions. The SDM showed higher habitat suitability for *A. microscaphus* at finer spatial resolution, while the SDM displayed lower habitat suitability for *C. humilis* var. *jonesii* at finer spatial resolution. Forecasting for the third objective showed decreasing suitable habitat for *A. microscaphus* for future climate scenarios but an increase in suitable habitat for *C. humilis* var. *jonesii* in future climate scenarios.

The results from the 30 m SDM models display similar findings with other studies regarding acceptable predictive power for high spatial resolution modeling of specialist species. Prior studies have displayed results that support higher predictive accuracy when modeling for specialist species opposed to generalist species, even when using fewer occurrence localities (Hernandez et al., 2006; Evangelista et al., 2008). Connor et al. (2017) found that SDMs for species in heterogenous landscapes perform better compared to homogenous landscapes. This likely occurs due to the SDMs ability to differentiate

extreme shifts in the heterogeneous landscape, allowing the model to delineate areas of high versus low suitability. This corresponds positively with *A. microscaphus* habitat, which often is in ravines and streams adjacent to steep cliffs hundreds of meters high. Similarly, *C. humilis* var. *jonesii* habitat is fragmented in areas that are dispersed in densely clustered colonies of ramets (US FWS 2008). These ramets are dispersed in microhabitats, or microrefugia, which are climatically unique pockets of suitable habitat. These microrefugia can often go undetected by SDMs when using low resolution environmental variables (Dobrowski, 2010). Furthermore, this study demonstrates that downscaling existing lower spatial resolution climate data can produce meaningful SDMs that display local scale species habitat distribution. This supports the studies that proposed downscaling climate data as a reliable method for mapping species distribution at a local scale (Franklin et al., 2013; Slavish et al., 2014; Meineri and Hylander, 2017).

Environmental variable contributions produced by MaxEnt can be an integral component to understanding the ecology that allows a species to persist within a set of abiotic conditions. NDVI displayed high variable contribution, likely due to the toad's habitat preference of relatively higher vegetated riparian habitat in arid environments where water and vegetation are sometimes scarce (Sweet, 1992). I also found that the contributing variables for *A. microscaphus* support the inferred distributional patterns which suggests that temperature sets the range limit for several amphibians (Schall and Pianka 1978; Duellman and Sweet 1999). Three of the top five contributing variables for the *A. microscaphus* SDM were derived from temperature. Annual mean temperature was

the most contributing environmental variable, along with isothermality the third most contributing variable, and mean diurnal range the fifth most contributing variable (Table 4). Moreover, Préau et al. (2018) reported that minimum temperature was the top two most contributing variable for three different European toads. Within that study, two different modeling approaches were used with high spatial resolution climate and topographic variables. Two SDM methods resulted in differing habitat suitability for each study species, thus leading to the recommendation of producing two or more modeling methods for local scale amphibians.

I observed increased variable contribution from both precipitation and NDVI for *C. humilis* var. *jonesii*. NDVI likely demonstrated high variable contribution due to the plants habitat preference to exist in communities of desert scrub and juniper (Tilley et al., 2010). The use of NDVI in this SDM allowed the model to capture the vegetation within areas and delineate high habitat suitability versus low habitat suitability. Likewise, precipitation was a main variable contributor in the plant SDM. Precipitation is a strong environmental indicator in many SDM plant studies; however, the absence of soil variables likely reduced the model performance for the plant (Woodward and Williams, 1987; Syfert et al., 2013; Yang et al., 2013). A study by Hageer et al. (2017) suggests that predictive power of SDMs perform better when models are calibrated with both climate and soil data. Soil data was limited within ZION for my study, therefore, I completely excluded soil from the SDM. The bare soil index variable was used as a proxy for soil,

but the remotely sensed data could not replicate the chemical and physical properties within soil needed to create a highly contributing environmental variable.

The AUC for both SDMs increased with increasing grain size. This finding contradicts previous studies which suggest, depending on the species, AUC will increase as the grain size becomes finer (Gottschalk et al. 2011; Scales et al. 2017; Connor et al., 2018). Guisan et al. (2007) found that an increase in grain size of the environmental variables reduced the predictive power of some SDMs for certain species but improved the SDMs for others. Additionally, Pradervand et al. (2014) conducted a study to compare the predictive power of 239 mountainous plant species at six different spatial resolutions (2, 5, 10, 25, 50, and 100 m) with three different types of SDMs. The study found that variations in predictive accuracy of the models AUCs displayed little change between the six spatial resolutions. Notably, I found that the AUC for both species increased slightly from 30 m to 900 m spatial resolution (Table 6). These observations in model performance are likely due to environmental variable contribution at different scales. This supports findings that environmental variables can have different meanings and respond to different resolutions when analyzing SDM predictive power (Lassueur et al. 2006; Guisan et al, 2007; Pradervand et al. 2014). For *C. humilis* var. *jonesii*, the highest suitable habitat increased as the grain size increased. This partially could be due to the plant habitat being found at higher elevations within the park where the landscape has increased homogeneity. Additionally, it could be due to the habitat features of the plant being less distinguishable. Unlike the toad which has contrasting habitat features

(i.e. elevation, vegetation, temperature), the plant has fewer distinct features, possibly making it difficult for high spatial resolution SDMs to capture the geographic landscape. After analyzing two spatial resolutions (30 m and 900 m), further model evaluation with multiple resolution types is recommended to produce higher accuracy models, especially when species modeling for conservation and land management purposes.

Understanding and expanding existing methods for mapping habitat distribution of microhabitat and microrefugia is imperative in understanding how species populations shift during periods of unfavorable climate. Typically, populations migrate in latitude or altitude during warming or cooling climates (Jump et al., 2009; Hampe and Jump 2011). In topographically heterogeneous landscapes, species are also capable of persisting in microrefugia, which may allow the species to persist until conditions outside microrefugia allow establishment (Scherrer and Körner, 2010; Auffret et al., 2015). However, amphibians often lack the mobility and dispersal ability needed to adapt to local climate stresses (Halpin, 1997). Amphibian abundance within the environment is linked to the interactions between temperature, precipitation, and vegetation. Where vegetation produces microhabitat that can mitigate climate impacts (Seebacher and Alford, 2002). These climatic factors greatly influence the distribution of amphibians through changes in their phenology. A study by Blaustein et al. (2001) observed fluctuations in temperature on a global scale, which altered the timing of breeding, hibernation periods, and the ability to find food for some species. Over a 17-year period, a gradual increase (0.11-0.24°C per year) in average maximum temperature between

March and April led to earlier breeding in two anurans and three salamanders. In the last five years of the study, the anurans were breeding 2-3 weeks earlier than the first five years of the study and 5-7 weeks earlier for the salamanders compared to the first five years. However, other amphibian species breeding activity within the study remained constant, despite rising temperatures over this timespan. I observed a reduction in available suitable habitat distribution in future climate scenarios for *A. microscaphus*. Contributing response curves for climate variables of the toad (Figure 18) show that as the annual mean temperature increases above 10°C habitat sustainability begins to decrease. Mean diurnal range, the difference between daily maximum and minimum temperature, begins to decrease rapidly below 17°C for toad suitability. The same can be said for precipitation seasonality, which begins to reduce rapidly in suitability below 30 mm. The future global climate model used in this study, CCSM4, demonstrates RCPs that predict future temperature increases and future precipitation decreases up to the year 2100 for 3 climate scenarios (4.5, 6.0, 8.5 W/m²) and a stabilization for RCP 2.6 W/m² globally (Meehl et al., 2012). Likewise, the International Panel on Climate Change projects the earth's surface in the Southwest to rise close to 1.7°C until 2100, with lower precipitation in the southern portion of the Southwest region and little change or a slight increase in precipitation in the northern portion (Garfin et al., 2013). Additionally, snowpack will decrease from February to May up to the year 2100 in addition to reductions in runoff and streamflow from the middle to the end of the twenty-first century (Garfin et al., 2013; IPCC, 2014).

Plant population response to changing climates varies from species to species, although two patterns appear consistent, particularly amongst arid species. First, precipitation is positively correlated with plant reproduction; and second, drought years often result in complete reproductive failure (Fox et al. 2006; Evans et al. 2007; Levine et al., 2008). With *C. humilis* var. *jonesii* forecasting models, I was able to observe significant increase in suitable habitat distribution for future climate scenarios of 2050 and 2070 for both the training extent and ZION maps. However, a decrease in suitable habitat occurred for the 2050 8.5 W/m² forecasting model. Response curves of the plant (Figure 19) show that increasing temperature seasonality favors plant suitability. Temperature seasonality is the measure of temperature change over the year, implying that *C. humilis* var. *jonesii* thrives in areas of higher temperature variation over the course of the year (USGS, 2012). Precipitation seasonality displays a decrease in suitability for the plant as it increases, indicating future habitat scenarios project a decrease in this variable based on the ubiquity of this species for both 2070 scenarios and the 2050 2.6 W/m² scenarios. Precipitation seasonality is the measure of variation in monthly precipitation totals over the course of a year (USGS, 2012). This finding is not consistent when observing IPCC projections that detail seasonally erratic and localized precipitation behavior for the desert southwest region for future years. In essence, the CCSM4 global climate model used in the forecasting SDMs displays *C. humilis* var. *jonesii* flourishing in most future scenarios. However, other climate models display high variability for future years, especially when observing precipitation, which could potentially display no

change or reduction of suitable habitat for the plant (Garfin et al., 2013). Understanding monthly climate variables opposed to yearly climate variables is especially important to plants because of their adaptability to erratic precipitation events in arid environments. These findings correspond with species modeling for plants and trees, in particular forecasting models, where a study has shown monthly climate variables rather than yearly variables improved SDM predictions of tree species (Zimmerman et al, 2009).

For higher performing SDM outputs, considerations to modify environmental variables and model calibration are suggested. First, the incorporation of soil data into the model would likely improve model predictive power. Incorporating Gridded National Soil Survey Geographic Database (GNATSGO) data, a consolidation of STATSGO2, SSURGO, and raster soil survey data would provide chemical and physical soil properties for model construction. The database is integrated with ArcGIS and a comprehensive effort created in 2019 to provide soil data up to 10 m in spatial resolution for more than 90 percent of the United States and island territories. Unfortunately, most likely due to the extreme changes in geography in ZION, an incomplete soil map remains for that area, making species modeling inadequate. Secondly, forecasting models within this study used a single global climate model, providing limited insight into future habitat changes for the study species. Inclusion of multiple GCMs and pathways using ensemble modeling will lead to a better understanding of future habitat based on an assortment of scenarios. Use of an ensemble platform, such as BIOMOD, will allow modelers to incorporate multiple model algorithms, GCMs, and RCPs to discover the optimum

grouping of variables and produce higher predictive models. BIOMOD is open source and implemented in R and allows assessing of species temporal turnover, response curves, and tests species interactions with environmental variables (Thuiller et al., 2009). Thirdly, expanding on the science and production of downscaling climate data will reduce downscaling inaccuracies and provide higher precision detection of microhabitats. Only recently have methods and procedures used to downscale climate data begun to expand the literature (Wang et al., 2011; Meineri and Hylander, 2017; Morgan and Guénard, 2019). Lastly, SDM construction and analysis is only the first step to properly map the habitat distribution for species. Further analysis by ground truthing and long-term species monitoring will strengthen model reliability and allow SDM construction to expand the ecological knowledge of study species (Rebelo and Jones, 2010).

Given the findings from the SDMs in this study, MaxEnt is a capable algorithm and platform for mapping the distribution of species using topographical, remotely sensed, and climate data. MaxEnt was capable of identifying suitable habitat for both study species within ZION. The use of presence-only data, along with downscaling of climate data to a finer resolution allows a better understanding of the ecological interaction with species and their abiotic environment. With the use of SDMs, conservation practitioners and land managers can work collaboratively to build and interpret model results, leading to better conservational efforts for current and future species distribution mapping.

LITERATURE CITED

- Anderson, R. P., D. Lew, and A. T. Peterson. 2003. Evaluating Predictive Models of Species' Distributions: Criteria for Selecting Optimal Models. *Ecological Modelling*. 162(3): 211–32. [https://doi.org/10.1016/S0304-3800\(02\)00349-6](https://doi.org/10.1016/S0304-3800(02)00349-6).
- Araújo, M. B. and A. Guisan. 2006. Five (or so) Challenges for Species Distribution Modelling. *Journal of Biogeography*. 33(10): 1677–1688. <https://www.jstor.org/stable/pdf/3838509.pdf>.
- Arora, V. K., J. F. Scinocca, G. J. Boer, J. R. Christian, K. L. Denman, G. M. Flato, V. V. Kharin, W. G. Lee, and W. J. Merryfield. 2011. Carbon Emission Limits Required to Satisfy Future Representative Concentration Pathways of Greenhouse Gases. *Geophysical Research Letters*. 38(5): 1-6. <https://doi.org/10.1029/2010GL046270>.
- Auffret, A. G., J. Plue, and S. A. O. Cousins. 2015. The Spatial and Temporal Components of Functional Connectivity in Fragmented Landscapes. *AMBIO*. 44(Suppl. 1): S51–S59. DOI 10.1007/s13280-014-0588-6.
- Beck, J., M. Böller, A. Erhardt, and W. Schwanghart. 2014. Spatial Bias in the GBIF Database and its Effect on Modeling Species' Geographic Distributions. *Ecological Informatics*. 19: 10–15. <https://doi.org/10.1016/j.ecoinf.2013.11.002>.
- Benestad, R. E. 2004. Empirical-Statistical Downscaling in Climate Modeling. *Eos, Transactions American Geophysical Union*. 85(42): 417–22. <https://doi.org/10.1029/2004EO420002>.
- Biedma, L., J. Calzada, J. A. Godoy, and J. Román. 2019. Local Habitat Specialization as an Evolutionary Response to Interspecific Competition between Two Sympatric Shrews. *Journal of Mammalogy*. 101(1): 80–91. doi.org/10.1093/jmammal/gyz203.
- Blais, B., M. J. Ryan, G. Gustafson, and J.T. Giermakowski. 2016. Natural History Notes. *Herpetological Review*. 47(3): 436-438. <https://ssarherps.org/herpetological-review-pdfs/>.

- Blair, A. P. 1955. Distribution, Variation, and Hybridization in a Relict Toad (*Bufo microscaphus*) in Southwestern Utah. *American Museum Novitates*. 1722: 1-38.
- Blaustein, A. R., L. K. Belden, D. H. Olson, D. M. Green, T. L. Root, and J. M. Kiesecker. 2001. Amphibian Breeding and Climate Change. *Conservation Biology*. 15(6): 1804–1809. <https://doi.org/10.1046/j.1523-1739.2001.00307.x>
- Boria, R. A., L. E. Olson, S. M. Goodman, and R. P. Anderson. 2014. Spatial Filtering to Reduce Sampling Bias can Improve the Performance of Ecological Niche Models. *Ecological Modelling*. 275: 73–77. <https://doi.org/10.1016/j.ecolmodel.2013.12.012>.
- Brabazon, H. K. 2015. Delimiting Species and Varieties of *Cycladenia humilis* (Apocynaceae). *All Student Publications*. pp. 172. <https://scholarsarchive.byu.edu/cgi/viewcontent.cgi?article=1178&context=studentpub>.
- Brabazon, H. K. 2015. Delimiting Species and Varieties of *Cycladenia Humilis* (Apocynaceae). *All Student Publications*. 172. <https://scholarsarchive.byu.edu/cgi/viewcontent.cgi?article=1178&context=studentpub>.
- Bradford, D. F., J. R. Jaeger, and S. A. Shanahan. 2005. Distributional Changes and Population Status of Amphibians in the Eastern Mojave Desert. *Western North American Naturalist*. 65(4): 462-472. <https://scholarsarchive.byu.edu/cgi/viewcontent.cgi?article=1828&context=wnan>.
- Brotons, L. 2014. Species Distribution Models and Impact Factor Growth in Environmental Journals: Methodological Fashion or the Attraction of Global Change Science. *PLOS ONE*. 9(11). doi:10.1371/journal.pone.0111996.
- Brown, J. L. 2014. SDMtoolbox: A Python-based GIS Toolkit for Landscape Genetic, Biogeographic, and Species Distribution Model Analyses. *Methods in Ecology and Evolution*. 5(7): 694–700. <https://doi.org/10.1111/2041-210X.12200>.
- Büchi, L and S. Vuilleumier, 2014. Coexistence of Specialist and Generalist Species is Shaped by Dispersal and Environmental Factors. *The American Naturalist*. 183(5): 612-624. <https://www.jstor.org/stable/pdf/10.1086/675756.pdf>.
- Canadell, J., R. B. Jackson, J. R. Ehleringer, H. A. Mooney, O. E. Sala, and E. D. Schulze. 1996. Maximum Rooting Depth of Vegetation Types at the Global Scale. *Oecologia*. 108(4): 583–595. <https://www.jstor.org/stable/pdf/4221458.pdf>.

- Cayan, D. R., T. Das, D. W. Pierce, T. P. Barnett, M. Tyree, and A. Gershunov. 2010. Future Dryness in the Southwest US and the Hydrology of the Early 21st Century Drought. *Proceedings of the National Academy of Sciences USA*. 107: 21271–21276. <https://www.pnas.org/content/107/50/21271>.
- Chase, J. M., M. A. Leibold. 2003. *Ecological Niches*. The University of Chicago Press.
- Chávez, R. O., J.G.P.W. Clevers, M. Decuyper, S. De Bruin, and M. Herold. 2016. 50 years of Groundwater Extraction in the Pampa del Tamarugal Basin: Can *Prosopis Tamarugo* Trees Survive in the Hyper-arid Atacama Desert (Northern Chile)? *Journal of Arid Environments*. 124: 293-303.
- Crawley, M. 2002. *Statistical Computing: An Introduction to Data Analysis Using S-plus*. Chichester, U.K: John Wiley & Sons.
- Connor, T., V. Hull, A. Viña, A. Shortridge, Y. Tang, J. Zhang, F. Wang, and J. Liu. 2018. Effects of Grain Size and Niche Breadth on Species Distribution Modeling. *Ecography* 41(8): 1270–82. <https://doi.org/10.1111/ecog.03416>.
- Cope, E. D. 1867 “1866”. On the Reptilia and Batrachia of the Sonoran Province of the Nearctic Region. *Proceedings of the Academy of Natural Sciences of Philadelphia*. 18: 300–314.
- Dahl, A., M. P. Donovan, and T. D. Schwaner. 2000. Egg Mass Deposition by Arizona Toads, *Bufo microscaphus*, Along a Narrow Canyon Stream. *Western North American Naturalist*. 60: 456-458. <https://scholarsarchive.byu.edu/cgi/viewcontent.cgi?article=1226&context=wnan>.
- Díaz, S., J. Fargione, F. S. Chapin III, and D. Tilman. (2006). Biodiversity Loss Threatens Human Well-Being. *PLOS Biology*, 4(8), e277. <https://doi.org/10.1371/journal.pbio.0040277>.
- Dobrowski, S. Z. 2011. A Climatic Basis for Microrefugia: The Influence of Terrain on Climate: A Climatic Basis for Microrefugia. *Global Change Biology* 17(2): 1022–35. <https://doi.org/10.1111/j.1365-2486.2010.02263.x>.
- Dodd, C. K. 2013. *Frogs of the United States and Canada*. John Hopkins University Press. 127-132. <https://ebookcentral.proquest.com/lib/sfasu-ebooks/reader.action?docID=3318708#>.

- Dominguez, F., J. Cañon, and J. Valdes. 2010. IPCC-AR4 Climate Simulations for the Southwestern US: The Importance of Future ENSO Projections. *Climatic Change* 99: 499–514. DOI 10.1007/s10584-009-9672-5.
- Drake, J. M., C. Randin, and A. Guisan. 2006. Modelling Ecological Niches with Support Vector Machines. *Journal of Applied Ecology*. 43(3): 424–432. <https://doi.org/10.1111/j.1365-2664.2006.01141.x>.
- Duellman, W.E. and Sweet, S.S. 1999. Distribution Patterns of Amphibians in the Nearctic Region of North America. *Patterns of Distribution of Amphibians: A Global Perspective*. pp. 31–10. Johns Hopkins University Press, Baltimore, MD.
- El-Gabbas, A. and C. F. Dormann. 2018. Wrong, but Useful: Regional Species Distribution Models may not be Improved by Range-wide Data Under Biased Sampling. *Ecology and Evolution*. 8(4): 2196–2206. <https://doi.org/10.1002/ece3.3834>.
- Elith, J., C. H. Graham, R. P. Anderson, M. Dudík, S. Ferrier, A. Guisan, R. J. Hijmans, F. Huettmann, J. R. Leathwick, A. Lehmann, J. Li, L. G. Lohmann, B. A. Loiselle, G. Manion, C. Moritz, M. Nakamura, Y. Nakazawa, J. M. Overton, A. T. Peterson, S. J. Phillips, K. Richardson, R. Scachetti-pereira, R. E. Schapire, J. Soberón, S. Williams, M. S. Wisz, and N. E. Zimmermann. 2006. Novel Methods Improve Prediction of Species' Distributions from Occurrence Data. *Ecography*. 29: 129–151. <https://onlinelibrary.wiley.com/doi/pdf/10.1111/j.2006.0906-7590.04596.x>.
- Elith, J. and J. Leathwick. 2007. Predicting Species Distributions from Museum and Herbarium Records Using Multiresponse Models Fitted with Multivariate Adaptive Regression Splines. *Diversity and Distributions*. 13(3): 265–275. <https://doi.org/10.1111/j.1472-4642.2007.00340.x>.
- Elith, J., J. R. Leathwick, and T. Hastie. 2008. A Working Guide to Boosted Regression Trees. *Journal of Animal Ecology*. 77(4): 802–813. <https://besjournals.onlinelibrary.wiley.com/doi/pdf/10.1111/j.1365-2656.2008.01390.x>.
- Elith J. and J. R. Leathwick. 2009. Species Distribution Models: Ecological Explanation and Prediction Across Space and Time. *Annual Review Ecology, Evolution, and Systematics*. 40: 667-697. <https://www.annualreviews.org/doi/pdf/10.1146/annurev.ecolsys.110308.120159>.

- Elith, J., S. J. Phillips, T. Hastie, M. Dudík, Y. E. Chee, and C. J. Yates. 2010. A Statistical Explanation of MaxEnt for Ecologists. *Diversity and Distributions*. 17(1): 43–57. <https://doi.org/10.1111/j.1472-4642.2010.00725.x>.
- Escalante, T., G. Rodríguez-Tapia, M. Linaje, P. Illoldi-Rangel, and R. González-López. 2013. Identification of Areas of Endemism from Species Distribution Models: Threshold Selection and Nearctic Mammals. *Revista Especializada en Ciencias Químico-Biológicas*. 16(1):5-17. <https://www.medigraphic.com/pdfs/revespcie/quibio/cqb-2013/cqb131a.pdf>.
- Evangelista, P. H., S. Kumar, T. J. Stohlgren, C. S. Jarnevich, A. W. Crall, J. B. Norman III, and D.T. Barnett. 2008. Modelling Invasion for a Habitat Generalist and a Specialist Plant Species. *Diversity and Distributions*. 14(5): 808–17. <https://doi.org/10.1111/j.1472-4642.2008.00486.x>.
- Evans, J. S., M. A. Murphy, Z. A. Holden, and S. A. Cushman. 2011. Modeling Species Distribution and Change Using Random Forest. *Predictive Species and Habitat Modeling in Landscape Ecology*. 139–159. https://doi.org/10.1007/978-1-4419-7390-0_8.
- Evans, M. E. K., R. Ferriere, M. J. Kane, and D. L. Venable. 2007. Bet Hedging via Seed Banking in Desert Evening Primroses (*Oenothera*, *Onagraceae*): Demographic Evidence from Natural Populations. *American Naturalist*. 169(2): 184–194. doi:10.1086/510599.
- Fick, S. E. and R. J. Hijmans. 2017. WorldClim 2: New 1km Spatial Resolution Climate Surfaces for Global Land Areas. *International Journal of Climatology*. 37(12): 4302-4315. <https://www.worldclim.org/data/worldclim21.html>.
- Fox, L. R., H. N. Steele, K. D. Holl, and M. H. Fusari. 2006. Contrasting Demographies and Persistence of Rare Annual Plants in Highly variable Environments. *Plant Ecology*. 183: 157 –170. doi:10.1007/s11258-005-9014-2.
- Franklin, J., F. W. Davis, M. Ikegami, A. D. Syphard, L. E. Flint, A. L. Flint, and L. Hannah. 2013. Modeling Plant Species Distributions under Future Climates: How Fine Scale Do Climate Projections Need to Be? *Global Change Biology*. 19(2): 473–83. <https://doi.org/10.1111/gcb.12051>.

- Garfin, G., A. Jardine, R. Merideth, M. Black, and S. LeRoy. 2013. Assessment of Climate Change in the Southwest United States: A Report Prepared for the National Climate Assessment. A report by the Southwest Climate Alliance. Washington, DC: Island Press.
- Gent, P., G. Danabasoglu, L. Donner, M. Holland, E. Hunke, S. Jayne, and D. Lawrence. 2011. The Community Climate System Model Version 4. *Journal of Climate*. (24): 4973–91. <https://doi.org/10.1175/2011JCLI4083.1>.
- Gottschalk, T. K., B. Aue, S. Hotes, and K. Ekschmitt. 2011. Influence of Grain Size on Species–habitat Models. *Ecological Modelling*. 222(18): 3403–3412. <https://doi.org/10.1016/j.ecolmodel.2011.07.008>.
- Grenouillet, G., L. Buisson, N. Casajus, and S. Lek. 2011. Ensemble Modelling of Species Distribution: The Effects of Geographical and Environmental Ranges. *Ecography*. 34(1): 9–17. <https://doi.org/10.1111/j.1600-0587.2010.06152.x>.
- Guisan, A. and N. E. Zimmermann. 2000. Predictive Habitat Distribution Models in Ecology. *Ecological Modelling*. 135(2–3): 147–186. [https://doi.org/10.1016/S0304-3800\(00\)00354-9](https://doi.org/10.1016/S0304-3800(00)00354-9).
- Guisan, A., T. C. Edwards, and T. Hastie. 2002. Generalized Linear and Generalized Additive Models in Studies of Species Distributions: Setting the Scene. *Ecological Modelling*. 157: 89-100. <https://www.sciencedirect.com/science/article/pii/S0304380002002041>.
- Guisan, A., C. H. Graham, J. Elith, F. Huettmann. 2007. Sensitivity of Predictive Species Distribution Models to Change in Grain Size. *Diversity and Distributions*. 13(3). <https://doi.org/10.1111/j.1472-4642.2007.00342.x>
- Guisan, A., R. Tingley, J. B. Baumgartner, I. Naujokaitis-Lewis, P. R. Sutcliffe, A. I. T. Tulloch, T. J. Regan, L. Brotons, E. McDonald-Madden, C. Mantyka-Pringle, T. G. Martin, J. R. Rhodes, R. Maggini, S. A. Setterfield, J. Elith, M. W. Schwartz, B. A. Wintle, O. Broennimann, M. Austin, and Y. M. Buckley. 2013. Predicting Species Distributions for Conservation Decisions. *Ecology Letters*. 16(12): 1424–1435. <https://doi.org/10.1111/ele.12189>.
- Hageer, Y. M. Esperón-Rodríguez, J. B. Baumgartner, and L. J. Beaumont. 2017. Climate, Soil or Both? Which Variables are Better Predictors of the Distributions of Australian Shrub Species? *PeerJ*. DOI 10.7717/peerj.3446.

- Halpin, P. N. 1997. Global Climate Change and Natural Area Protection: Management Responses and Research Directions. *Ecological Applications*. 7: 828-843. doi.org/10.1890/1051-0761(1997)007[0828:GCCANA]2.0.CO;2.
- Hernandez, P. A., C. H. Graham, L. L. Master, and D. L. Albert. 2006. The Effect of Sample Size and Species Characteristics on Performance of Different Species Distribution Modeling Methods. *Ecography*. 29(5): 773–85. https://doi.org/10.1111/j.0906-7590.2006.04700.x.
- Hess, G. R., R. A. Bartel, A. K. Leidner, K. M. Rosenfeld, M. J. Rubino, S. B. Snider, and T. H. Ricketts. 2006. Effectiveness of Biodiversity Indicators Varies with Extent, Grain, and Region. *Biological Conservation*. 132: 448–457. https://www.sciencedirect.com/science/article/pii/S0006320706001960.
- Hickman, J. C. 1993. *The Jepson Manual Higher Plants of California*. University of California Press. pp. 1424.
- Hijmans, R. J., S. E. Cameron, J. L. Parra, P. G. Jones, and A. Jarvis. 2005. Very High-Resolution Interpolated Climate Surfaces for Global Land Areas. *International Journal of Climatology*. 25(15): 1965–1978. https://doi.org/10.1002/joc.1276.
- Hutchinson, M. F. and T. Xu. 2013. ANUSPLIN Version 4.4 User Guide. Fenner School of Environment and Society. Australian National University. http://fennerschool.anu.edu.au/files/anusplin44.pdf.
- Intergovernmental Panel on Climate Change (IPCC). 2007. Report of the 26th Session of the IPCC. Bangkok. April 30–May 4 2007. Intergovernmental Panel on Climate Change, Geneva, Switzerland.
- Intergovernmental Panel on Climate Change (IPCC). 2014. *Climate Change 2014: Impacts, Adaptation, and Vulnerability. Part B: Regional Aspects. Contribution of Working Group II to the Fifth Assessment Report of the Intergovernmental Panel on Climate Change*. Cambridge University Press, New York, New York, USA.
- Jasmin, J. N., and R. Kassen. 2007. On the Experimental Evolution of Specialization and Diversity in Heterogeneous Environments. *Ecology Letters*. 10: 272–281. https://doi.org/10.1111/j.1461-0248.2007.01021.x
- Jenness, J. 2006. Topographic Position Index Extension for ArcView 3.x. Jenness Enterprises. http://www.jennessent.com/arcview/tpi.html.

- Jetz, W., C. H. Sekercioglu, and J. E. M. Watson. 2007. Ecological Correlates and Conservation Implications of Overestimating Species Geographic Ranges. *Conservation Biology*. 22(1): 110–19. <https://doi.org/10.1111/j.1523-1739.2007.00847.x>.
- Jiménez-Valverde, A. 2012. Insights into the Area under the Receiver Operating Characteristic Curve (AUC) as a Discrimination Measure in Species Distribution Modelling. *Global Ecology and Biogeography*. 21(4): 498–507. <https://doi.org/10.1111/j.1466-8238.2011.00683.x>.
- Kattan, G. H. 1992. Rarity and Vulnerability: The Birds of the Cordillera Central of Colombia. *Conservation Biology*. 6(1): 64–70. <https://www.jstor.org/stable/pdf/2385851.pdf>.
- Kulkarni, S. S., I. Gomez-Mestre, C. L. Moskalik, B. L. Storz, and D. R. Buchholz. 2011. Evolutionary Reduction of Developmental Plasticity in Desert Spadefoot Toads. *Journal of Evolutionary Biology*. 24(11): 2445–2455. <https://doi.org/10.1111/j.1420-9101.2011.02370.x>.
- Lassueur T., J. S, C. F. Randin. 2006. Very High-Resolution Digital Elevation Models: Do they Improve Models of Plant Species Distribution? *Ecological Modelling*. 198(1–2): 139–153. <https://www.sciencedirect.com/science/article/abs/pii/S0304380006001712>.
- Lawlor, L. R., and J. M. Smith. 1976. Co-evolution and Stability of Competing Species. *American Naturalist*. 110(971): 79–99. <https://www.jstor.org/stable/pdf/2459878.pdf>.
- Lawler, J. J., Y. F. Wiersma, and F. Huettmann. 2011. Using Species Distribution Models for Conservation Planning and Ecological Forecasting. *Predictive Species and Habitat Modeling in Landscape Ecology*. Springer New York. pp. 271–290. https://doi.org/10.1007/978-1-4419-7390-0_14.
- Lenoir, J., J. C. Gegout, P. A. Marquet, P. de Ruffray, and H. Brisse. 2008. A Significant Upward Shift in Plant Species Optimum Elevation During the 20th Century. *Science*. 320: 1768–1771. <https://science.sciencemag.org/content/320/5884/1768>.
- Levine, J. M., A. K. McEachern, and C. Cowan. 2008. Rainfall Effects on Rare Annual Plants. *Journal of Ecology*. 96: 795–806. doi:10.1111/j.1365-2745.2008.01375x.

- Levins, R. 1968. *Evolution in Changing Environments*. Princeton University Press. Princeton, NJ.
- Li, F. and H. He. 2018. Assessing the Accuracy of Diagnostic Tests. *Shanghai Archives of Psychiatry*. 30(3): 207–12. <https://doi.org/10.11919/j.issn.1002-0829.218052>.
- Liu, C., P. M. Berry, T. P. Dawson, and R. G. Pearson. 2005. Selecting Thresholds of Occurrence in the Prediction of Species Distributions. *Ecography* 28(3): 385–93. <https://doi.org/10.1111/j.0906-7590.2005.03957.x>.
- Liu, C., M. White, and G. Newell. 2013. Selecting Thresholds for the Prediction of Species Occurrence with Presence-only Data. *Journal of Biogeography*. 40(4): 778–789. <https://www.jstor.org/stable/pdf/23463638.pdf>.
- Liu, C., G. Newell, and M. White. 2015. On the Selection of Thresholds for Predicting Species Occurrence with Presence-only Data. *Ecology and Evolution*. 6(1): 337–48. <https://doi.org/10.1002/ece3.1878>.
- Lorini, M. L. and M. M. Vale. 2015. Publication Trends in Species Distribution Modeling and the Pioneer Contribution of Dr. Rui Cerqueira to Ecological Biogeography and Distribution Modeling in Brazil. *Oecologia Australis*. 19(01): 16–31. <https://doi.org/10.4257/oeco.2015.1901.02>.
- Luoto, M., J. Pöyry, R. K. Heikkinen and K. Saarinen. 2005. Uncertainty of Bioclimate Envelope Models Based on the Geographical Distribution of Species. *Global Ecology and Biogeography*. 14(6): 575–584. <https://www.jstor.org/stable/pdf/3697674.pdf>.
- Martes, K. and W. Jetz. 2018. Disentangling Scale Dependencies in Species Environmental Niches and Distributions. *Ecography*. 41: 1604–1615. <https://onlinelibrary.wiley.com/doi/pdf/10.1111/ecog.02871>.
- Marvier, M., P. Kareiva, and M. G. Neubert. 2004. Habitat Destruction, Fragmentation, and Disturbance Promote Invasion by Habitat Generalists in a Multispecies Metapopulation. *Risk Analysis* 24(4): 869–878. <https://onlinelibrary.wiley.com/doi/abs/10.1111/j.0272-4332.2004.00485.x>
- McKinney, M. L., and L. J. Lockwood. 1999. Biotic Homogenization: A Few Winners Replacing Many Losers in the Next Mass Extinction. *Trends in Ecology & Evolution*. 14(11): 450–453. [https://doi.org/10.1016/S0169-5347\(99\)01679-1](https://doi.org/10.1016/S0169-5347(99)01679-1).

- McShea, W. 2014. What are the Roles of Species Distribution Modeling in Conservation Planning? *Environmental Conservation*. 41(2): 93-96.
https://www.researchgate.net/publication/278188304_What_are_the_roles_of_species_distribution_models_in_conservation_planning.
- Meehl, G. A., W. M. Washington, J. M. Arblaster, A. Hu, H. Teng, C. Tebaldi, B. N. Sanderson. 2012. Climate System Response to External Forcings and Climate Change Projections in CCSM4. *Journal of Climate* 25(11): 3661–3683.
<https://doi.org/10.1175/JCLI-D-11-00240.1>.
- Meineri, E. and K. Hylander. 2017. Fine-grain, Large-domain Climate Models Based on Climate Station and Comprehensive Topographic Information Improve Microrefugia Detection. *Ecography*. 40 (8): 1003–1013.
<https://doi.org/10.1111/ecog.02494>.
- Melo-Merino, S. M., H. Reyes-Bonilla, and A. Lira-Noriega. 2020. Ecological Niche Models and Species Distribution Models in Marine Environments: A Literature Review and Spatial Analysis of Evidence. *Ecological Modelling*. 415.
<https://doi.org/10.1016/j.ecolmodel.2019.108837>.
- Morgan, B. and B Guénard. 2019. New 30 m Resolution Hong Kong Climate, Vegetation, and Topography Rasters Indicate Greater Spatial Variation than Global Grids within an Urban Mosaic. *Earth System Science Data*. 11(3): 1083–1098. <https://doi.org/10.5194/essd-11-1083-2019>.
- Moss, R., M. Babiker, S. Brinkman, E. Cal NPS o, T. Carter, J. Edmonds, I. Elgizouli, S. Emori, and K. A. Hibbard. 2008. Towards new scenarios for analysis of emissions, climate change, impacts, and response strategies. IPCC Expert Meeting Report on New Scenarios. Intergovernmental Panel on Climate Change, Noordwijkerhout.
- National Park Service (NPS). 2013. Foundation Document: Zion National Park.
https://www.nps.gov/zion/learn/management/upload/ZION_Foundation_Document_SP-2.pdf.
- National Park Service (NPS). 2018. Nezer & Science. <https://www.nps.gov/zion/learn/nature/index.htm>.
- New Mexico Department of Game and Fish. 2006. Comprehensive Wildlife Conservation Strategy for New Mexico. New Mexico Department of Game and Fish. Santa Fe, New Mexico. pg. 526.

- Nezer, O., S. Bar-David, T. Gueta, and Y. Carmel. 2017. High-resolution Species-distribution Model Based on Systematic Sampling and Indirect Observations. *Biodiversity and Conservation*. 26(2): 421–437. <https://doi.org/10.1007/s10531-016-1251-2>.
- Notaro, M. and A. Zarrin. 2011. Sensitivity of the North American Monsoon to Antecedent Rocky Mountain Snowpack. *Geophysical Research Letters*. 38: L17403. <https://agupubs.onlinelibrary.wiley.com/doi/pdf/10.1029/2011GL048803>
- Papeş, M. and P. Gaubert. 2007. Modelling Ecological Niches from Low Numbers of Occurrences: Assessment of the Conservation Status of Poorly Known Viverrids (Mammalia, Carnivora) Across Two Continents. *Diversity and Distributions*. 13(6): 890–902. <https://doi.org/10.1111/j.1472-4642.2007.00392.x>.
- Parmesan C., N. Ryrholm, C. Stefanescu, J. K. Hill, C. D. Thomas, H. Descimon, B. Huntley, L. Kaila, J. Kullberg, T. Tammaru, W. J. Tennent, J. A. Thomas, and M. Warren. 1999. Poleward Shifts in Geographical Ranges of Butterfly Species Associated with Regional Warming. *Nature*. 399: 579-583. <https://www.nature.com/articles/21181>.
- Pearson, R. G., T. P. Dawson, P. M. Berry, and P. A. Harrison. 2002. SPECIES: A Spatial Evaluation of Climate Impact on the Envelope of Species. *Ecological Modelling*. 154(3): 289–300. [https://doi.org/10.1016/S0304-3800\(02\)00056-X](https://doi.org/10.1016/S0304-3800(02)00056-X).
- Pearson, R. G., C. J. Raxworthy, M. Nakamura, and P. A. Townsend. 2006. Predicting Species Distributions from Small Numbers of Occurrence Records: A Test Case Using Cryptic Geckos in Madagascar. *Journal of Biogeography*. 34(1): 102–117. <https://doi.org/10.1111/j.1365-2699.2006.01594.x>.
- Pepe, M.S. 2000. Receiver Operating Characteristic Methodology. *Journal of the American Statistical Association*. 95(449): 308–11. <https://doi.org/10.1080/01621459.2000.10473930>.
- Phillips, S. J., R. P. Anderson, and R. E. Schapire. 2006. Maximum Entropy Modeling of Species Geographic Distributions. *Ecological Modelling*, 190(3): 231–259. <https://doi.org/10.1016/j.ecolmodel.2005.03.026>.
- Phillips, S.J. and M. Dudik. 2008. Modeling of Species Distributions with MaxEnt: New Extensions and a Comprehensive Evaluation. *Ecography*. 31(2): 161–75. <https://doi.org/10.1111/j.0906-7590.2008.5203.x>.

- Phillips, S. J., M. Dudík, J. Elith, C. H. Graham, A. Lehmann, J. Leathwick, and S. Ferrier. 2009. Sample Selection Bias and Presence-only Distribution Models: Implications for Background and Pseudo-absence Data. *Ecological Applications*. 19(1): 181–97. <https://doi.org/10.1890/07-2153.1>.
- Phillips, J. S. and J. Elith. 2013. On Estimating Probability of Presence from Use-availability or Presence-background Data. *Ecology*. 94(6): 1409-1419. <https://pubmed.ncbi.nlm.nih.gov/23923504/>.
- Phillips, S. J. 2017. A Brief Tutorial on MaxEnt. https://biodiversityinformatics.amnh.org/open_source/maxent/Maxent_tutorial2017.pdf.
- Pollock, L. J., R. Tingley, W. K. Morris, N. Golding, R. B. O’Hara, K. M. Parris, P. A. Vesk, and M. A. McCarthy. 2014. Understanding Co-occurrence by Modelling Species Simultaneously with a Joint Species Distribution Model (JSDM). *Methods in Ecology and Evolution*. 5(5): 397–406. <https://doi.org/10.1111/2041-210X.12180>.
- Préau, C., A. Troche, R. Bertrand., and F. Isselin-Nondedeu. 2018. Modeling Potential Distributions of Three European Amphibian Species Comparing ENFA and MaxEnt. *Herpetological Conservation and Biology*. 13(1):91–104. LINK.
- Radosavljevic, A. and R.P. Anderson. 2014. Making Better MaxEnt Models of Species Distributions: Complexity, Overfitting and Evaluation. *Journal of Biogeography*. 41(4): 629–643. <https://onlinelibrary.wiley.com/doi/abs/10.1111/jbi.12227>.
- Raes, N. 2012. Partial Versus Full Species Distribution Models. *Natureza & Conservação*. 10(2): 127–38. <https://doi.org/10.4322/natcon.2012.020>.
- Rebelo, H. and G. Jones. 2010. Ground Validation of Presence-only Modelling with Rare Species: A case study on *Barbastelles* *Barbastella barbastellus* (Chiroptera: Vespertilionidae). *Journal of Applied Ecology*. 47: 410-420. doi: 10.1111/j.1365-2664.2009.01765.x.
- Reddy, S. and L. M. Dávalos. 2003. Geographical Sampling Bias and its Implications for Conservation Priorities in Africa. *Journal of Biogeography*. 30(11): 1719-1727. <https://onlinelibrary.wiley.com/doi/10.1046/j.1365-2699.2003.00946.x>.
- Ricketts, T. H. 2001. The Matrix Matters: Effective Isolation in Fragmented Landscapes. *American Naturalist*. 1(158): 87-99. <https://www.jstor.org/stable/pdf/10.1086/320863.pdf>.

- Riley, S. J., S. D. DeGloria, and R. Ellis. 1999. A Terrain Ruggedness Index that Quantifies Topographic Heterogeneity. *Intermountain Journal of Sciences*. 5(1-4): 23-27. http://download.osgeo.org/qgis/doc/reference-docs/Terrain_Ruggedness_Index.pdf.
- Ruiz-Gutiérrez, V. and E. F. Zipkin. 2011. Detection Biases Yield Misleading Patterns of Species Persistence and Colonization in Fragmented Landscapes. *Ecosphere*. 2(5): 1-14. <https://esajournals.onlinelibrary.wiley.com/doi/full/10.1890/ES10-00207.1>.
- Ryan, M. J., I. M., Latella, and J. T. Giermakowski. 2014. Final Report: Current Status of the Arizona Toad (*Anaxyrus microscaphus*) in New Mexico: Identification and Evaluation of Potential Threats to its Persistence. New Mexico Department of Game and Fish.
- Ryan, M. J., I. M. Latella, J. T. Giermakowski, and H. L. Snell. 2015. Final Report: Status of the Arizona Toad (*Anaxyrus microscaphus*) in New Mexico. <https://doi.org/10.25844/PRK4-NR28>.
- Ryan, M. J., J. T. Giermakowski, I. M. Latella, and H. L. Snell. 2017. Final Report: Status of the Arizona Toad (*Anaxyrus microscaphus*) in New Mexico. Submitted to New Mexico Department of Game and Fish. Available at the University of New Mexico's Digital Repository, <https://digitalrepository.unm.edu/>.
- Sappington, J. M., K. M. Longshore, and D. B. Thompson. 2007. Quantifying Landscape Ruggedness for Animal Habitat Analysis: A Case Study Using Bighorn Sheep in the Mojave Desert. *Journal of Wildlife Management*. 71(5): 1419–26. <https://doi.org/10.2193/2005-723>.
- Scales, K. L., E. L. Hazen, M. G. Jacox, C. A. Edwards, A. M. Boustany, M. J. Oliver, and S. J. Bograd. 2016. Scale of Inference: On the Sensitivity of Habitat Models for Wide-ranging Marine Predators to the Resolution of Environmental Data. *Ecography*. 40(1). <https://doi.org/10.1111/ecog.02272>.
- Schalk, C. M., C. G. Moñtana, L. Springer. 2015. Morphological Diversity and Community Organization of Desert Anurans. *Journal of Arid Environments*. 122: 132-140. <https://www.sciencedirect.com/science/article/abs/pii/S0140196315300069?via%3Dihub>.
- Schall, J.J. and Pianka, E.R. 1978. Geographic Trends in Number of Species. *Science*. 201(4357): 679–686. <https://science.sciencemag.org/content/201/4357/679>

- Scherrer, D. and C. Körner. 2010. Infra-red Thermometry of Alpine Landscapes Challenges Climatic Warming Projections. *Global Change Biology*. 16: 2602-2613. <https://onlinelibrary.wiley.com/doi/abs/10.1111/j.1365-2486.2009.02122.x>.
- Schwaner, T. D., and B.K. Sullivan. 2005. *Bufo microscaphus* Cope, 1867 “1866”: Arizona Toad. Pp. 422–424 In *Amphibian Declines: The Conservation Status of United States Species*. University of California Press, Berkeley, California, USA.
- Schwaner, T. D. and B. K. Sullivan. 2009. Fifty Years of Hybridization: Introgression Between the Arizona Toad (*Bufo microscaphus*) and Woodhouse’s Toad (*B. Woodhousii*) Along Beaver Dam Wash in Utah. *Herpetological Conservation and Biology*. 9. [http://www.herpconbio.org/Volume_4/Issue_2/ Schwaner Sullivan_2009.pdf](http://www.herpconbio.org/Volume_4/Issue_2/Schwaner_Sullivan_2009.pdf).
- Seager, R. and G. A. Vecchi. 2010. Greenhouse Warming and the 21st Century Hydroclimate of Southwestern North America. *Proceedings of the National Academy of Sciences USA* . 107: 21277–21282. <https://www.pnas.org/content/107/50/21277>.
- Seebacher, F. and R. Alford. 2002. Shelter Microhabitats Determine Body Temperature and Dehydration Rates of a Terrestrial Amphibian (*Bufo Marinus*). *Journal of Herpetology*. 36: 69–75. [https://doi.org/10.1670/00221511\(2002\)036\[0069:smdbta\]2.0.co;2](https://doi.org/10.1670/00221511(2002)036[0069:smdbta]2.0.co;2).
- Segurado, P. and M. B. Araújo. 2004. An Evaluation of Methods for Modelling Species Distribution. *Journal of Biogeography*. 31(10): 1555-1568. <https://www.jstor.org/stable/pdf/3554758.pdf>.
- Shannon, C. 1948. A Mathematical Theory of Communication. *The Bell System Technical Journal*. 27(3): 379-423. https://pure.mpg.de/rest/items/item_2383162_7/component/file_2456978/content.
- Sipes, S. D., P. G. Wolf, V. J. Tepedino, and J. Boettinger. 1994. Population Genetics and Ecology of *Jones cycladenia*. Bureau of Land Management Cost Share Program. Utah State Office.
- Sipes, S. D. and V. J. Tepedino. 1996. Pollinator Lost? Reproduction by the Enigmatic *Jones cycladenia*, *Cycladenia humilis* var. *jonesii* (Apocynaceae) in Southwestern Rare and Endangered Plants. Flagstaff, Arizona. Gen. Tech. Rep. RM-GTR-283. p. 328.

- Sipes, S. D. and P. G. Wolf. 1997. Clonal Structure and Patterns of Allozyme Diversity in the Rare Endemic *Cycladenia humilis* var. *jonesii* (apocynaceae). *American Journal of Botany*. 84(3): 401-409.
<https://bsapubs.onlinelibrary.wiley.com/doi/pdf/10.2307/2446013>.
- Slavich, E., D. I. Warton, M. B. Ashcroft, J. R. Gollan, and D. Ramp. 2014. Topoclimate versus Macroclimate: How Does Climate Mapping Methodology Affect Species Distribution Models and Climate Change Projections? *Diversity and Distributions* 20(8): 952–63. <https://doi.org/10.1111/ddi.12216>.
- Soberón, J. and A. T. Peterson. 2005. Interpretation of Models of Fundamental Ecological Niches and Species' Distributional Areas. *Biodiversity Informatics*. 2: 1-10. <https://www.researchgate.net/publication/26539066>.
- Stockwell, D. R. B. and A. T. Peterson. 2002. Effects of Sample Size on Accuracy of Species Distribution Models. *Ecological Modelling*. 148(1): 1–13.
[https://doi.org/10.1016/S0304-3800\(01\)00388-X](https://doi.org/10.1016/S0304-3800(01)00388-X).
- Sullivan, B. K. and T. Lamb. 1988. Hybridization Between the Toads *Bufo microscaphus* and *Bufo woodhousii* in Arizona: Variation in Release Calls and Allozymes. *Herpetologica*. 44(3): 325–333. <https://www.jstor.org/stable/3892347>.
- Sullivan, B. K. 1992. Calling Behavior of Southwestern Toad (*Bufo microscaphus*). *Herpetologica*. 48(4): 383-389. <https://www.jstor.org/stable/pdf/3892856.pdf>
- Sullivan, B. K. 1993. Distribution of the Southwestern Toad (*Bufo microscaphus*) in Arizona. *Great Basin Naturalist*. 53(4): 402-406.
<https://scholarsarchive.byu.edu/cgi/viewcontent.cgi?article=2794&context=gbn>.
- Sweet, S. S. 1992. Initial Report on the Ecology and Status of the Arroyo Toad (*Anaxyrus Microscaphus Californicus*) on the Los Padres National Forest of Southern California, with Management Recommendations. Contract Report to USDA, Forest Service, Los Padres National Forest, Goleta, California. pp. 198.
- Syfert, M. M., M. J. Smith, and D. A. Coomes. 2013. The Effects of Sampling Bias and Model Complexity on the Predictive Performance of MaxEnt Species Distribution Models. *PLOS ONE* 8. 2: e55158. <https://doi.org/10.1371/journal.pone.0055158>.

- Tang, J., X., Niu, S., Wang, H., Gao, X., Wang, and J. Wu. 2016. Statistical Downscaling and Dynamical Downscaling of Regional Climate in China: Present Climate Evaluations and Future Climate Projections. *Journal of Geophysical Research: Atmospheres*. 121(5): 2110–29. <https://doi.org/10.1002/2015JD023977>.
- Tilley, D., L. St. John, and D. Ogle. 2010. Plant Guide for Jones' Waxy Dogbane (*Cycladenia humilis* var. *jonesii*). USDA-Natural Resources Conservation Service. https://plants.usda.gov/plantguide/pdf/pg_cyhuj.pdf.
- Turner, M. G., R. V. O. R. H. Gardner, R. V. O'Neill, R. H. Gardner, and B. T. Milne. 1989. Effects of Changing Spatial Scale on the Analysis of Landscape Pattern. *Landscape Ecology*. 3: 153-162. <https://link.springer.com/article/10.1007/BF00131534>.
- US Department of the Interior (US DOI). National Park Service (NPS). 2001. Zion National Park: General Management Plan. https://www.nps.gov/zion/learn/management/upload/zion_gmp.pdf
- US Department of the Interior (US DOI). National Park Service (NPS). 2009. Zion National Park. Reptiles and Amphibians. <https://www.nps.gov/zion/learn/nature/upload/Reptiles&Amph2009.pdf>
- US Department of the Interior (US DOI). National Park Service (NPS). 2013a. Foundation Document. Zion National Park. Utah. <http://npshistory.com/publications/foundation-documents/zion-fd-2013.pdf>.
- US Department of the Interior (US DOI). National Park Service (NPS). 2013b. Virgin River Comprehensive Management Plan/Environmental Assessment. Zion National Park and Bureau of Land Management. <https://www.rivers.gov/documents/plans/virgin-plan.pdf>
- US Department of the Interior (US DOI). National Park Service (NPS). 2014. The Basics of Compliance with the National Environmental Policy Act and Section 106 of the National Historic Preservation Act: Instructional Manual, Version 1. Denver, Colorado: NPS Intermountain Region.
- US Fish and Wildlife Service (US FWS). 1986. Rule to Determine *Cycladenia humilis* var. *jonesii* (Jones' cycladenia) to be a Threatened Species. Federal Register 51(86): 16526-16530.

- US Fish and Wildlife Service (US FWS). 2008. Recovery Outline for the Jones' cycladenia (*Cycladenia humilis* var. *jonesii*). <https://www.fws.gov/mountain-prairie/es/species/plants/jonescycladenia/RecoveryOutlineDecember2008.pdf>.
- Vuuren, D. P. V., J. Edmonds, M. Kainuma, K. Riahi, A. Thomson, K. Hibbard, and G. C. Hurtt. 2011. The Representative Concentration Pathways: An Overview. *Climatic Change*. 109(1). <https://doi.org/10.1007/s10584-011-0148-z>.
- Vrba, E. S. 1987. Ecology in Relation to Speciation Rates: Some Case Histories of Miocene-Recent Mammal Clades. *Evolutionary Ecology*. 1: 283–300. <https://link.springer.com/content/pdf/10.1007/BF02071554.pdf>.
- Wang, T., A. Hamann, D. L. Spittlehouse, T. Q. Murdock. 2011. ClimateWNA—High-Resolution Spatial Climate Data for Western North America. *Journal of Applied Meteorology and Climatology*. 51: 16-29. DOI: 10.1175/JAMC-D-11-043.1.
- Welsh, S. L., N. D. Atwood, L. C. Higgins, and S. Goodrich. 1987. A Utah Flora. Great Basin Naturalist Memoirs No. 9. Brigham Young University. Provo, UT.
- Williams, J. N., C. Seo, J. Thorne, J. K. Nelson, S. Erwin, J. M. O'Brien, and M. W. Schwartz. 2009. Using Species Distribution Models to Predict New Occurrences for Rare Plants. *Diversity and Distributions*. 15(4): 565–576. <https://doi.org/10.1111/j.1472-4642.2009.00567.x>.
- Wisz, M. S., R.J. Hijmans, J. Li, A.T. Peterson, C. H. Graham, and A. Guisan. 2008. Effects of Sample Size on the Performance of Species Distribution Models. *Diversity and Distributions*. 14(5): 763–773. <https://doi.org/10.1111/j.1472-4642.2008.00482.x>.
- Woodward, F. I. and B. G. Williams. 1987. Theory and Models in Vegetation Science. *Vegetatio*. 69(1&3): 189-197. <https://www.jstor.org/stable/20038116>.
- Yang, X., S. Kushwaha, S. Saran, J. Xu, and P. Roy. 2013. MaxEnt Modeling for Predicting the Potential Distribution of Medicinal Plant, *Justicia Adhatoda* L. in Lesser Himalayan Foothills. *Ecological Engineering* 5: 83–87. <https://doi.org/10.1016/j.ecoleng.2012.12.004>.
- Yackulic, C. B., R. Chandler, E. F. Zipkin, J. A. Royle, J. D. Nichols, E. H. C. Grant, and S. Veran. 2013. Presence-only Modelling Using MaxEnt: When can we Trust the Inferences? *Methods in Ecology and Evolution*. 4(3): 236–243. <https://doi.org/10.1111/2041-210x.12004>.

Yiwen, Z., L. B. Wei, and D. C. J. Yeo. 2016. Novel Methods to Select Environmental Variables in MaxEnt: A Case Study Using Invasive Crayfish. *Ecological Modelling*. 341: 5–13. <https://doi.org/10.1016/j.ecolmodel.2016.09.019>.

Zimmerman, N. E., N. G. Yoccoz, T. C. Edwards, E. S. Meier, W. Thuiller, A. Guisan, D. R. Schmatz, and P. B. Pearman. 2009. Climatic Extremes Improve Predictions of Tree Species. *PNAS*. 106(2): 19726-19728. https://www.pnas.org/content/pnas/106/Supplement_2/19723.full.pdf

VITA

Sam Driver attended Woden High School, Woden Texas from 2004 to 2007. In the fall of 2007, he began his undergraduate degree at Texas State University in San Marcos, Texas, finishing the degree of Bachelor of Science in Biology with a minor in Chemistry in 2012. In January 2018, he entered the Graduate School of Stephen F. Austin State University. During the summer of 2019, the U.S. National Park Service at Zion National Park employed him as an intern working under the Environmental Protection Specialist. During the spring of 2020 he was employed as the GIS intern for Conservation Equity Partners in Nacogdoches, Texas. He completed his graduate studies from Stephen F Austin in the fall of 2020 with the degree of Master of Science in Environmental Science with a minor in Spatial Science.

This thesis was typed by Samuel M. Driver